MECHANISMS OF γ-LINOLENIC ACID INDUCTION OF APOPTOSIS IN T CELLS CHRONICALLY INFECTED WITH HIV-1

By

ONESMO MPANJU

BPharm, University of Dar es Salaam, 1985
MSc, Vrije Universiteit Brussel (VUB), 1992

A THESIS SUBMITTED IN PARTIAL FULFILLMENT OF THE REQUIREMENTS FOR THE DEGREE OF

DOCTOR OF PHILOSOPHY

In

THE FACULTY OF GRADUATE STUDIES

Experimental Medicine Program

We accept this thesis as conforming to the required standard

THE UNIVERSITY OF BRITISH COLUMBIA

May 2001

In presenting this thesis in partial fulfilment of the requirements for an advanced degree at the University of British Columbia, I agree that the Library shall make it freely available for reference and study. I further agree that permission for extensive copying of this thesis for scholarly purposes may be granted by the head of my department or by his or her representatives. It is understood that copying or publication of this thesis for financial gain shall not be allowed without my written permission.

Department of EXPERIMENTAL MEDICINE

The University of British Columbia
Vancouver, Canada

Date 10/10/2001

University of British Columbia

Abstract

MECHANISMS OF γ-LINOLENIC ACID INDUCTION OF APOPTOSIS IN T CELLS CHRONICALLY INFECTED WITH HIV-1

By Onesmo Mpanju

Chairperson of the Supervisory Committee: Brian Conway, MD

BACKGROUND: The polyunsaturated fatty acid (PUFA) gamma-linolenic acid (GLA) kills HIV-1-infected cells at concentrations that are relatively harmless to uninfected cells. The mechanism of this effect is unclear but evidence implicates oxidative stress. The aim of this study was to define mechanisms of GLA cytotoxicity in HIV-infected T cells.

METHODS: The test model comprised uninfected A3.01 and HIV-1-infected 8E5 T cells. Cell proliferation was measured using WST-1 and Trypan blue dye-exclusion assays. Colorimetric analysis for lipid peroxidation, and supplementation with antioxidants and lipoxygenase (LOX) or cyclooxygenase (COX)-mediated PUFA metabolism inhibitors probed for involvement of oxidative stress. Apoptosis was assayed flow cytometrically using FITC-conjugated Annexin V and bromodeoxyuridine. We examined cells for specific apoptosis signaling using caspase inhibitors, and by ribonuclease protection and immunoblot assays. Propidium iodide staining helped to investigate association of apoptosis and cell cycling. As validation, GLA effects were assessed in $CD4^+$ cells infected *de novo* with isolates of HIV-1, or freshly isolated from HIV^+ patients.

RESULTS: GLA was more cytotoxic to 8E5 cells (IC_{50} = 14.5 μg/ml) than A3.01 cells (IC_{50} = 43.0 μg/ml). GLA-induced cytotoxicity in 8E5 was associated with a four-fold increase in concentration of lipid peroxidation metabolites. The thiol antioxidant, 2-mercaptoethanol, and glutathione peroxidase-mimic, ebselen, inhibited GLA actions. Concentration-specific inhibition was also achieved with LOX and COX inhibitors. Flow cytometric analysis with Annexin V-FITC and BrdU-FITC, and inhibition by caspase inhibitor BD.fmk confirmed occurrence of apoptosis in GLA-treated cells. The majority of apoptotic cells were found in the G_0/G_1 cell cycle-phase. Immunoblot analysis demonstrated cleavage of caspase-3 and poly (ADP-ribose) polymerase (PARP). Differential GLA cytotoxicity was also observed in cells acutely infected with $HIV\text{-}1_{IIIB}$ but not in cells infected with other isolates. There was a negative correlation between GLA IC_{50} in $CD4^+$ cells from HIV^+ patients and plasma viral load.

CONCLUSION: GLA induces apoptosis in 8E5 cells through a mechanism that involves lipid peroxidation and cleavage of caspase-3 and PARP. GLA cytotoxicity against $CD4^+$ cells of HIV^+ patients increases with viral load. Therefore, GLA and its homologues deserve further study in the search for compounds that target HIV-infected cells for selective killing.

TABLE OF CONTENTS

Abstract ..... *ii*
List of Tables ..... *v*
List of Figures ..... *vi*
Acknowledgements ..... *viii*
List of Abbreviations ..... *ix*

CHAPTER 1 **INTRODUCTION** *1*

CHAPTER 2 **MATERIALS AND METHODS** *9*
Cell culture conditions *9*
T cell lines *9*
Isolation of $CD4^+$ T cells *10*
HIV-1 isolates *11*
Cytotoxicity assay *12*
Apoptosis assay *12*
Flow cytometric analysis *14*
Isolation of total RNA *14*
Biotin or [^{32}P] labeling of RNA probes *15*
Ribonuclease protection assay (RPA) *15*
Gel electrophoresis of ribonuclease protected probes *16*
Detection of Ribonuclease protected probes *17*
Western blot analysis of apoptosis-related cellular factors *17*
Colorimetric assay for lipid peroxidation *19*

CHAPTER 3 **RESULTS** *21*

The productively and chronically HIV-1 infected cell line 8E5 is three times more sensitive to GLA-induced cytotoxicity than the parental uninfected A3.01 cell line *21*

Lack of distinctive modulation of GLA-induced cytotoxicity by inhibitors of lipoxygenase and cyclooxygenase pathways of PUFA metabolism *23*

GLA selective cytotoxicity in chronically HIV-infected cells is associated with elevated lipid peroxidation *26*

GLA induces programmed cell death in the HIV-1-infected 8E5 cell line at a median concentration that does not affect viability of the parental uninfected A3.01 cell line *32*

The induction of apoptosis in 8E5 cells by GLA is associated with arrest of cells in the G_0/G_1 cell cycle phase *39*

Susceptibility to GLA-induced apoptosis is only partially associated with active production of HIV-1 core antigen *44*

Modification of apoptosis-related genes during GLA-induced cell death..... *46*

GLA induces apoptosis via a pathway that is blocked by a broad-spectrum inhibitor of caspases..... *49*

Induction of apoptosis by GLA is associated with cleavage of caspase-3 and poly (ADP-ribose) polymerase (PARP)..... *51*

Effect of GLA on primary $CD4^+$ T cells acutely infected with clinical and laboratory-adapted isolates of HIV-1 ..... *58*

GLA cytotoxicity against $CD4^+$ T cells isolated from HAART-treated AIDS patients is negatively correlated with patients' viral load..... *61*

CHAPTER 4 **DISCUSSION** *64*

REFERENCES *76*

LIST OF TABLES

Table 1: *27*

Table 2: *63*

LIST OF FIGURES

Figure 1: Apoptosis pathway 7

Figure 2: Cytotoxicity of GLA in A3.01 and 8E5 cells 22

Figure 3: Effect of inhibitors of lipoxygenase and cyclooxygenase enzymes on GLA-induced cytotoxicity 24

Figure 4: Effect of antioxidants on GLA-induced cytotoxicity in 8E5 cells 30

Figure 5: Annexin V flow cytometric analysis for GLA induction of apoptosis in A3.01 and 8E5 cells 34

Figure 6: Apo-BrdU flow cytometric analysis for GLA induction of apoptosis in A3.01 and 8E5 cells 36

Figure 7: Time-course of apoptosis induction in 8E5 cells 38

Figure 8a: Bivariate analysis of GLA-treated A3.01 cells for cell cycling and apoptosis 40

Figure 8b: Bivariate analysis of GLA-treated 8E5 cells for cell cycling and apoptosis 41

Figure 9: Effect of GLA on cycling of G_0/G_1-synchronized 8E5 cells 43

Figure 10: Bivariate analysis of GLA-treated 8E5 cells for apoptotic status and production of HIV-1 core antigen 45

Figure 11: Expression of apoptosis-related genes in 8E5 cells exposed to GLA 48

Figure 12: Effect of broad-spectrum caspase inhibitors on GLA- and α-Fas antibody-mediated programmed death of 8E5 cells 50

Figure 13: GLA and α-Fas antibody- mediated regulation of upstream factors of the apoptosis cascade in apoptotic 8E5 cells 52

Figure 14: GLA- and α-Fas antibody- mediated cleavage of effector molecules of the apoptosis cascade in apoptotic 8E5 cells 57

Figure 15: Cytotoxicity of GLA in primary donor $CD4^+$ T cells infected *de novo* with HIV-1_{657}, HIV-1_{714}, HIV-1_{NL43} or HIV-1_{RF} isolates 59

Figure 16: Cytotoxicity of GLA in primary donor $CD4^+$ T cells infected *de novo* with HIV-1_{IIIB} isolates 60

Figure 17: Cytotoxicity of GLA in primary $CD4^+$ T cells isolated from HAART-treated HIV^+ patients..... *62*

Figure 18: Oxidation and regeneration of vitamin E..... *68*

ACKNOWLEDGMENTS

I wish to express my sincerest thanks to Dr. Brian Conway, University of British Columbia, for giving me the chance to undertake this work and for his constant guidance. My very deep appreciation goes to Dr. Robert Shoemaker, Screening Technologies Branch (STB) – NCI, for giving me the opportunity to work at NCI, and Dr. Judy Mikovits, Laboratory of Antiviral Drug Mechanisms – NCI-Frederick, for her invaluable supervision and constructive review of the manuscript. I am also grateful to Dr. Howard Young, Laboratory of Experimental Immunology – NCI-Frederick, for assistance on RPA, Mac Trubey for technical support on FACS analysis and Quan-En Yang for technical help on protein analysis. I wish to thank everyone in the laboratories of Drs. Conway, Mikovits and Francis Ruscetti who helped me along. I owe much gratitude to Drs. Michael Currens, STB – NCI and Michael O'Shaughnessy, British Columbia Centre for Excellence in HIV/AIDS, for reviewing the manuscript.

A very special thanks goes to my family, especially my loving wife Joyce who has been there always, and my daughter Melanie who put it all in perspective. Finally, this would not have been possible without my parents who instilled in me the value of education.

I am indebted to the National Institutes of Health for awarding me a predoctoral fellowship that enabled me to conduct part of my research at NCI-Frederick.

This thesis is dedicated to Vincent.

LIST OF ABBREVIATIONS

γ-GCE	Gamma-glutamylcysteine ethyl ester
2-ME	2-Mercaptoethanol
^{32}P-UTP	^{32}Phosphorus-labeled uridine tri-phosphate
4-HNE	4-hydroxy-2(E)-nonenal
AA	Arachidonic acid
ADP	Adenosine 5′-diphosphate
AIDS	Acquired immune defficiency syndrome
APAF-1	Apoptotic protease activating factor-1
ATP	Adenosine 5′-triphosphate
BCA	Bicinchoninic acid
BD.fmk	Boc-Asp(OMe)-CH_2F
BHT	Butylated hydroxytoluene
BrdU	Bromodeoxyuridine
BSA	Bovine serum albumin
$CCID_{50}$	Cell culture infective dose 50%
COX	Cyclooxygenase
CTL	Cytotoxic T lymphocyte
DAIDS	Division of AIDS
DD	Death domain
DED	Death effector domain
DGLA	Dihommo gamma-linolenic acid
DNA	Deoxyribonucleic acid
dNTP	Deoxyribonucleoside 5′-triphosphate
DR3	Death receptor 3
DR5	Death receptor 5
DTT	Dithiothreitol
ECL	Electrogenerated chemiluminescence
EDTA	Tetrasodium ethylene diaminetetraacetate
ELISA	Enzyme-linked immunosorbent assay
EPA	Eicosapentaenoic acid
ETYA	8,11,14-eicosatetraynoic acid
FACS	Fluorescent-activated cell sorting
FADD	Fas-associated death domain
FAF	Fas-associated factor
FAP	Fas-associated phosphatase
FASL	Fas ligand
FITC	Fluorescein isothiocyanate
FLAP	Five-lipoxygenase activating protein
GLA	Gamma-linolenic acid
GPx	Glutathione peroxidase
GSH	Reduced glutathione
GSSG	Oxidized glutathione
H_2O_2	Hydrogen peroxide
HAART	Highly active antiretroviral therapy
HAT	Hypoxanthine-aminopterin-thymidine
HETE	Hydroxyeicosatetraenoic acid
HIV-1	Human immune deficiency virus type-1
HPETE	Hydroperoxyeicosa-tetraenoic acid
HSV-1	Herpes simplex virus type-1
HSV-2	Herpes simplex virus type-2
IC_{50}	Inhibitory concentration 50%
LARD	Lymphocyte-associated receptor of death
LLP-I	Lentiviral lytic peptide I
LOX	Lipoxygenase
MACS	Magnetic cell sorting
MDA	Malondialdehyde

MOI	Multiplicity of infectivity
MPA	Mycophenolic acid
NAC	N-acetyl cysteine
NaCl	Sodium chloride
NADPH	Nicotinamide adenine dinucleotide phoshphate reduced form
NDGA	Nordihydroguiaretic acid
NH_4OAc	Ammonium acetate
NIAID	National Institute of Allergy and Infectious Diseases
NIH	National Institutes of Health
PARP	Poly (ADP) ribose polymerase
PBMC	Peripheral blood mononuclear cells
PBS	Phosphate buffered saline
PCD	Programmed cell death
PG	Prostaglandin
PHA-P	Purified phytohemaglutinin
PI	Propidium iodide
PKA	Protein kinase A
PKC	Protein kinase C
PMSF	Phenylmethylsulfonyl fluoride
PS	Phosphatidylserine
PUFA	Polyunsaturated fatty acid
PVDF	polyvinylidene difluoride
RIP	Receptor interacting protein
RNA	Ribonucleic acid
ROS	Reactive oxygen species
RPA	Ribonucleic protection assay
RT	Reverse transcriptase
SDS-PAGE	Sodium dodecyl sulfate - polyacrylamide gel electrophoresis
SMAC	Secondary mitochondria-derived activator of caspases
SOD	Superoxide dismutase
TCR	T cell receptor
TdT	Terminal deoxynucleotidyl-transferase
TNF-α	Tumor necrosis factor-alpha
TNFR1	Tumor necrosis factor receptor 1
TNFRp55	Tumor necrosis factor receptor 55-kilo-Dalton protein
TPA	12-O-tetradecanoxylphorbol 13-acetate
TRADD	TNF receptor 1-associated death domain
TRAIL	TNF-related apoptosis inducing ligand
TRAMP	TNF receptor apoptosis mediating protein
WST-1	Water-soluble tetrazolium
zVAD-FMK	Z-Val-Ala-Asp(OMe)-

Chapter 1

INTRODUCTION

The polyunsaturated fatty acid (PUFA) γ-linolenic acid (GLA) was shown in previous studies to induce differential cytotoxicity of T cells chronically infected with human immunodeficiency virus type-1 (HIV-1) *[70]*. In a study of the H9/$H9_{RF}$ model of chronic HIV infection, authors reported a 90% killing of the chronically and productively HIV-1 infected H9/$HTLV\text{-}III_{RF}$ cell line by GLA compared to 20% of the uninfected parental H9 cell line during four days of culture. This GLA – induced cytotoxicity correlated with lipid peroxidation and was preventable by preincubating cells with the antioxidant vitamin E (α-tocopherol). Previously, we demonstrated preferential cytotoxicity of GLA in the productively HIV-1 infected 8E5 cell line when compared to its uninfected parental A3.01 cell line *[88]*. Moreover, GLA has been demonstrated to induce differential cytotoxicity in cells infected with viruses such as Herpes simplex virus type-1 (HSV-1) and HSV-2 *[116]*.

Mechanisms of GLA-induced Cytotoxicity

Besides its effects in virally infected cells, GLA is also known to induce selective cytotoxicity in a number of malignant cells relative to normal cells *[4, 9, 10, 32, 66, 100]*. The exact mechanism by which GLA exerts its effects is still unclear. Although there are a number of potential biochemical pathways that may lead to GLA-induced cell death, the majority of published data suggest increased levels of oxygen free radicals or reactive oxygen species (ROS). This is caused by a state of altered oxidative metabolism in malignant and certain virally infected cells *[70, 126]*. Mammalian cells are naturally incapable of *de novo* biosynthesis of essential (ω-3 and ω-6) PUFA such as GLA and must obtain them through diet. Following dietary intake, GLA is converted to arachidonic acid (AA) by Δ6-desaturase and microsomal elongase enzymes. AA can be oxygenated to a large series of metabolites with very important physiological activities. Metabolism of AA by cyclooxygenase (COX) enzyme results in the formation of prostaglandins while that by lipoxygenase (LOX) enzymes generate highly reactive hydroperoxyeicosatetraenoic acids (HPETEs) *[84]*, which under normal biochemical conditions are quickly converted to leukotrienes and lipoxins via a series of reactions involving

glutathione S-transferase and glutathione peroxidase (GPx) enzymes. HPETEs are free radical molecules that readily react with cellular macromolecules to initiate destructive cascades like apoptosis [75, 108, 133].

There are also reports of ROS-independent mechanisms of GLA-induced apoptosis. GLA may induce apoptosis by triggering the release of the second messenger ceramide, an inducer of apoptosis [91]. AA, the product of Δ6-desaturase metabolism of GLA, activates sphingomyelinase, which in turn metabolizes phospholipid sphingomyelin and results in the release of ceramide [65]. The third possible pathway of GLA-induced apoptosis is one that involves elevation of cAMP levels and activation of protein kinase A (PKA) due to increased formation of E-prostaglandins following GLA metabolism via the cyclooxygenase (COX) pathway [85]. Finally, GLA has been shown to induce apoptosis by decreasing MAP kinase activity and c-Jun levels [32].

Oxidative Stress and Programmed Cell Death in HIV Infection

HIV-infected cells possess elevated levels of reactive oxygen species (ROS) and exhibit deficiency in ROS scavenger molecules such as reduced glutathione (GSH) and GPx [7, 13, 15, 40, 118]. Furthermore, evidence suggests that oxidative stress is an integral part of HIV pathogenesis [40]. For example, intracellular concentration of free radical scavenger molecules like GSH is significantly reduced in peripheral blood mononuclear cells (PBMC) and monocytes isolated from HIV infected individuals [38].

One possible explanation for GSH deficiency in HIV infected cells might be extrusion of GSH from the cell during apoptotic signaling [29]. Accumulation of ROS in HIV infected cells and ensuing programmed cell death (PCD) or apoptosis have been implicated in the T cell depletion characteristic of HIV disease [40, 74, 123] but other factors such as T cell co-signaling, Bcl-2 and Fas dysregulation, might play a larger role in this respect. On the opposing side of the apoptosis equation in HIV infection is the observation that products of accessory genes *Nef* and *tat* can prevent infected cells from undergoing PCD [41, 52, 55, 131]. As well, HIV-1 *vpr* was shown to protect infected PBMC and Jurkat cells from activation-induced apoptosis during early stages of the viral life cycle but to have the opposite effect at later stages [28]. *Vpr* and *Nef* have been shown to promote depletion of 'bystander' cells while prolonging survival of HIV-infected cells [8]. Moreover, lymph node studies in HIV infected patients point to occurrence of apoptosis predominantly in 'bystander' rather than productively

infected T cells [41, 42] and inhibition of apoptosis in HIV – infected cells is reported to enhance virus production and facilitate persistent infection [5].

This apparent dichotomy in the role of apoptosis in HIV cytophathology warrants further investigation. In particular, there appears to be a need by the virus to counteract host cell 'suicide', at least transiently, in a manner reminiscent of other viruses [12, 86, 115, 125]. For instance, the human dermatotropic poxvirus molluscum contagiosum encodes a novel anti-oxidant selenoprotein (MC066L) which functions as a scavenger of ROS. This protein protects human keratinocytes against cytotoxic effects of ultraviolet irradiation and hydrogen peroxide. Although production of similar proteins has not been demonstrated in other viruses, it is noteworthy that sequence motifs similar to that of MC066L have been observed in HIV-1 and Ebola virus [86, 121].

Host-cell Targeted Antiretroviral Strategies

The presence of a long-lived HIV reservoir *in vivo*, probably comprised of both monocytes and lymphocytes, is further evidence that a proportion of HIV infected cells manage to escape both immune-mediated and virally induced apoptosis. This elusive reserovoir persists despite administration of highly active antiretroviral therapy (HAART) [56, 58]. As a result, initial speculation that continuous treatment with HAART could achieve complete eradication of the virus in infected individuals within a period of two to three years if complete viral suppression was sustained throughout the treatment period, has proven improbable [95]. Studies show that, despite HAART, a stable reservoir of infected $CD4^+$ T cells continue to seed the infection indefinitely [21, 43, 128] and that even after two years of HAART and suppression of viremia below the detection limit (as low as 3 copies per mililiter) viral replication continues to occur, as evidenced by genotypic variation of the progeny [36, 48, 130, 132]. Moreover, interruption of HAART results in a rebound of plasma viremia [27, 80] with virus that is genetically distinct from both cell-associated HIV RNA and replication-competent virus within the detectable pool of latently infected resting $CD4^+$ T cells, implicating existence of other persistent HIV reservoirs [24]. By all indications, a proportion of chronically infected cells is responsible for persistent virus production during HAART. Even with the most optimistic estimates, the time required to fully eradicate HIV from the body under HAART has been put at between 10 to 60 years [106].

Hence, the need to develop approaches that can kill virus-infected cells and eliminate the reservoir has been recognized in both vaccine development and therapy. Although the concept

of therapeutically targeting HIV-infected cells for selective killing – similar to cytotoxic T lymphocyte (CTL) activity -- has been around for several years [76], its study has been inadequate due to lack of appropriate experimental models and candidate molecules that are selective.

Besides GLA, the literature contains reports of other compounds that exhibit selective cytotoxicity against HIV infected T cells *in vitro*. In one study [6], using the antitumor agent benzaldehyde, sodium 5,6-benzylidene-L-ascorbate (SBA), a dose-dependent apoptotic cell death of chronically HIV – infected monocytic U1 cells was observed only when cells were induced to produce HIV by treatment with either TNF-α or 12-O-tetradecanoxylphorbol 13-acetate (TPA). Hydroxyurea is another agent which may induce a cytostatic effect by inhibiting cellular ribonucleotide reductase [79]. Another compound that possesses direct antiviral activity and is also capable of inducing apoptosis in activated $CD4^+$ T cells is mycophenolic acid (MPA) [19]. Both hydroxyurea and MPA have been investigated clinically for the treatment of AIDS. Selective cytotoxicity was also demonstrated in HIV-1 infected H9 T cells cultured in the presence of γ-glutamylcysteine ethyl ester (γ-GCE) [71]. The cytotoxic effects of γ-GCE were synergistically enhanced by the lentiviral lytic peptide I (LLP-I) of HIV-1 gp41 or the amphipathic peptide toxin, melliten. Selective killing of HIV – infected cells was also demonstrated in the chronically and productively HIV-1–infected 8E5 T cell line, which was shown to be preferentially susceptible to apoptotic cell death when cultured in the presence of hydroperoxides of arachidonic, linoleic and linolenic acids [109]. The uninfected parental cell line, A3.01, and its chronically HIV-infected but low viral antigen - producing derivative, 8E5L, were resistant to this cell killing.

Although currently none of these compounds have proved efficacious enough for clinical application, they may prove useful to eradicate HIV-1 reservoirs when used in combination or together with conventional HAART drugs. Moreover, these cytotoxic compounds serve as valuable tools in the study of novel host-cell targeted antiretroviral approaches. Their investigation also provides further insight into the mechanism of apoptotic cell death in HIV infection. Better understanding of the mechanisms involved in selective killing of HIV infected cells might form a basis for devising strategies to eliminate the viral reservoir.

Methodological Approach

Based on the aforementioned as well as previous demonstration of GLA-mediated selective killing of chronically HIV infected cells, we performed a comprehensive investigation of the mechanisms involved in GLA cytotoxicity. For this purpose, we chose the commonly used A3.01/8E5 model of chronic HIV infection for examination of specific induction of apoptosis by GLA and the biochemical pathways involved. This model consists of the parental uninfected CEM-derived cell line, A3.01, and its chronically and productively HIV-1-infected derivative, 8E5 *[14, 44, 45, 46]*.

The A3.01/8E5 model was picked over other models of chronic HIV infection because 8E5 cells are known to possess deficiencies in redox regulators *[109]* that are typical of HIV infected cells, which makes these cells well-suited to study GLA;. Moreover, similar to long-lived virus-producing cells in vivo, 8E5 cells are resistant to HIV-induced cytotoxicity, thus making it possible to delineate GLA-induced from virally induced cytotoxicity. However, the biggest limitation of the model derives from the fact that transformed T cell lines are physiologically different from non-transformed T lymphocytes that are targeted by HIV in vivo. To address the in vivo relevance of the model, we investigated the occurrence of similar GLA-induced cytotoxicity in freshly isolated $CD4^+$ cells of HAART-treated AIDS patients and HIV-seronegative donor $CD4^+$ cells acutely infected with laboratory or clinical isolates of HIV.

Pathways of Cell Death

There are two processes by which nucleated eukaryotic cells die, necrosis and apoptosis *[37, 69, 129]*. These processes derive from different stimuli, are mechanistically distinct and play disparate roles in cell functioning. Apoptosis is a well regulated physiologic process characterized by loss of membrane symmetry, cytoplasm condensation and internucleosomal cleavage of cellular DNA *[69]*. This leads to fragmentation of the dying cell into "apoptotic bodies". Necrosis, on the other hand, is largely a result of cell exposure to damaging substances and is characterized by swelling and rupture of the cell membrane. Unlike apoptosis, necrosis results in the release of cytoplasmic contents into the extracellular milieu, often with inflammatory consequences.

In addition to well-defined ultrastructural and morphological changes, apoptosis is also regulated by a series of molecular cascades that involve death receptors, death adapter domains, activation of cysteine proteases (caspases) and proteins of the Bcl-2 family. Activation of caspases is especially useful in characterizing apoptotic cell death and, depending

on the type of initiator-caspase (8 or 9) involved, identifying the specific pathway of apoptosis. There are two broad pathways of apoptosis (Summarized in **Figure 1**) *[105]*. The caspase-8 (also referred to as extrinsic) pathway involves ligand binding to death receptor complexes, e.g. CD95/Fas, and recruitment of initiator caspase-8 via adapter domains, e.g. FADD (Fas-associated death domain). The caspase-9 (or intrinsic) pathway depends on ratio of anti- and pro-apoptotic Bcl-2 family proteins, release of secondary mitochondria-derived activator of caspases (SMAC) and cytochrome C from the mitochondria. The latter enables interaction of apoptotic protease activating factor (APAF)-1 with caspase-9 [77]. In contrast to engagement of CD95 by ligand, this pathway is typical of apoptosis induced by cytotoxic substances [57, 72] and is more responsive to inhibition by the *bcl-2* family than is the CD95 route *[2]*. The two pathways converge at the level of effector or death executing caspases (caspase-3 and caspase-7) *[105]*.

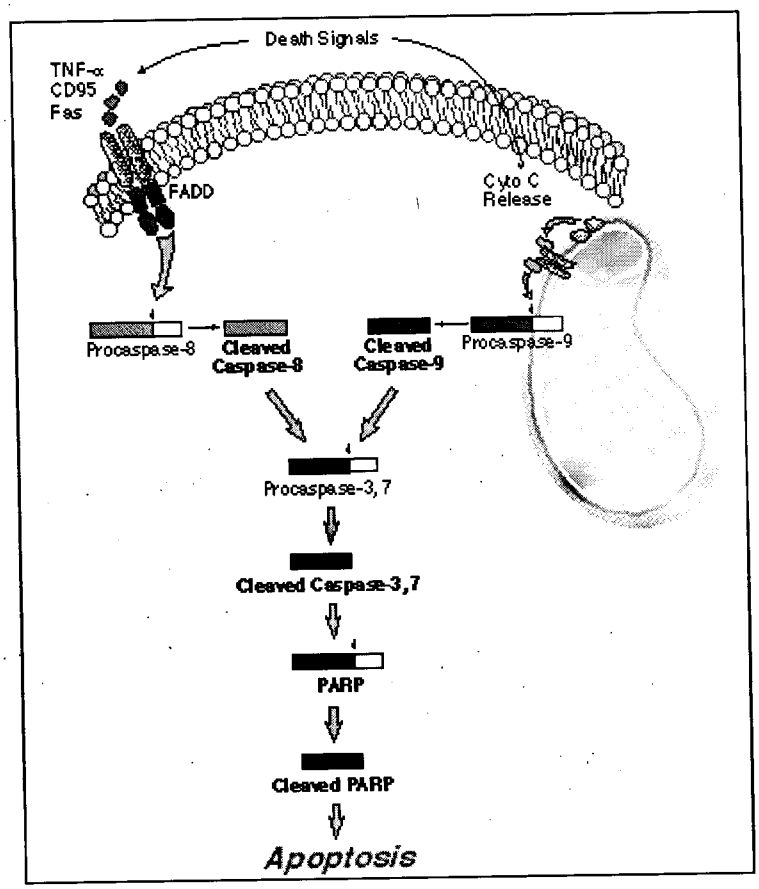

Figure 1: Apoptosis pathway: Death signals cleave and activate large prodomain caspases (caspase- 8 and 9), which in turn cleave and activate effector caspases (caspase- 3 and 7) [*Adopted from Apoptosis Sampler insert, Cell Signaling Technology, Beverly, MA*]

Activation-induced apoptosis of HIV-1-infected cells is largely mediated via the CD95/Fas pathway *[127]*. By contrast, ROS and lipid peroxides regulate activation-induced T cell apoptosis through a mechanism that involves loss of mitochondrial membrane potential, release of cytochrome C from mitochondria and is independent of Fas and tumor necrosis factor alpha (TNF-α) *[60, 81]*. Still, 4-hydroxynonenal (4-HNE), a diffusible aldehyde produced by lipid peroxidation and a key mediator of oxidative stress-induced cell death, does cause activation of both caspase-8 and caspase-9 *[78]*.

The data presented here show that GLA-induced cell death of chronically HIV-infected 8E5 cells is apoptotic and not necrotic, and, at the concentration tested, GLA cytotoxicity is specific to infected cells. We also demonstrate that induction of apoptosis in 8E5 cells occurs via a mechanism that involves cleavage of caspase-3 and poly (ADP-ribose) polymerase (PARP), as well as activation of caspase-9 and can be inhibited by a caspase inhibitor. Occurrence of apoptosis in 8E5 cells was also associated with arrest of cells in the G_0/G_1 phase of the cell life cycle. Evidence implicating a state of oxidative stress in GLA-induced cytotoxicity of 8E5 cells is shown but involvement of LOX rather than COX metabolism as a pathway that generates GLA-related apoptosis trigger molecules could not be confirmed. Finally, we provide preliminary data to show a correlation between GLA IC_{50}, as a measure of GLA cytotoxicity, and plasma HIV-1 mRNA copy number of HAART-treated AIDS patients.

Chapter 2

MATERIALS AND METHODS

Cell Culture Conditions

All cells were grown at 37°C in a humidified incubator containing 5% CO_2. Cell lines were maintained in growth medium--complete RPMI-1640 medium (Gibco BRL, ON, Canada or Burlington, CA) supplemented with 2mM L-glutamine, 10μM HEPES buffer, 10U/ml penicillin, 10 μg/ml streptomycin and 10% heat-inactivated fetal bovine serum (Gibco BRL, ON, Canada or Burlington, CA) except where indicated. Prior to virus adsorption during acute infection experiments, peripheral blood mononuclear cells (PBMC) or $CD8^+$ T cell-depleted mononuclear cells were grown for 72 hours in stimulation medium [growth medium supplemented with 1 μg/ml purified phytohemaglutinnin (PHA-P) (Sigma, St. Louis, MO), or 1 ng/ml PHA in the case of AIDS patient $CD8^+$ T cell-depleted mononuclear cells]. Mononuclear or $CD4^+$cell cultures were maintained in growth medium as described above but supplemented with 20 U/ml of recombinant IL-2 (AIDS Research and Reference Program, Division of AIDS, NIAID, NIH or Boehringer Mannheim Biochemica, Mannheim, Germany), except AIDS patient cells which were grown in medium supplemented with 50 U/ml IL-2.

T Cell Lines

The majority of experiments were performed on matched T lymphocytic cell lines comprised of A3.01 and 8E5 cells. These cell lines were obtained from Dr. Thomas Folks through the AIDS Research and Reference Program, Division of AIDS, NIAID, NIH. The initial batch of cell lines was kindly donated by Paul Sandstrom (Retrovirus Diseases Branch, Centers for Disease Control and Prevention, Atlanta, GA, USA).

The A3.01 cell line is a hypoxanthine-aminopterin-thymidine (HAT)-sensitive cloned derivative of the CEM line *[14, 46]*, which is sensitive to infection with HIV and is over 95% susceptible to the cytopathic effects induced by the virus. CEM is a continuous line of lymphoblastic cells isolated from the peripheral blood of a child suffering from acute leukemia

by the cultivation of buffy coats directly in suspension cultures [44]. The 8E5 cell line, a commonly used *in vitro* model of chronic and productive HIV infection, was established through limited dilution cloning of A3.01 cells surviving acute infection by the HIV-1_{LAI} isolate [45]. Each 8E5 cell carries a single copy of integrated HIV-1 genome with a frame shift mutation in the *pol* region—single base addition at position 3241--of the provirus reverse transcriptase (RT) gene [51, 98]. Likely, due to this mutation, 8E5 cells were previously observed to be incapable of expressing *pol* gene products and to produce viral particles that were replication defective [45]. However, later studies have demonstrated that 8E5 cells do produce infectious virus with reversion to wild type *pol* sequence and RT positivity [98]. In a few experiments, we used the 8E5L cell line, a spontaneous derivative of 8E5, which does not express HIV mRNA or proteins [108].

Isolation of $CD4^+$ T cells

Peripheral blood mononuclear cells (PBMC) were obtained from whole blood of HIV-seronegative donors or HAART-treated AIDS patients. The HIV+ patients used in this study were from the Wilford Hall Medical Center, Lackland AFB, Texas, and the voluntary, fully informed consent of the patients was obtained as required by Air Force Regulation 169-9. Blood collection was performed using institutional review board-approved protocols. Mononuclear cells were isolated by gradient sedimentation in Lymphocyte Separation Media (ICN, Aurora, OH). The buffy interface was collected and washed twice in PBS following which the number of viable cells was determined by their exclusion of Trypan Blue dye when observed under light microscope. Cells were then re-suspended in sorting buffer (PBS supplemented with 2% bovine serum albumin, 0.01% sodium azide and 2mM EDTA) at 10^7 cells/ml.

Subsequently, the PBMC suspension was enriched for $CD4^+$ T Cells by depletion of $CD8^+$ T cells using magnetic cell separation (MACS) with anti-CD8 immunoreactive microbeads (Miltenyi Biotec, Auburn, CA). Briefly, 20 µl of α-CD8-labeled magnetic microbeads were added to each ml of cell suspension and the mix incubated in the refrigerator for 15 minutes. Cells were washed once in sorting buffer and resuspended in 1 ml of buffer and run through a magnetic VS+ column (Miltenyi Biotec) assembled in a MACS separator, all done in accordance with manufacturer's instructions. The effluent was collected, cells washed in PBS and retained for further experimentation.

HIV-seronegative donor cells to be used in *de novo* infection experiments were stimulated by culturing in media supplemented with 1 μg/ml phytohemaglutinin (PHA) for 24-72 hours at 37°C in a humidified incubator, with 5% CO_2. Following stimulation, cells were centrifuged and pellets infected with virus stock for 2-4 hours at multiplicities of infection (M.O.I.) shown in figure legends. At the end of this incubation period, unadsorbed virus was removed by washing in cold phosphate buffered saline (PBS) and cells re-suspended in IL-2 -containing growth medium.

HIV-1 Isolates

For acute *de novo* infection experiments, we used the following laboratory adapted HIV-1 isolates obtained through the AIDS Research and Reference Reagent Program, Division of AIDS (DAIDS), National Institute of Allergy and Infectious Diseases (NIAID), National Institutes of Health (NIH): HIV-1 IIIB from Dr. Robert Gallo *[18, 96, 97, 99]* and HIV-1 RF NIH 1983 *[97, 119]*. We also tested HIV-1 NL4.3, which is a full length cloned infectious isolate of HIV-1 *[1]*. Two clinical, R5, non-syncytium-inducing HIV-1 isolates were tested: HIV-1 92US657 and HIV-1 92US714, both belonging to the HIV-1 envelope subtype B. The two isolates were obtained through the NIH AIDS Research and Reference Reagent Program. To generate virus stock, primary lymphocyte cultures were infected with specific virus isolates for seven to fourteen days during which supernatants were pooled and clarified. Virus titer in viral supernatants was determined using the NIH DAIDS protocol *[124]*. Briefly, seven serial four-fold dilutions of virus stock, ranging from 1:16 through 1:65,635, were used to infect three day old PHA-stimulated donor PBMC in a 96-well microculture plate. Infected cells were incubated at 37°C, 5% CO_2 in a humidified incubator for seven days, following which supernatants were tested for HIV p24 antigen concentration by ELISA. The 50% endpoint was determined by counting the number of wells scored positive (≥50 pg/ml HIV-1 p24 antigen) and those scored negative (<50 pg/ml HIV-1 p24 antigen). The cell culture infective dose 50% ($CCID_{50}$) was calculated using the Spearman-Karber formula, $M = xk + d\,[0.5 - (1/n)\,(\sum r)]$, where: xk = dose of highest dilution, r = number of "negative" responses, d = spacing between dilutions, n = wells per dilution, and $\sum r$ = sum of r.

Cytotoxicity Assay

The Trypan Blue dye exclusion and water-soluble tetrazolium (WST-1) bioassay techniques were used to determine proliferation of cells. Based on experimental protocol, cells were grown in 96-, 48-, 24- 6-well culture plates or T-25 tissue culture flasks. Cells were incubated for the prescribed length of time with or without the test compound as appropriate. Periodically, or at the end of the experiment, cultures were resuspended and an aliquot of the cell suspension taken for cell enumeration in Trypan Blue. Counting of cells was carried out in glass counting chambers (hemacytometers) under a light microscope. The 50% inhibitory concentration (IC_{50}) of GLA in test cell lines and $CD4^+$ T cells was obtained through sigmoidal fitting of the curve of cell proliferation data versus GLA concentration using the Boltzman equation in Microcal Origin™ data and graphics software (Northampton, MA).

The WST-1 assay (Roche Molecular Biochemicals, Mannheim, Germany) was performed as described previously [*64*], and according to manufacturer's recommendation. This assay is based on the ability of mitochondrial succinate tetrazolium reductase system in viable cells to reduce the slightly red colored tetrazolium salt [4-{3-(4-Iodophenyl)-2-(4-nitrophenyl)-2H-5-tetrazolio}-1,3-benzene disulphonate] or WST-1 to a dark red soluble product, formazan. The concentration of formazan in a test well depends on the number of actively metabolizing cells and is quantified using a scanning multi-well spectrophotometer (ELISA plate reader). To each test well of a 96-well microculture plate was added 10^5 cells in 200µl of phenol red - free RPMI growth medium containing appropriate concentration of test compound. Culture plates were incubated at 37°C for a specified period of time at the end of which 20µl of WST-1 Reagent were added to each test well and blank wells containing culture medium alone. Culture plates were then incubated for four hours after which absorbances were read at a measurement wavelength of 450nm and reference wavelength of 690nm in a Molecular Devices ThermoMax plate reader running SoftMax software for MS Windows.

Apoptosis Assay

Two different methodological approaches were utilized to assay for apoptosis in control and drug treated cultures:

Annexin V Staining

A commercial kit (Pharmingen, San Diego, CA) was used to measure apoptosis by Annexin V staining according to manufacturer's instructions. Cells were washed twice with cold PBS and

resuspended in single-strength binding buffer (0.1 M HEPES, pH 7.4; 1.4 M NaCl; 25 mM $CaCl_2$), at a concentration of ~1 x 10^6 cells/ml. A 100 µl aliquot of the cell suspension was transferred to a 5 ml polystyrene flow cytometry tube to which 5 µl of fluorescein isothiocyanate (FITC)-conjugated Annexin V and 2 µl of propidium iodide (PI) were added. Cells were gently mixed and incubated for 15 minutes at room temperature in the dark. At the end of the incubation, 400 µl of binding buffer was added to each tube and cells analyzed by flow cytometry within an hour.

Flow Cytometric TUNEL Assay for DNA Fragmentation

We also used the APO-BRDU™ and modified BrdU Flow™ (Pharmingen, San Diego, CA) methods to measure apoptosis. In the APO-BRDU™ kit, 2 x 10^6 cells of the sample were resuspended in 0.5 ml of PBS and added to 4.5 ml of a 1% (w/v) paraformaldehyde solution in PBS in 12 x 75 mm polystyrene flow cytometry tubes. After vortexing, tubes were incubated on ice for 15 minutes. Cells were pelleted and washed in PBS twice after which they were resuspended in 0.5 ml PBS and added to 4.5 ml of ice-cold 70% (v/v) ethyl alcohol. Cells were incubated at -20°C for at least 12 hours prior to staining for flow cytometric analysis. After incubation, ethyl alcohol was removed by centrifugation and aspiration of test sample tubes and those containing assay-kit control cells. Cells were washed twice using buffer provided in the kit and resuspended in 50 µl of a buffered DNA labeling solution containing terminal deoxynucleotidyltransferase (TdT) enzyme and bromolated deoxyuridine triphosphate (Br-dUTP). Cells were incubated for 60 minutes at 37°C in a water bath with continuous shaking. At the end of the incubation, cells were washed twice in rinse buffer and each pellet resuspended in 100 µl of a buffer solution containing Fluorescein-labeled anti-BrdU monoclonal antibody. Cells were incubated for 30 minutes in the dark at room temperature. Next, cells were resuspended in 0.5 ml of PI plus Ribonuclease A (RNase A) solution and incubated for 30 minutes at room temperature in the dark. Cells were analyzed the same day in PI/RNase A solution.

The BrdU Flow kit is designed to measure the frequency and nature of cells that have synthesized DNA. We modified the assay to measure extent of DNA cleavage in cells undergoing apoptosis and expression of intracellular antigen in these cells. Cells were fixed/permeabilized using the Cytofix/Cytoperm buffer contained in the kit, incubated for 15

minutes at room temperature and washed once with a buffer containing permeabilization agent (Perm/Wash) to keep membrane pores open. Subsequently, cells were incubated on ice in another permeabilization buffer (Cytoperm Plus) for 10 minutes and washed once in Perm/Wash buffer. To re-fix cells, each pellet was resuspended in 100 µl of Cytofix/Cytoperm buffer, incubated on ice for 5 minutes and washed once in Perm/Wash. At this point, cells were resuspended in DNA labeling solution prepared as described under the Apo-BrdU™ procedure above and incubated for 60 minutes at 37°C in a water bath. After incubation, cells were washed once with Perm/Wash buffer and resuspended with 50 µl of Perm/Wash buffer containing FITC-conjugated anti-BrdU monoclonal antibody and antibody specific for intracellular HIV-1 core antigen. Cells were washed and resuspended with 1 ml of staining buffer for analysis by flow cytometry.

Flow Cytometric Analysis

Samples were analyzed on a Becton Dickinson FACScan™ flow cytometer equipped with an argon laser using CELLQuest acquisition software. Analysis of listmode data was carried out using FCS Express software (De Novo Software, Thornhill, ON, Canada).

Isolation of total RNA

Total RNA for ribonuclease protection assay (RPA) was isolated using TRIzol® reagent (Life Technologies) according to recommended protocol. Briefly, approximately 10 million cells were lysed in 1 ml of TRIzol reagent by repetitive pipetting. This was followed by incubation of homogenized samples for five minutes at room temperature to permit complete dissociation of nucleoprotein complexes. To the homogenate, 0.2 ml of chloroform was added and tubes shaken vigorously by hand for 15 seconds. Samples were incubated for three minutes at room temperature followed by centrifugation at 12,000 X g for 10 minutes at 4°C in a refrigerated tabletop microcentrifuge. The upper aqueous phase was separated from the phenol-chloroform phase and transferred to a fresh Eppendorf tube. The RNA in each tube was precipitated from the aqueous phase by mixing with 0.5 ml of ice-cold isopropyl alcohol. Samples were incubated at room temperature for 10 minutes and the RNA precipitate spun down at 12,000 X g for 15 minutes at 4°C. The supernatant was discarded and the pellet washed once by adding 1 ml of 75% ethyl alcohol to each tube, vortexing the tubes and centrifuging at 12,000 X g for 10 minutes at 4°C. Pellets were air-dried briefly and the RNA

redissolved in 20 µl of RNase-free water. The concentration of RNA in each sample was determined spectrophotometrically.

Biotin or [^{32}P] Labeling of RNA Probes

Anti-sense RNA multi-probe template sets (Pharmingen, San Diego, CA) were biotin-labeled using the BioArray™ HighYield™ RNA transcript labeling kit (Enzo Diagnostics, Farmingdale, NY). Briefly, template DNA was mixed with biotin labeled ribonucleotides, DTT, RNase inhibitor mix, T7 RNA polymerase, reaction buffer and deionized water in an RNase-free microfuge tube. Tubes were vortexed, centrifuged briefly and incubated in a 37°C water bath for 4 hours. After incubation, to each tube was added 1 µl of DNase I and the tubes incubated for 15 minutes at 37°C. Transcripts were purified using the TE MIDI SELECT®-D G-50 microcentrifuge spin columns (Eppendorf-5 Prime, Boulder, CO). The columns were inverted several times to resuspend the gel and then placed in the collection tubes, securely capped and centrifuged at maximum speed in the microcentrifuge for two minutes. Collection tubes were discarded and columns placed in new collection tubes. A 50 µl sample of biotin-labeled transcript was added to the surface of gel bed in each column and caps secured. The loaded columns were allowed to sit undisturbed for 3 minutes, then the column/collection tube assembly placed in the centrifuge and spun at maximum speed for 90 seconds. Labeled probes were recovered in collection tubes, aliquoted in small volumes and stored at -80°C until ready for use. Alternatively, multi-probe template sets were used for in vitro transcription reactions using T7 polymerase to direct synthesis of high specific activity [^{32}P]-labeled antisense RNA. Templates were transcribed using a Maxiscript kit (Ambion, Austin, TX) in the presence of a ^{32}P-UTP (800 Ci/mmol, NEN, Beverly, MA) and further purified as described above.

Ribonuclease Protection Assay

This assay was performed using the standard hybridization procedure of the RPA III™ kit (Ambion, Austin, TX). Briefly, 10 µg of sample RNA was mixed with labeled probe in RNase-free 1.5 ml microfuge tube. The optimal amount of probe to be added was pre-determined by running a gel electrophoresis of probe at several dilutions and selecting a concentration showing optimal resolution. For each probe used, two control tubes containing the same amount of labeled probe used for the experimental tubes plus Yeast RNA equivalent to the

highest amount of sample RNA were included. The probes and sample RNA were co-precipitated by adjusting the concentration of ammonium acetate (NH_4OAc) in the reaction mix to 0.5 M using the 5 M NH_4OAc solution supplied with the kit and adding 2.5 volumes of 75% ethyl alcohol. Tubes were placed at -20°C overnight. RNA was pelleted by centrifuging tubes at maximum speed in a microcentrifuge for 15 minutes at 4°C. The ethyl alcohol was removed and pellets left on the bench to air-dry for about five minutes following which they were resuspended in 10 µl of hybridization buffer. Tubes were vortexed for a few seconds and spun briefly to collect liquid at the bottom. To denature and solubilize the RNA, samples were incubated at 95°C for four minutes. Tubes were vortexed, centrifuged briefly and incubated overnight at 42°C to hybridize probes to their complement in sample RNA. After hybridization, 150 µl of RNase A/RNase T1 mixture diluted 1:50 in RNase digestion buffer was added to each sample tube and one of the two Yeast RNA controls. To the second Yeast RNA control tube was added 150 µl of RNase digestion buffer. Tubes were incubated at 37°C for 30 minutes to digest unprotected single-stranded RNA. After this incubation, 225 µl of RNase inactivation/precipitation solution was added to each tube followed by 2 µl of yeast RNA to increase the size and visibility of final pellets. To each tube was also added 100 µl of ethanol to improve precipitation of RNA. Samples were then incubated at -20°C for 15 minutes and then microcentrifuged for 15 minutes at top speed at 4°C. Supernatant was removed and discarded, pellets air-dried and resuspended in gel loading buffer--diluted 1:1 in water--ready for electrophoresis.

Gel Electrophoresis of Ribonuclease Protected Probes

Electrophoretic separation of hybridized samples (biotin-labeled) was carried out using the NOVEX™ QuickPoint™ rapid nucleic acid separation system, which consists of pre-cast mini-gels, buffers and electrophoresis cell. Samples diluted in loading buffer were heated at 95°C for 3 minutes, microfuged briefly and placed on ice until ready to load. The electrophoresis cell and mini-gel were assembled and the 5X and 1X running buffers added to the upper and lower chambers of the apparatus, respectively, according to manufacturer's instructions. The gel was pre-run at 250 volts for at least 15 minutes before sample loading. 1 µl of each sample was loaded into the corresponding well. The gels were run at 250 volts for

approximately 2.5 hours. At the end of the run, the apparatus was disassembled and the pre-cast gel glass cassette pried open to remove the top glass plate and expose the gel. The gel was transferred to a positively-charged nylon membrane by electroblotting as follows: a piece of BrightStar-Plus™ nylon membrane (Ambion, Austin, TX) was cut to roughly the same dimensions of the gel, wetted in methanol and washed in molecular grade water. The glass slab carrying the gel was placed on a flat surface and the wet membrane carefully placed on top of the gel. Two pieces of thick filter paper of similar size were stacked on top of the membrane and a weighted flask laid on top of the stack. The transfer was carried out overnight. Alternatively, protected fragments of radiolabeled samples were precipitated and electrophoresed on a 6% sequencing gel.

Detection of Ribonuclease Protected Probes

Biotin-labeled probes hybridized with RNA were detected nonisotopically using the Brightstar™ BioDetect™ system for chemiluminescent detection of biotinylated RNA probes. An ultra-violet (UV) automatic crosslinker, which delivers 120 milliJoules over 30 seconds was used to immobilize RNA on the membrane. The membrane was washed twice in wash buffer followed by three washes in blocking buffer. Subsequently, the membrane was washed for 30 minutes in wash buffer containing Streptavidine-Alkaline Phosphatase conjugate at a 1:10,000 dilution in blocking buffer. Afterwards the membrane was washed for 10 minutes in blocking buffer, followed by three five minute washes in wash buffer and two 2 minute washes in assay buffer. Finally, the membrane was washed for five minutes in the CDP-Star™ reagent, which provides a substrate for alkaline-phosphatase. At the end of the five-minute wash, excess CDP-Star solution was shaken off and the membrane wrapped in cling-wrap. Imaging of the membrane was carried out on a NucleoVision desktop imaging system using GelExpert image acquisition and processing software (Nucleotech, Hayward, CA). On the other hand, gels of radiolabeled samples were dried and scanned on a phosphorimager (Molecular Dynamics, Palo Alto, CA). Dried gels were also photographed on XAR-5 film at -70°C.

Western Blot Analysis of Apoptosis-related Cellular Factors

8E5 cells incubated with GLA and anti-Fas antibody with or without inhibitor were collected by gentle centrifugation and washed with cold PBS. Pelleted cells were placed on ice and resuspended in lysis buffer (100 mM NaCl, 50 mM Tris, pH 7.4, 1 mM EDTA, 1% Tween-20)

containing 1% phenylmethylsulfonyl fluoride (PMSF). Lysates were left on a mechanical rocker for 30 minutes and then centrifuged at 16,000 X g. Supernatants were transferred to fresh tubes and frozen at -80°C until further processing. Before analysis, the lysates were thawed at 37°C in a water bath and checked for protein concentration using the microwell plate protocol of a commercial bicinchoninic acid (BCA) protein assay kit (Pierce, Rockford, IL). Briefly, serial dilutions (0.011 – 1.410 mg/ml) of freshly diluted BSA protein standards were prepared in PBS as per kit instructions. The BCA working reagent was prepared by mixing 50 parts of reagent A (sodium carbonate, sodium bicarbonate, BCA detection reagent and sodium tartrate in 0.1M sodium hydroxide) with one part of 4% copper sulphate pentahydrate ($CuSO_4 \cdot 5H_2O$). To 25 µl of each standard, sample or PBS (blank) in a microwell was added 200 µl of the BCA working reagent and the plates mixed for 30 seconds. The plate was covered and incubated at 37°C for 30 minutes following which they were cooled and the absorbance measured at 562 nm on a plate reader subtracting the average blank readings from those of standards and samples. The standard curve was generated by plotting the average blank-protected mean optical density for each standard against the logarithm of its concentration in mg/ml. The protein concentration for each sample was determined using the standard curve. 120 µg protein per sample lysates was transferred to an Eppendorf tube and mixed with appropriate amount of reducing agent (Novex) and sample loading buffer. The samples were heated at 70°C for 10 minutes, spun briefly and subjected to SDS-PAGE in a 10-well, 1mm, 4-12% BT gel (Novex, San Diego, CA), with 360 mA/6 gels/3 boxes, at room temperature for one hour. Multicolor molecular weight markers were included and an antibody against β-actin (Sigma) was used as a control for protein input. Gels were electrophoretically transferred to a Millipore polyvinylidene difluoride (PVDF) membrane (0.45 µm pore size) in a Novex transfer buffer with 10% methanol at 480 mA/6 membranes/3 boxes, room temperature for three hours. Membranes were blocked in 100 ml of I-Block (PBS with 0.1% Tween 20 and 0.2% I-Block) on the rocker for at least 4 hours at 4°C then washed three times with 100 ml 0.1% Tween 20 in PBS for 10 minutes at room temperature. Next, membranes were stained with primary antibody diluted in I-Block at 4°C, overnight, then washed in I-Block as previously described and stained with appropriate second antibody at room temperature for two hours. Following another wash step, membranes were incubated at room

temperature for three minutes with ECL substrate (Amersham). Excess substrate was drained off membranes using paper towel; membranes were then wrapped in plastic wrap and exposed to X-ray film.

Colorimetric Assay for Lipid Peroxidation

As a measure of lipid peroxidation in test cells, levels of lipid peroxide metabolites of polyunsaturated fatty acid breakdown, namely malondialdehyde (MDA) and the hydroxyalkenal 4-hydroxy-2(E)-nonenal (4-HNE), were determined using a colorimetric assay (Oxford Biomedical Research, Oxford, MI). 2×10^6 cells were lysed by repetitive freezing/thawing in distilled water containing Triton X-100 to inactivate the virus and 5 mM butylated hydroxytoluene (BHT). After lysis, samples were clarified by centrifugation at 15,000 X g for 10 minutes. 200 µl of sample supernatant was added to 650 µl of a 10.3 mM acetonitrile solution of N-methyl-2-phenylindole (R1 solution) diluted in a 1:3 volume of methanol in a glass test tube. The mixture was vortexed for a few seconds. To assay both MDA and 4-HNE simultaneously, 10 µl of 0.5 M BHT and 150 µl of a 15.4 M methanesulfonic acid solution (R2 solution) was added to the sample solution. Tubes were stoppered tightly and incubated at 45°C for 40 minutes. At the end of the incubation, samples were cooled on ice and the absorbance measured at 586 nm in a Beckman DU650 spectrophotometer using 1 ml cuvettes with 1 cm optical path length.

To generate standard curves for interpolation of MDA and 4-HNE concentrations in test samples, standard serial dilutions of the two compounds were prepared and their absorbances read as described above. Solutions of 10 mM 4-hydroxynonenal as the diethylacetal in acetonitrile (S1) and 10 mM 1,1,3,3-tetramethoxypropane in 20 mM Tris-HCl buffer, pH 7.4 (S2), were diluted in 650 µl of R1. Increasing volumes of S1 or S2 and decreasing volumes of water were added to each of six consecutive tubes to obtain final concentrations of either S1 or S2 of 0, 2.5, 5, 10, 15 and 20 µM. After mixing, 150 µl of R2 or 37% HCl—for MDA—and 150 µl of R2—for 4-HNE—were added to each tube and the contents mixed well. Tubes were closed tightly and incubated at 45°C for 60 minutes for MDA, and at 45°C for 40 minutes in the case of 4-HNE. After incubation, tubes were cooled on ice and absorbance determined spetrophotometrically at 586 nm. A least-squares linear regression analysis of blanked standard solution absorbance values ($A-A_0$) against final enaldehyde concentration

conformed to linear functionality. The apparent molar extinction coefficient (ε) of the measured product was defined in this assay to be equal to the slope of the straight line generated from the plot of ($A-A_0$) versus MDA or 4-HNE standard concentrations. Finally, concentration of the two enaldehydes in test samples was obtained from the following equation:

[MDA + 4-hydroxyalkenals (HNE)] = $(A-A_0) \times 5/\varepsilon$

where, A = Absorbance in the presence of sample, A_0 = Absorbance in the absence of sample or blank, 5 = Sample dilution factor in the cuvette (200 µl of sample in total volume of 1 ml), and ε = Apparent molar extinction coefficient.

Chapter 3

RESULTS

The productively and chronically HIV-1 infected cell line 8E5 is three times more sensitive to GLA – induced cytotoxicity than the parental uninfected A3.01 cell line

It has been demonstrated previously that GLA causes selective cytotoxicity in certain HIV-1-infected cells relative to uninfected controls. In one study *[70]*, GLA was shown to cause a higher rate of cell death in the chronically HIV-1-infected $H9_{HTLV\text{-}IIIRF}$ cells than in the parental uninfected H9 cells. In order to study the mechanism by which GLA induces selective cytotoxicity, we chose a different model system previously used in our laboratory. The chosen model consists of the parental uninfected cell line – A3.01, and its derivative cell line – 8E5, which is chronically and productively HIV infected.

First, we determined the pattern of GLA toxicity in these cell lines in order to validate the model system. To do this, cells were cultured in growth medium supplemented with increasing concentrations of GLA and their viability was measured using Trypan Blue dye exclusion and WST-1 methods, as described under Materials and Methods. These two methods were selected because of their different mechanisms for evaluating cell viability as outlined earlier. Using these assays, the chronically HIV-1 infected 8E5 cell line was observed to be at least three-fold more sensitive to GLA-induced cytotoxicity than its uninfected parental cell line (**Fig. 1**). The concentration causing 50 percent inhibition of cell growth (inhibitory concentration 50% or IC_{50}) in each cell line was calculated using Microcal™ Origin software (Northampton, MA) by means of sigmoidal (Boltzmann) linear curve fit to GLA concentration versus cell viability (% viable cells relative to untreated control) data, with weight given by error bars (standard deviation from the mean). Using data generated by the Trypan Blue dye exclusion assay, the IC_{50} values in the A3.01 and 8E5 cell lines were calculated at 39.6 ± 3.1 μg/ml and 13.8 ± 0.5 μg/ml, respectively. When viability was measured using the WST-1 assay, the respective IC_{50} values for A3.01 and 8E5 were 47.1 ± 1.1 and 15.1 ± 2.2 μg/ml.

Cytotoxicity of GLA in A3.01 and 8E5 cells

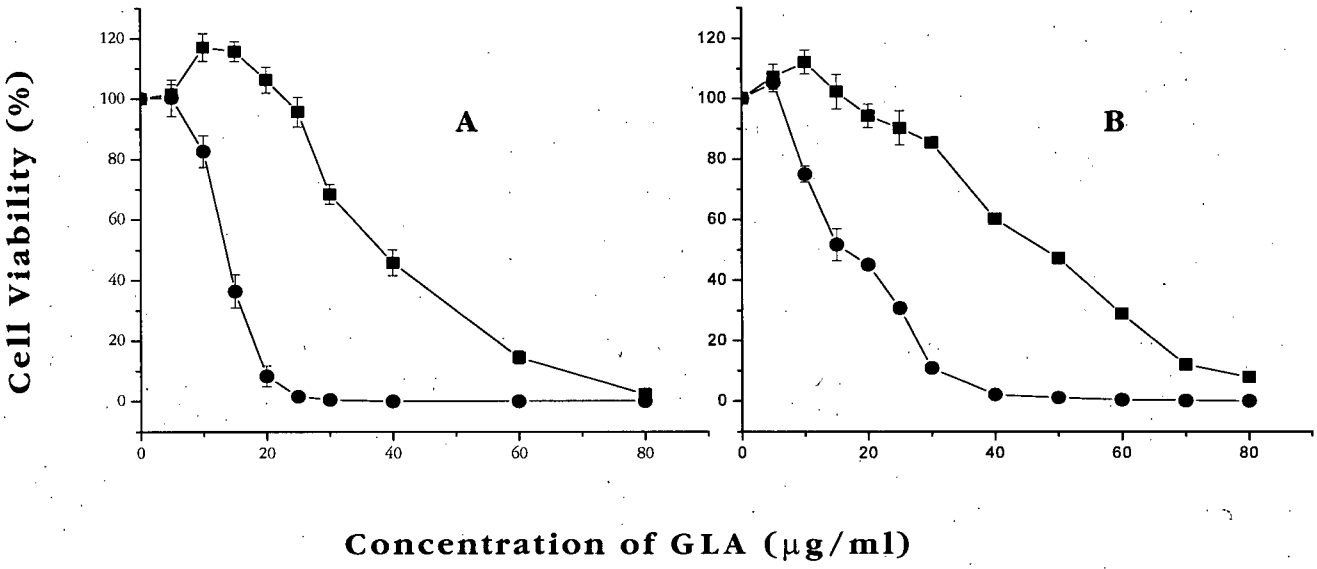

Figure 2: The effect of GLA on viability of A3.01 (HIV-) (■) and 8E5 (HIV+) (●) cell lines was determined by means of Trypan Blue dye exclusion assay (**A**) and WST-1 assay (**B**) as described in Materials and Methods. Cells were incubated, with or without drug, for 72 hours at 37°C. Cell proliferation was determined by counting cells (A) or measuring the absorbance of each well at 450 nm (650 nm reference) wavelength (B) and using the cell counts and absorbance readings to calculate the percentage of viable cells in each GLA-treated well relative to untreated controls and plotted as above. Each point on both graphs represents an average of triplicate measurements from two independent experiments. The concentration of GLA resulting in 50% inhibition of cell proliferation (IC_{50}) was calculated by means of a sigmoidal (Boltzmann) fit of plotted curves to yield a GLA IC_{50} of 39.6 ± 3.1 μg/ml for A3.01 and 13.8 ± 0.5 μg/ml for 8E5, when using dye exclusion data. When calculation was based on WST-1 assay data, the IC_{50} of GLA in A3.01 cultures was found to be 47.1 ± 1.1 μg/ml and 15.1 ± 2.2 μg/ml for 8E5 cultures.

Lack of distinctive modulation of GLA-induced cytotoxicity by inhibitors of lipoxygenase versus cyclooxygenase pathways of PUFA metabolism

The selective induction of cytotoxicity in virally infected cells by GLA may be the result of altered oxidative metabolism, which leads to accumulation of reactive oxygen species (ROS). Two major pathways of PUFA metabolism involve, respectively, lipoxygenase (LOX) and cyclooxygenase (COX) enzymes as summarized earlier, and generation of ROS is mainly a consequence of LOX activity. Under conditions of cellular oxidative metabolism impairment, the LOX pathway may lead to elevation of oxidative stress through generation of lipid free radical intermediates such as hydroperoxyeicosatetraenoic (HpETE) acids, which have been shown to induce apoptosis in virus-infected cells *[109]*. Mammalian LOX enzymes are divided into four subtypes according to tissue distribution: 5-, 8-, 12-, and 15-LOX *[30]*. LOX enzymes and their metabolic products play a complex regulatory role in cell survival and death *[120]*, promoting proliferation or apoptosis depending on cell type and/or biochemical environment.

Effect of LOX inhibition on GLA cytotoxicity

The role of LOX enzymes in T cell metabolism is a subject of intensive study. There is a preponderance of evidence suggesting that LOX-associated eicosanoids play an important role in T cell proliferation *[94]*. It was reasoned that inhibition of the LOX pathway and interference with GLA metabolism should modulate GLA cytotoxicity in these cells and shed light on its mechanism of cytotoxicity. Several inhibitors of LOX have been described, and one of these - nordihydroguaiaretic acid (NDGA) was picked for experimentation based on its broad-spectrum LOX inhibitory activity *[94, 31]*. NDGA possess concentration-specific selectivity for LOX enzymes, inhibiting 5-, 12- and 15-LOX with an IC_{50} of 0.2, 30 and 30 μM, respectively. To determine a possible role for the LOX pathway in GLA induced cytotoxicity, we examined the ability of NDGA to block GLA induced cytotoxicity. A concentration of 15 μg/ml GLA was selected for further experimentation because it represented the IC_{50} of GLA in the 8E5 cell line as discussed in susceptibility experiments above. Results of LOX inhibition experiments are summarized in **Fig. 3**, panel **A**. In cultures of 8E5 cells not treated with GLA, inhibition of LOX by NDGA (1.25-20 μM) resulted in a 27-95% increase in 8E5 cell viability but higher concentrations of NDGA were inhibitory.

Effect of inhibitors of lipoxygenase and cyclooxygenase enzymes on GLA-induced cytotoxicity in 8E5 cells

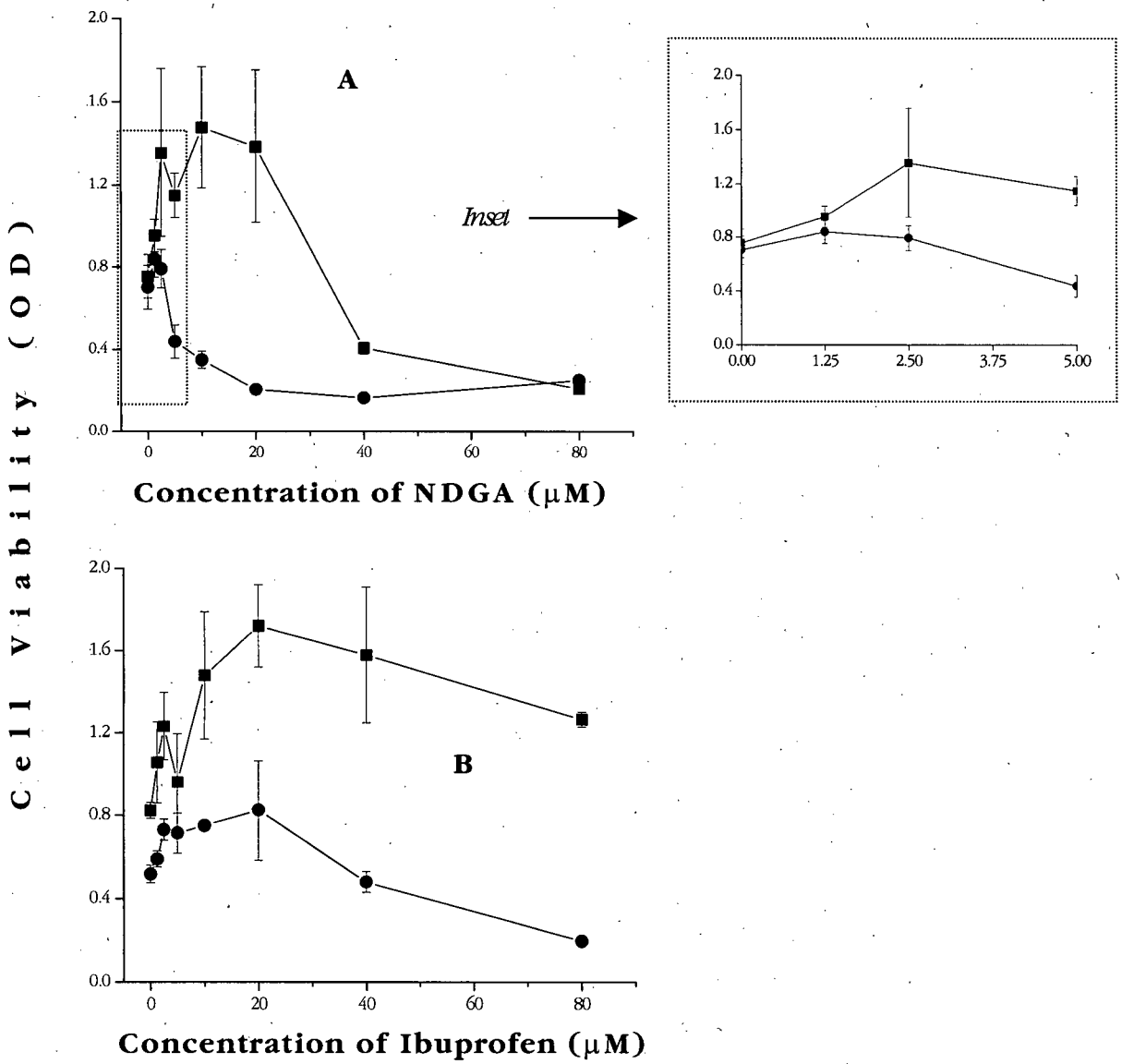

Figure 3: Cytotoxicity assay of 8E5 cells exposed to 0 μg/ml GLA (■) or 15 μg/ml GLA (●) in the presence of increasing concentration of the nonspecific lipoxygenase inhibitor nordihydroguaiaretic acid (NDGA) (**A**) or the cyclooxygenase inhibitor ibuprofen (**B**). Exponentially growing cells were added to wells of a 96-well plate containing quadruplet concentrations of either inhibitor and preincubated at 37°C for at least four hours followed by addition of GLA. Cultures were grown for 72 hours and subjected to WST-1 proliferation assay described in detail under Materials and Methods. Each point on the graph represents four measurements from two independent experiments.

At 40 and 80 μM NDGA, 8E5 cell viability was reduced to 54.6% and 28.1%, respectively. By contrast, 1.25 μM and 2.5 μM NDGA caused a 20.3% and 13.0% reduction of GLA-induced cytotoxicity, respectively, in 8E5 cultures treated with 15 μg/ml GLA (Fig. 3, panel A inset). Addition of GLA to 8E5 cultures pretreated with higher concentrations of NDGA (5-80 μM) resulted in a dose-dependent reduction of 8E5 cell viability. When the viability data were analyzed by One-Way ANOVA at the 0.05 significance level, there was a statistically significant difference between the means of cell viability data between cultures treated with NDGA alone or NDGA + GLA ($p = 0.02$). In summary, addition of 15 μg/ml GLA to cultures preincubated with non-cytotoxic concentrations (5-20 μM) of NDGA results in higher toxicity than seen with GLA alone. Interpretation of these results in the context of LOX inhibition is confounded by the possible existence of multiple forms of LOX enzyme in 8E5 cells and their complex interaction with NDGA as discussed earlier. It is possible that one or more forms of LOX mediate GLA cytotoxicity in 8E5 cells. Based on previous reports, only 5-LOX is inhibited by NDGA at concentrations of 2 μM or less. Conceivably, inhibition of 5-LOX or other forms of LOX shunts more GLA to alternative metabolic pathways, e.g. 15-LOX, leading to increased GLA toxicity as was observed in these experiments. Alternatively, it is possible that GLA toxicity is mediated via the COX pathway and therefore inhibition of LOX potentiates GLA cytotoxicity.

Similar to LOX and its products, COX and its metabolic products have also been shown to modulate cell survival and apoptosis, especially of tumor cells *[120]*. Some COX metabolites, notably prostaglandins E_1 and E_2, have suppressive effects on the interleukin 2-driven proliferative phase that follows T cell activation *[110]*. The COX pathway can be inhibited by non-steroidal anti-inflammatory drugs such as indomethacin, ibuprofen and acetyl salicylic acid.

Effect of COX inhibition on GLA cytotoxicity

To address the possible involvement of COX metabolism in mediating GLA cytotoxicity, we examined the profile of 8E5 cell viability in cultures exposed to both GLA and the COX inhibitor Ibuprofen. In the absence of GLA, we observed a concentration-dependent increase in viability of 8E5 cells preincubated with 0-20 μM Ibuprofen, reaching a maximum of 110% above that of control at 20 μM Ibuprofen. There was a relative decline in viability of 8E5 cells

above this concentration of Ibuprofen (up to 80 μM), but viability remained higher at all concentrations in comparison to untreated control (**panel B**, **Fig. 3**). A similar trend was observed in cultures incubated with a combination of Ibuprofen and GLA - peaking at 59.2% increase in cultures treated with 20 μM Ibuprofen - but One-Way ANOVA revealed a statistically significant difference ($p < 0.0001$) between the means of viability data between cultures treated with Ibuprofen alone or Ibuprofen + GLA.

In the past, COX (and LOX) inhibitors have been shown to inhibit the DNA synthesis and proliferation of, among many cell types, several human lymphocytic cell lines such as HL-60, K562 and KG-1 *[120]* and also to trigger apoptosis of cultured cells. Recent studies seem to suggest that these disparate effects of LOX and COX are probably mediated through separate mechanisms than those of PUFA metabolism. Thus, it is difficult to offer a conclusive interpretation of the role of LOX or COX inhibitors on GLA induced cytotoxicity.

GLA selective cytotoxicity in chronically HIV-infected cells is associated with elevated lipid peroxidation

Despite the inconclusive nature of LOX and COX inhibition experiments, several reports dealing with GLA activity in malignant and transformed cells have demonstrated an association of GLA cytotoxicity (and that of other PUFA) with an increase in lipid peroxidation and free radical generation *[126, 39]*. There are also numerous reports in the literature linking abnormal oxidative metabolism and elevated oxidative stress in individuals infected with HIV *[Reviewed in 83]*. A higher state of oxidative stress was also the hypothesized mechanism of GLA selective cytotoxicity in HIV-1_{RF}-infected H9 cells *[70]*.

Therefore, we next determined the extent of lipid peroxidation in relation to GLA cytotoxicity. To measure the level of lipid peroxidation in A3.01 and 8E5 cells treated with GLA, the products of PUFA breakdown, which include malondialdehyde (MDA) and 4-hydroxy-2(E)-nonenal (4-HNE), were measured colorimetrically. Untreated control and GLA treated cells were assayed for concentration of MDA and 4-HNE using a protocol based on the reaction of N-methyl-2-phenylindole with MDA and 4-HNE to yield a chromophore, which shows maximal absorbance at 586 nm. From cultures of A3.01 and 8E5 cells grown with or without 15 μg/ml GLA for 72 hours, two million cells were lysed and incubated as described under Materials and Methods. Absorbance was measured spectrophotometrically and concentration

of MDA/4-HNE in test samples was calculated from the standard curve. Results of the lipid peroxidation assay are summarized in **Table 1** below:

	Concentration of MDA + 4-HNE (μM)
A3.01 Control	2.3 ± 0.2
A3.01 + GLA	2. 7 ± 0.2
8E5 Control	2.1 ± 0.2
8E5 + GLA	7.9 ± 0.6

Table 1: Effect of GLA on lipid peroxidation in A3.01 and 8E5 cells. The concentration of malonaldehyde (MDA) and 4-hydroxy-2(E)-nonenal (4-HNE) in A3.01 and 8E5 cells cultured with 0 or 15 μg/ml GLA was assayed using a lipid peroxidation colorimetric assay (Oxford Biomedical Research) as described in Materials and Methods.

The concentration of MDA + 4-HNE remained virtually unchanged between untreated and GLA treated A3.01 cells at 2.258 μM and 2.67 μM, respectively, confirming that even after GLA treatment A3.01 cells do not acquire increased oxidative stress. By contrast, treating 8E5 cells with GLA resulted in a four-fold (2.094 μM to 7.870 μM) increase in the concentration of MDA/4-HNE, an indication of GLA-induced elevation in oxidative stress in these cells. There was no difference in MDA/4-HNE concentration between lysates of control untreated cells of either A3.01 or 8E5: 2.258 μM in A3.01 cells as opposed to 2.094 μM in 8E5 cells. Thus, there does not seem to be a pre-existing state of oxidative stress in 8E5 cells. If GLA-induced cytotoxicity in 8E5 cells is a consequence of oxidative stress, then it is likely due to an inability of these cells to overcome GLA-induced oxidative stress rather than exacerbation of pre-existing stress.

Effect of Antioxidants on GLA cytotoxicity

In order to probe the role of oxidative stress in mediation of GLA toxicity in 8E5 cells, we next attempted to inhibit GLA effects by pre-incubating cells with known antioxidants and modulators of oxidative stress. The compounds tested included the non-enzymatic free radical scavenger α-tocopherol (Vitamin E) (Sigma, St. Louis, MO) and the antioxidant enzyme superoxide dismutase (SOD) (Sigma-Aldrich, St. Louis, MO). Similar to most HIV-infected cells, 8E5 cells have been reported to have a deficiency in glutathione (GSH) peroxidase (GPx) and catalase enzymes *[108, 109]*. These enzymes act in tandem to detoxify PUFA-derived and other oxygen free radicals and thus protect the cell from ROS-induced toxicity. Therefore, we tested the capacity of Ebselen [2-phenyl-1,2-benzisoselenazol-3(2H)-one] (Sigma-Aldrich, St. Louis, MO), a seleno-organic compound with GPx-like activity, to inhibit GLA cytotoxicity in 8E5 cells. Also tested were the thiol reducing agent, 2-mercaptoethanol (2-ME) (Sigma, St. Louis, MO), and N-acetyl cysteine (NAC) (Sigma, St. Louis, MO).

Viability of cells in cultures of test cell lines exposed to increasing concentration of these antioxidants in the presence of GLA was determined by means of the WST-1 method described in Materials and Methods. Results are shown in **Fig. 4**. Each histogram represents the average of five separate measurements (n = 5).

The most effective protection of 8E5 cells against GLA-induced cytotoxicity was achieved by supplementing culture media with 2-ME (**Fig. 4, panel A**). As expected, treating cultures with GLA reduced the viability of 8E5 cells by 50% compared to untreated control cultures. This difference was statistically significant ($p < 0.001$). Supplementation of cultures with 2-ME (5, 10 or 20 μM), however, inhibited GLA induced reduction of 8E5 viability. The growth of 8E5 cells in 2-ME supplemented cultures was not statistically different from that of control untreated cultures, $p = 0.7$, 0.8 and 0.9 at 5, 10 and 10 μM 2-ME, respectively. The protective effect of 2-ME is strong evidence that a deficiency of thiol reducing molecules predisposes 8E5 cells to GLA cytotoxicity. 2-ME is a known enhancer of cysteine uptake, which increases intracellular GSH levels. GSH is a key cellular antioxidant.

Further evidence of GSH and/or GPx impairment role in GLA cytotoxicity was provided by inhibition experiments using the GPx mimic, Ebselen (**panel E, Fig. 4**). In the absence of GLA, the viability of 8E5 cells in cultures supplemented with 5, 10 or 20 μM Ebselen was

approximately 59%, 164% and 177%, respectively, with respect to the untreated control. Cultures treated with 15 μg/ml GLA had 45% viability compared to untreated cultures. Supplementation of GLA-treated cultures with 5 or 10 μM Ebselen, increased viability to 77% and 123%, respectively, relative to the GLA-untreated control. The increase was statistically significant, $p < 0.01$, in both instances. However, cultures exposed to 20 μM Ebselen and GLA had viability of 41% relative to untreated control cultures, even though cells treated with inhibitor alone had a higher viability (177%) than control cultures. Ebselen might be less effective than 2-ME at preventing GLA cytotoxicity because of its dependence on normal cellular levels of catalase and GSH to exert its antioxidant effects. However, it is difficult to explain the low viability observed at 20 μM Ebselen. One possibility is the involvement of non-GPx effects at high concentrations, such as induction of TNF-α *[63, 112]*. Nonetheless, there was not a statistically significant ($p = 0.59$) difference between viability of cells in cultures treated with GLA alone or GLA + Ebselen (20 μM), suggesting that the two compounds did not have additive cytotoxicity under these conditions.

In contrast to 2-ME and Ebselen, which act primarily on the GPx pathway to modulate hydroperoxide metabolism, the antioxidant scavenger α-tocopherol (Vitamin E) did not protect 8E5 cells against GLA-induced cytotoxicity (**panel B**, **Fig. 4**). This might be related to the inability of 8E5 cells to recycle oxidized vitamin E to its reduced form due to impaired expression of GSH. Relative cell proliferation in all GLA-treated cultures was approximately 40% regardless of vitamin E concentration used (0-20 μM). Likewise, our test of SOD (0-40 U/ml) revealed that this enzyme did not influence proliferation of 8E5 cells, whether GLA treated or not (**panel D**). Proliferation of cells in cultures not treated with GLA was the same as that of control while that of GLA-treated cultures remained at approximately 45% at all concentrations of SOD, relative to untreated control. SOD has a crucial role in reduction of superoxide radicals (especially the superoxide anion, $O_2^{\bullet-}$) to H_2O_2, which is in turn converted to water by catalase enzyme. The deficiency of catalase enzyme in 8E5 cells may explain why SOD did not protect these cells against GLA toxicity.

Effect of antioxidants on GLA-induced cytotoxicity in 8E5 cells

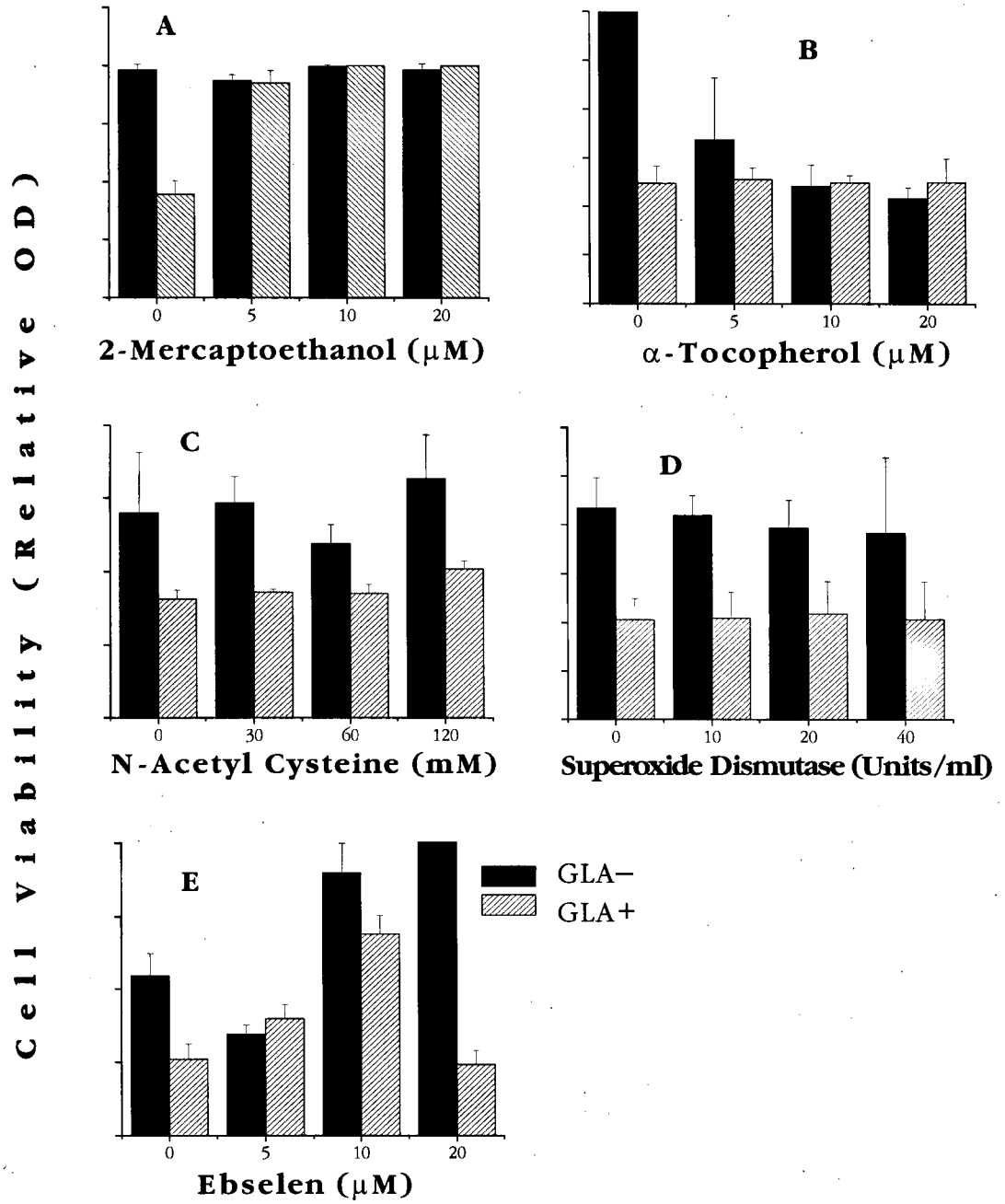

Figure 4: Effect of antioxidants on GLA-induced cytotoxicity in 8E5 cells. Exponentially growing 8E5 cells were pre-incubated at 37°C with antioxidant for 4 hours after which cells were transferred to media supplemented with 15 μg/ml GLA and incubated for 72 hours. Cell viability was assessed by means of WST-1 method as described in Materials and Methods. Each histogram represents an average of five measurements from two independent experiments. Dark histograms represent cultures treated with antioxidant alone and hatched histograms those treated with both GLA and inhibitor.

Another antioxidant tested was N-acetyl cysteine (NAC), which like 2-ME increases cellular GSH concentration in many cell types. NAC ultimately depends on normal levels of catalase and especially GPx in order to exert its antioxidant effects. We observed a statistically significant reduction in viability of cells in GLA-treated compared to control untreated cultures ($p = 0.01$). A small but statistically significant ($p < 0.001$) protective effect was observed at the highest concentration of NAC tested—120 mM, increasing viability by 20% above that of cultures treated with GLA alone. However, even at this concentration, NAC did not return 8E5 cell viability to the level of control untreated cultures. Lower concentrations of NAC did not protect 8E5 cells against GLA-induced cytotoxicity (**panel C, Fig. 4**). The deficiency of catalase and GPx in 8E5 cells might explain the inability of NAC to inhibit GLA-induced cytotoxicity in these cells.

GLA induces programmed cell death in the HIV-1-infected 8E5 cell line at a median concentration that does not affect viability of the parental uninfected A3.01 cell line

We have established that 8E5 cells are at least three times more sensitive to GLA-induced cytotoxicity than the parental A3.01 cells, and that this cytotoxicity is associated with an inability of 8E5 cells to overcome GLA-induced oxidative stress. Next, we sought to establish whether this cytotoxicity was necrotic or apoptotic, the two ways by which eukaryotic cells die. Necrosis and apoptosis can be distinguished experimentally based on their biochemical and morphological characteristics. In order to determine the specific mode of cell death in cultures treated with GLA, cells were harvested at designated time points and subjected to one of three flow cytometric techniques for assay of apoptosis using commercially available kits.

The first method is based on interaction of the protein Annexin V and a membrane phospholipid phosphatidylserine (PS). One of the early events in apoptosis involves translocation of PS from the cytoplasmic interface of the cell membrane to the cell surface. Annexin V binds to negatively charged phospholipids such as PS with high affinity. When conjugated to a fluorochrome like FITC, PS can be used in flow cytometry to label cells in the stages of apoptosis before loss of membrane integrity. Annexin V remains bound to apoptotic cells throughout the cell death process. Cells that are either necrotic or in the last stages of apoptosis, and therefore have lost membrane integrity, can simultaneously be identified by staining with PI, a fluorescent vital dye that stains DNA stoichiometrically.

In the Annexin V and PI assay, viable cells are double negative for Annexin V-fluorochrome and PI. Cells that are in early stages of apoptosis are positive for Annexin V-fluorochrome but negative for PI. Double positive cells are those in either late apoptosis or simply necrotic. Therefore, to distinguish between apoptosis and necrosis in cells dying due to GLA treatment, cells were examined for expression of phosphatidylserine using a commercial kit (Pharmingen, San Diego, CA) as described under Materials and Methods.

Figure 5 summarizes results of a representative experiment. A3.01 and 8E5 cells treated with 15 μg/ml GLA for 12 or 36 hours were stained with Annexin V-FITC and PI, and analyzed by flow cytometry. The majority of cells in control untreated cultures of both cell lines were double negative for Annexin V-FITC and PI--83.63% of A3.01 and 80.45% of 8E5 (lower left quadrants of panels **A** & **D**). Each cell line showed presence of a late-apoptotic population that

was not related to GLA treatment – 13.35% in A3.01 and 15.10% in 8E5 (upper right quadrants of panels A & D). Treatment of A3.01 cells with 15 μg/ml GLA for 12 or 36 hours did not increase percentage of necrotic or apoptotic cells compared to control (lower and upper right quadrants of panels **B** & **C**). The percentage of GLA-treated A3.01 cells found in early apoptosis was similar to that of untreated control—2.15% of untreated cultures (lower right quadrant, A) versus 2.55 and 3.31% in cultures incubated with GLA for 12 or 36 hours (lower right quadrants, B &C). A slight decrease in percentage of A3.01 cells found in late apoptotic cells was noted in GLA-treated cells--from 13.55% of untreated control (upper right quadrant, A) to 7.86% and 7.68% in cultures incubated with GLA for 12 or 36 hours (upper right quadrants, B & C), respectively.

By contrast, a substantial increase was apparent in the percentage of 8E5 cells undergoing apoptosis, from basal 2.72% of untreated control (lower right quadrant, **D**) to 16.30% after 12 hours of treatment (lower right quadrant, **E**), with little difference in percentage of late apoptotic or necrotic cells (upper right quadrant, E) at this time point. After 36 hours, 92.40% of 8E5 cells treated with GLA were positive for phosphatidylserine and permissive of PI dye (upper left quadrant, panel **F**), indicating that they were in late apoptosis. These results indicate that apoptosis and not necrosis is the predominant mode of cell death in 8E5 cells at this concentration of GLA.

Annexin V flow cytometric analysis for GLA induction of apoptosis in A3.01 and 8E5 cells

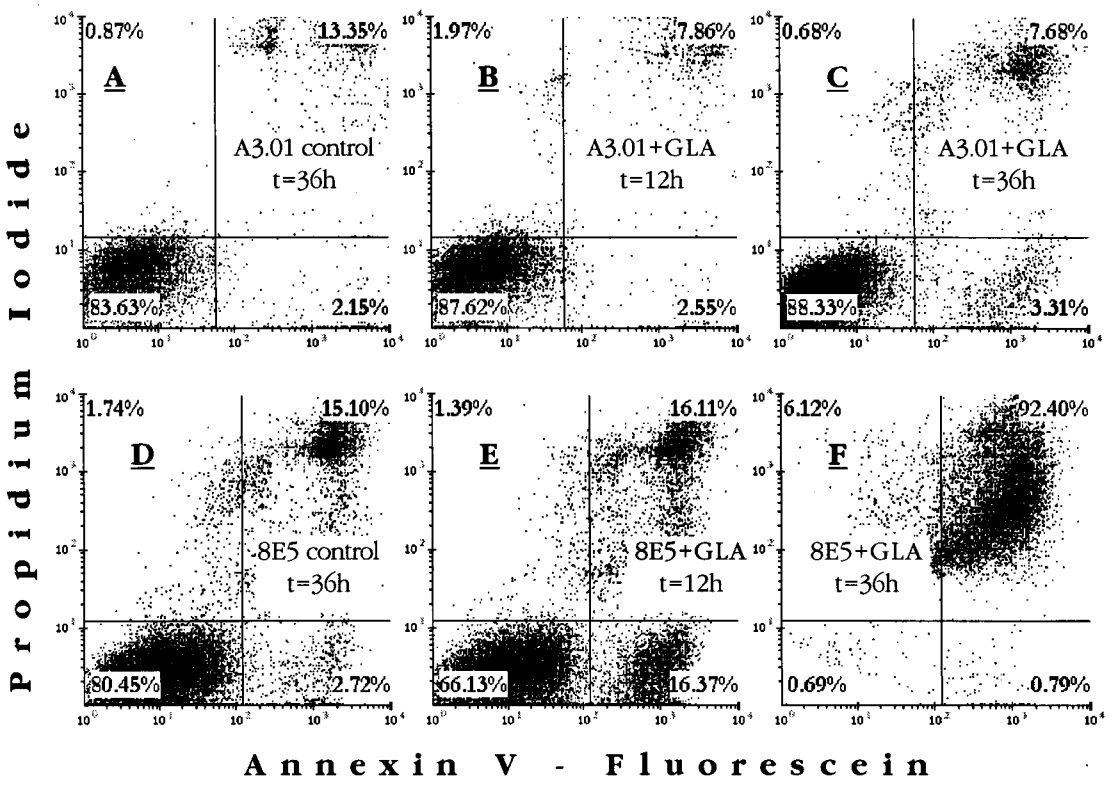

Figure 5: Cultures of A3.01 and 8E5 cells were resuspended at 5 X 10^5 cells/mL in growth medium supplemented with 0 or 15 μg/mL GLA. Cultures were incubated in a humidified CO_2 (5%) incubator for 12 or 24 hours after which cells were prepared for Annexin V analysis as described in Materials and Methods. Samples were analyzed by flow cytometry on a Becton Dickinson FACScan in a Cell Quest™ acquisition environment and further analysis was carried out using FCS Express software. Cells are sorted in four quadrants: Annexin V-FITC negative and PI negative or non-apoptotic and non-necrotic (lower left), Annexin V-FITC negative and PI positive or necrotic (upper left), Annexin V-FITC positive and PI negative or early apoptotic (lower right) and Annexin V-FITC positive and PI positive or late apoptotic (upper right).

To confirm occurrence of apoptosis in GLA - treated 8E5 cells, we employed the APO-BrdU assay, which analyzes cells for presence of DNA fragmentation – a key feature of late apoptosis. The apoptosis cascade involves activation of cellular endonucleases, which eventually degrade chromatin of the dying cell into smaller DNA fragments of approximately 50 base pairs in length. These double- and single-stranded DNA pieces possess exposed hydroxyl (OH) groups on their 3'-termini. In a reaction commonly known as TUNEL [terminal deoxynucleotidyltransferase (TdT) dUTP nick end labeling], exogenous TdT is used to catalyze a template-independent addition of bromodeoxyuridine triphosphates (Br-dUTP or BrdU) to exposed OH-termini. Cells are incubated with an anti-BrdU monoclonal antibody conjugated to a fluorochrome to permit detection of cells undergoing apoptosis.

Flow cytometric analysis of GLA treated cells for occurrence of apoptosis was carried out by measuring the percentage of cells incorporating bromodeoxyuridine using the APO-BRDU™ commercial kit (Pharmingen, San Diego, CA) as described under Materials and Methods. Panels **A** & **B** of **figure 6** represent assay control human lymphoma cells that were used to validate assay results. Cells in the M1 gate are non-apoptotic, while those in M2 are positively apoptotic and show a higher labeling intensity for BrdU-FITC. Panel **A** of Fig. 6 represents negative control cells showing that 95% of cells are negative for BrdU-FITC (gate M1) while only 5% are apoptotic (gate M2). Panel **B** represents positive control cells, with 73% (M1) being negative and 27% (M2) positive for BrdU-FITC, respectively.

When used to test A3.01 and 8E5 cells, the APO-BRDU assay confirmed earlier observations obtained using the Annexin V assay. GLA did not induce apoptosis in A3.01 cells at the concentration tested. In untreated control A3.01 culture, 99% of the cells were non-apoptotic and 1% was apoptotic (panel **C**), and after a 48-hour exposure to GLA only a 4% increase in BrdU uptake was demonstrated (panel **D**). In contrast, under similar conditions, 95% of GLA-treated 8E5 cells became apoptotic after 48 hours of culture with GLA (Gate M2 of panel **F**).

Apo-BrdU flow cytometric analysis for GLA induction of apoptosis in A3.01 and 8E5 cells

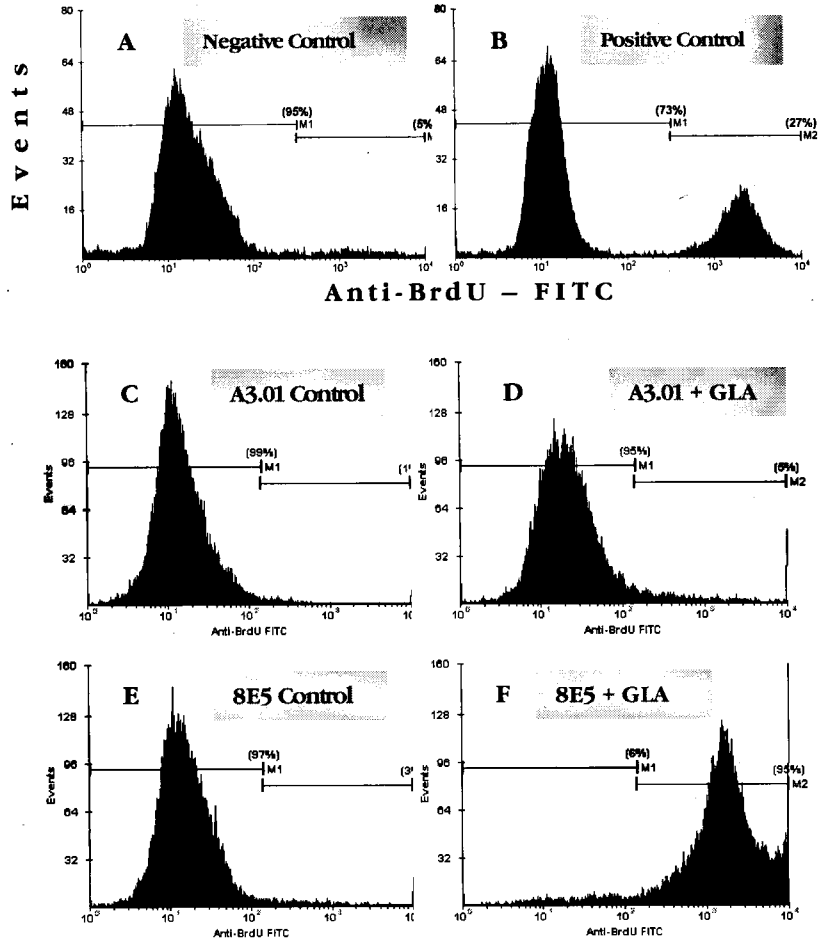

Figure 6: APO-BRDU™ apoptosis assay demonstrating incorporation of bromodeoxyuridine into DNA strand breaks of positive apoptotic cells and lack of labeling in negative cells. Control non-apoptotic cells (panel A) and positive apoptotic cells (panel B) were fixed and incubated with Br-dUTP in the presence of TdT enzyme in order to incorporate Br-dUTP into exposed 3'-OH DNA ends, formed during apoptotic cell death. Incorporated Br-dUTP was detected with a FITC – labeled anti-BrdU monoclonal antibody. Non-apoptotic cells (M1 gates) have insignificant fluorescence due to absence of exposed 3'-OH ends. Cells in the M2 gates are apoptotic and show significantly higher incorporation of Br-dUTP. Likewise, A3.01 and 8E5 cells grown in the presence of 0 or 15 μg/ml of GLA for 48 hours were harvested and prepared for flow cytometric analysis using the APO-BRDU™ method. Cells were acquired within three hours of staining on a Becton Dickinson FACScan flow cytometer equipped with Cell Quest ™ software and analyzed using FCS Express™ listmode data analysis software.

Some experimental variation in the kinetics of apoptosis in GLA-treated cultures was observed with both Annexin V and APO-BRDU analyses. Therefore, we next performed a time course experiment to determine kinetics of apoptosis by sampling GLA-treated cultures at 6, 12, 24 and 48 hours. Although the exact kinetics of apoptosis showed minor variation from experiment to experiment, the induction of apoptosis by GLA in 8E5 cells was time – dependent. Results from a representative experiment are shown in **figure 7**. No incorporation of BrdU was observed in the first six hours of incubation as shown in the first (top) panel of figure 7. A small peak of apoptotic cells emerged after 12 hours and after 48 hours of incubation 95% of cells had become apoptotic (bottom panel). The time lag of apoptosis induction by GLA could be related to the need for GLA to undergo metabolic transformation in order to exert its activity. However, this can only be confirmed in experiments designed to follow metabolic transformation of GLA in apoptotic cells.

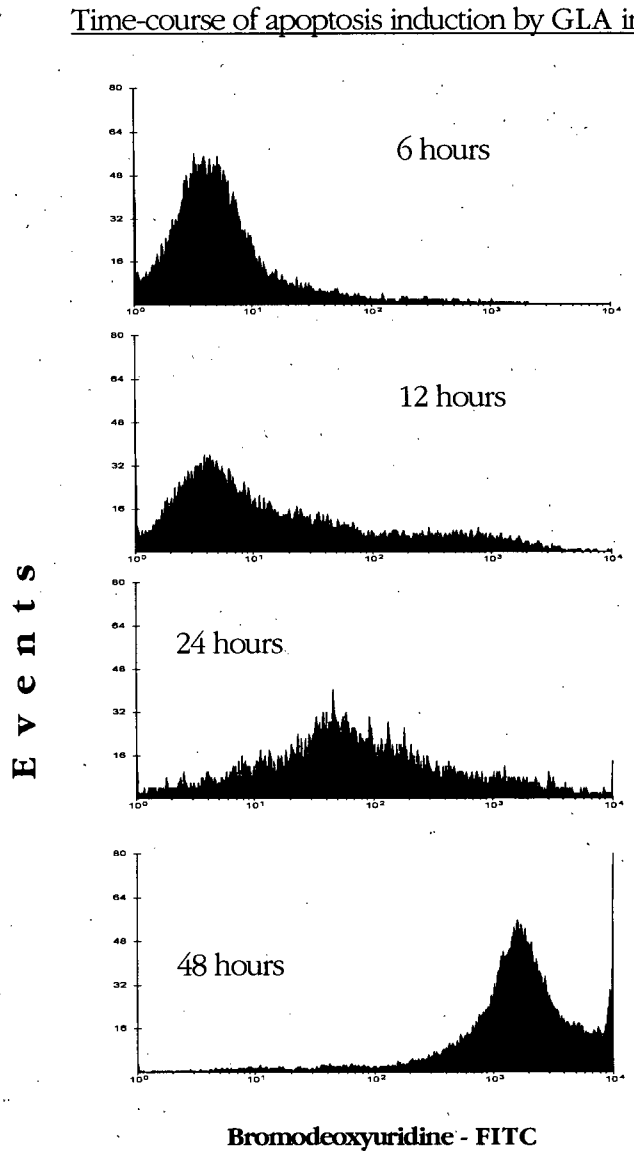

Figure 7: Time-course of programmed cell death in 8E5 cells exposed to 15µg/ml GLA over a period of 48 hours. 8E5 cells were treated as described in Materials and Methods. An equivalent of two million cells were drawn from the culture at 6, 12, 24 and 48 hours of incubation and prepared for FACS analysis using the APO-BrdU™ assay as described previously. The diagram shows results obtained from a representative experiment.

The induction of apoptosis in 8E5 cells by GLA is associated with arrest of cells in the G0/G1 cell cycle phase

The induction of apoptosis in many cell types often follows perturbation of the cell cycle. For instance, in previous studies GLA was shown to cause inhibition of cell division and mitosis in osteogenic sarcoma MG-63 cells *[34]* and inhibition of mitosis and apoptosis induction in HeLa cells *[33]*. S- and G_2/M-phase arrests and G_1-phase arrest were demonstrated in fibroblast cell lines (HSF43 and E8T4) and lymphoblast cell lines (TK6 and WTK1), respectively *[114]*. We performed a series of experiments to examine if an association exists between cycling of cells and occurrence of apoptosis. The cell cycle stage and apoptotic status of control and GLA-treated A3.01 and 8E5 cells were determined simultaneously using the APO-BRDU flow cytometric method. A3.01 and 8E5 cells were grown in presence of GLA for 24 hours after which they were stained with anti-BrdU-FITC monoclonal antibody to identify true apoptotic cells and propidium iodide to resolve cell cycle stage of live and dying cells. Analysis was performed using doublet discrimination to gate around singlet populations on the FL2-W (DNA Width) versus FL2-A (DNA Area) plots in order to discriminate against doublets (region R1, panels **A**, **C**, **E** & **G**, **figure 8**). In panels **B**, **D**, **F** and **H**, the upper rectangle encompasses cells that are positively staining for BrdU-FITC (apoptotic) and the bottom rectangle those cells that are not apoptotic. Bivariate analysis demonstrated that, following GLA treatment, the majority of apoptotic 8E5 cells were found in the G_0/G_1-phase (**panel H**) as opposed to control untreated cells which were not undergoing programmed cell death and were found in all three stages of the life cycle (**panel F**). By contrast, A3.01 cells were non-apoptotic and able to cycle through the S-phase to G_2/M-phase in the presence of drug (**panel D**). In discriminating against doublets, many of the GLA-treated 8E5 cells were left out of analysis due to their tendency to fluoresce in the doublet range (**panel G**). However, with regards to panel H, the only effect of this phenomenon was an underestimation of apoptotic cells but not the overall results.

Bivariate analysis of control and GLA-treated A3.01 and 8E5 cells for cell cycling and occurrence of apoptosis

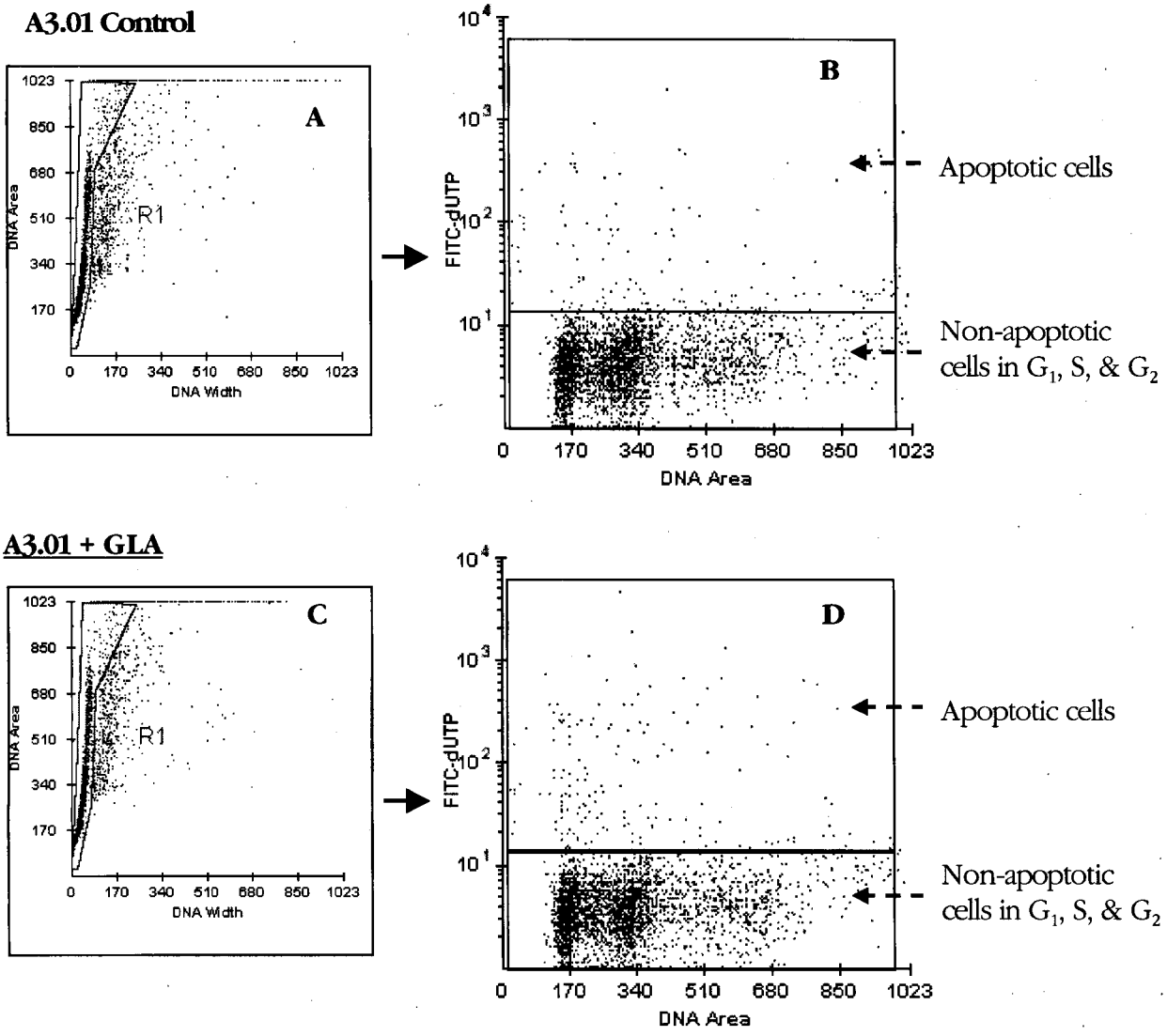

Figure 8a: Bivariate flow cytometric analysis to determine the cell cycle phase and apoptotic status of A3.01 cells following exposure to 0 or 15 µg/ml GLA for 24 hours. Cells were labeled with PI (total cellular DNA) and Fluorescein-BrdU monoclonal antibody (apoptotic cells) as detailed under Materials and Methods, and analyzed by dual parameter DNA doublet discrimination on a Becton Dickinson FACScan cytometer. Panels A & C are dual parameter DNA doublet discrimination displays with the DNA Area signal on the Y-axis and the DNA Width on the X-axis. A gate (R1) is drawn around the non-clumped cells to generate the second gated dual parameter displays (B & D) with DNA (Linear Red Fluorescence) on the X-axis and dUTP-FITC (Log Green Fluorescence) on the Y-axis. Panels B and D resolve non-apoptotic and apoptotic cell populations, bottom and top rectangles respectively, into their respective cell cycle stage as illustrated.

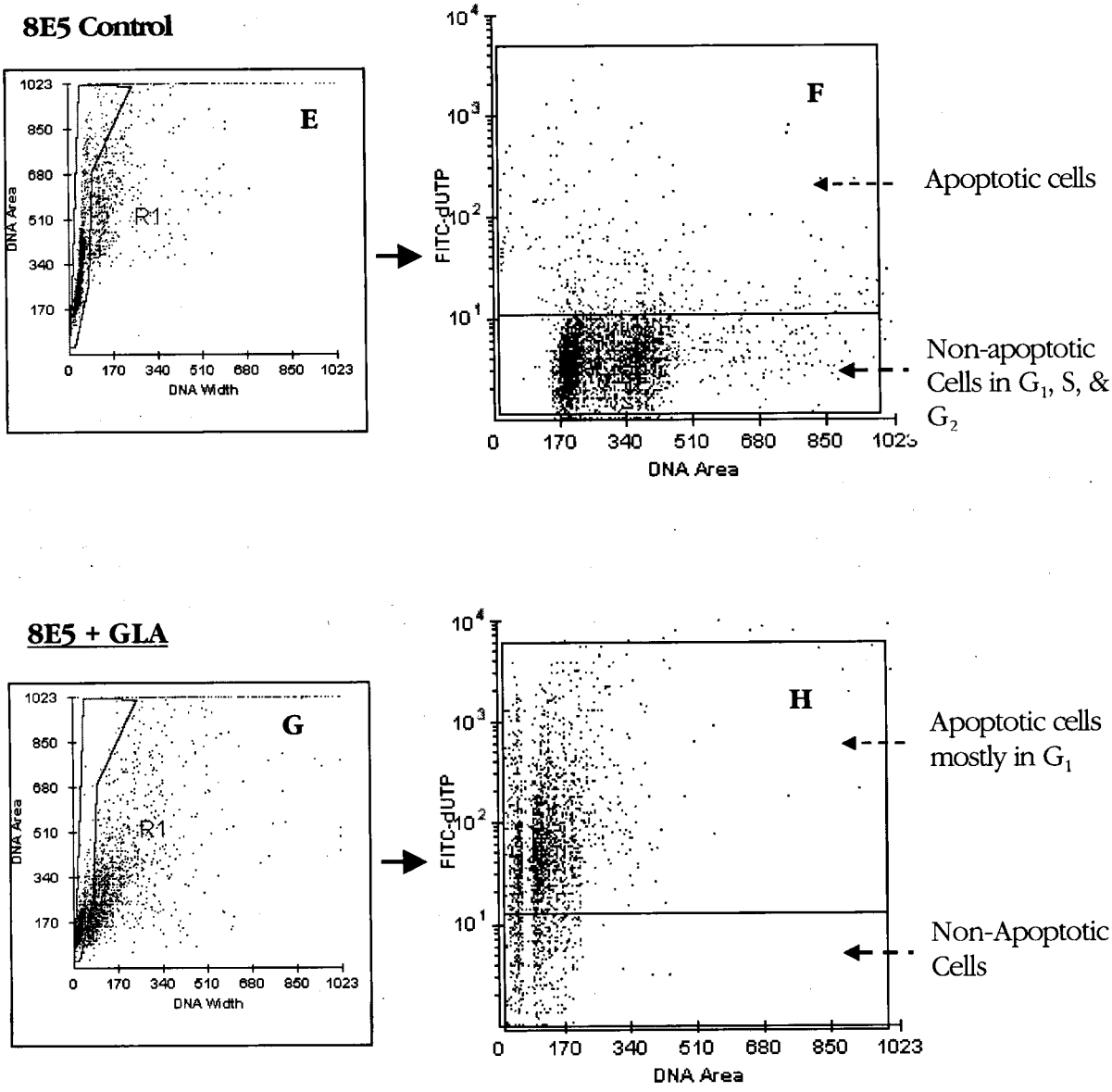

Figure 8b: Bivariate flow cytometric analysis to determine the cell cycle phase and apoptotic status of 8E5 cells following exposure to 0 or 15 μg/ml GLA for 24 hours. Cells were labeled with PI (total cellular DNA) and Fluorescein-BrdU monoclonal antibody (apoptotic cells) as detailed under Materials and Methods, and analyzed by dual parameter DNA doublet discrimination on a Becton Dickinson FACScan cytometer. Panels E & G are dual parameter DNA doublet discrimination displays with the DNA Area signal on the Y-axis and the DNA Width on the X-axis. A gate (R1) is drawn around the non-clumped cells to generate the second gated dual parameter displays F & H, respectively, with DNA (Linear Red Fluorescence) on the X-axis and dUTP-FITC (Log Green Fluorescence) on the Y-axis. Panels F and H resolve non-apoptotic and apoptotic cell populations, bottom and top rectangles respectively, into their respective cell cycle stage as illustrated.

In order to confirm arrest of GLA-treated 8E5 cells in the G_0/G_1-phase of the cell cycle, an analysis of DNA distribution was carried out on unsynchronized cultures and those enriched for G_0/G_1-phase. After exposure to 15 μg/ml GLA for 24 hours, cells were harvested and stained with PI as described under Materials and Methods. The results of DNA content distribution analysis using doublet discrimination is summarized in **figure 9**. Cells that were neither synchronized nor treated with GLA (control) (panel **A**) were able to cycle through G_0/G_1-, S- and G_2/M-phases. As expected, following GLA treatment, the majority of cells were found in a sub-G_0 peak, most likely comprised of apoptotic cells (panel **B**). The emergence of a sub-G_0 peak was accompanied by a reduction in both G_0/G_1 and G_2/M. Since earlier results (figure 8) had indicated that GLA prevent cells from passing G_0/G_1, further attempts were made to examine the possibility of augmenting GLA-induced cytotoxicity of cells in this stage. Ultimately, the best experimental strategy to enrich 8E5 cultures for cells in G_0/G_1-phase was by means of serum deprivation since other approaches, such as treatment with Mimosine or double-block with Aphidocolin, proved unsuccessful. To synchronize cultures in G_0/G_1, cells were grown in serum-reduced (0.5%) media for 48 hours. Serum deprivation reduced the proportion of cells in G_2/M-phase and resulted in emergence of a sub-G_0 peak or apoptotic cells (panel **C**, fig. 9). Subsequently, these cells were returned to normal growth medium and cultured with or without GLA for 24 hours before further analysis. Cells that were not exposed to GLA managed to continue cycling as normal but those growing in GLA-supplemented were unable to do so, and in fact were more susceptible to GLA than were unsynchronized cells (panel **D**, Fig. 9).

Effect of GLA on cycling of G_0/G_1-synchronized 8E5 cells

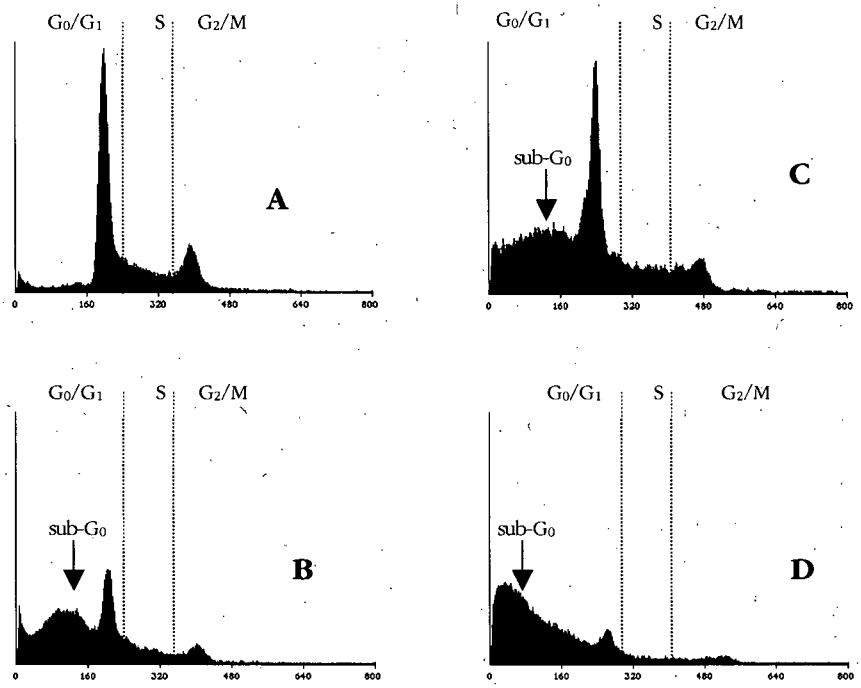

Figure 9: DNA content frequency histograms of fixed 8E5 cells stained with PI. Cells were fixed/permeabilized using 70% ethanol and their nuclei stained with PI in a solution containing RNase A to denature RNA. PI fluorescence was measured using a Becton Dickinson FACScan flow cytometer using doublet discrimination. Panel **A** represents untreated and unsynchronized cultures whereas **B** shows the distribution of DNA in GLA-treated unsynchronized cultures. Panel **C** represents cells of cultures synchronized by serum starvation to enrich for cells in the G_0/G_1-phase of the cell cycle. Subsequent to G_0/G_1-enrichment, cells were transferred to serum-supplemented media and exposed to GLA (panel **D**). The different stages of the cell cycle are as indicated in the panels, including appearance of a sub-G_0 (apoptotic) peak in GLA-treated and serum-starved cultures (panels B, C and D).

Susceptibility to GLA-induced apoptosis is only partially associated with active production of HIV-1 core antigen

Since uninfected A3.01 cells were more resistant to killing by GLA than the HIV-1-infected 8E5 cells, we next asked whether HIV antigen production was necessary for GLA cytotoxicity. Although each 8E5 cell carries a single copy of integrated HIV genome, repeated flow cytometric analysis of intracellular HIV core antigen expression in these cells demonstrated that, on average, about 20% of cells in the population did not stain positively for HIV-1 antigen. Therefore, an attempt was made to identify any difference in susceptibility to GLA between HIV-1 antigen producing and non-productive cells within the 8E5 mixed cell population.

The APO-BrdU method described above for assay of BrdU incorporation in apoptotic cells utilizes ethyl alcohol for cell permeabilization. However, alcohol is unsuitable in assays where integrity of target epitopes is critical, as is the case with intracellular HIV antigen. Therefore, a combination of the APO-BrdU assay and the BrdU Flow staining protocol (BD Pharmingen, San Diego, CA) was used to measure intracellular HIV-1 core antigen and BrdU incorporation as a measure of apoptosis. The results are summarized in **figure 10.** In agreement with previous experiments, GLA did not induce apoptosis in A3.01 cells as evidenced by percentage of cells positive for BrdU-FITC (two right hand quadrants of panels **A** and **B**) – 3.79% of control cells and 1.73% of GLA-treated cells. As expected, A3.01 cells were negative for HIV-1 core antigen. Dual parameter flow cytometric analysis of 8E5 cells showed that, without GLA treatment, 84.29% of cells stained positive for HIV-1 core antigen and only about 7% were apoptotic (panel **C**). Following GLA treatment, 73.37% of 8E5 cells became apoptotic (lower and upper right quadrants, panel **D**) and the percentage of cells staining positive for HIV antigen (upper two quadrants, panel D) decreased to 61.4% from 84.29%. Of the apoptotic cells, approximately 20% were negative for intracellular viral antigen (lower right quadrant panel D). Since an excess of anti-HIV-1 core monoclonal antibody was used, these results suggest that productively infected cells are more susceptible to GLA-induced apoptosis. Also this could mean that cells with low copies of HIV-1 core antigen are less susceptible to GLA cytotoxicity, assuming 100% of cells are producing antigen but at different levels of intensity.

Bivariate analysis of GLA-treated 8E5 cells for apoptosis and HIV-1 core antigen production

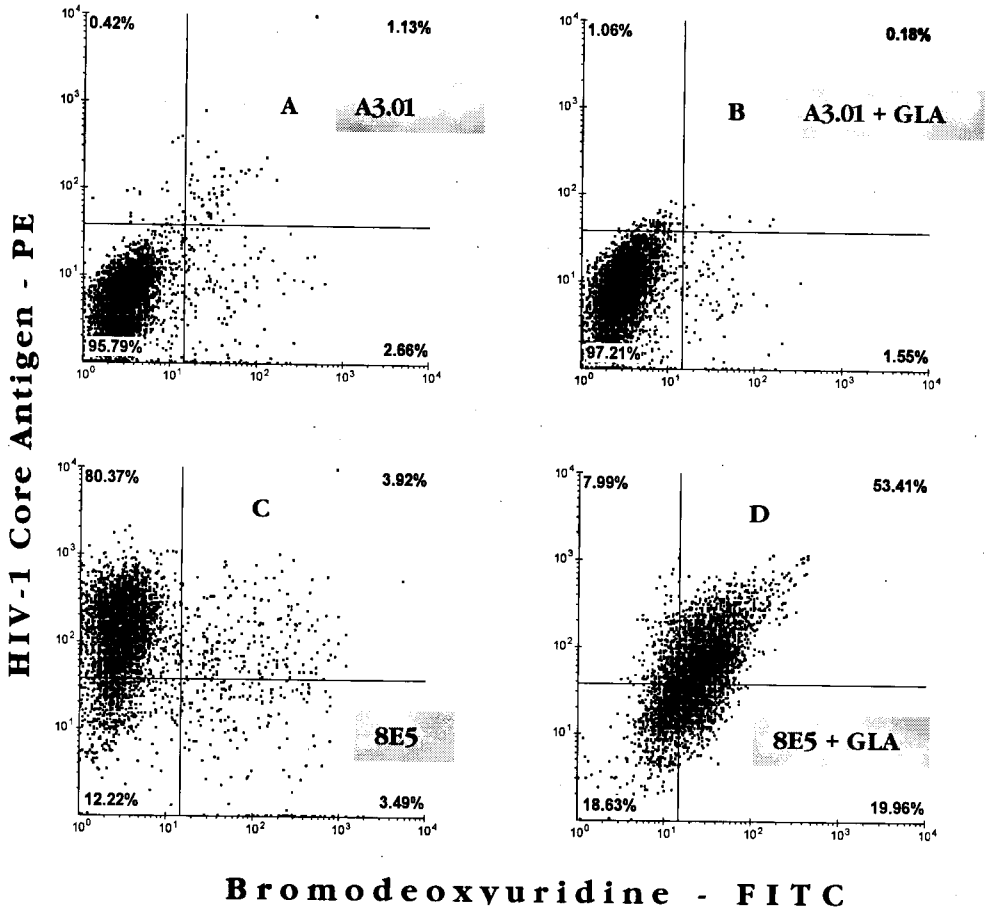

Figure 10: Assay of apoptosis and intracellular HIV-1 core antigen concentration in control and GLA-treated A3.01 (panels A & B) and 8E5 (panels C & D) cells was carried out using a hybrid APO-BRDU™ and BRDU FLOW™ on cells grown for 48 hours as described under Materials and Methods. Cells were resuspended in 1 ml of staining buffer and acquired in a Becton Dickinson FACScan cytometer equipped with Cell Quest™ software. Further analysis was carried out in FCS Express™ software. The diagram shows results from a representative experiment, with the x-axis representing the number of cells incorporating BrdU-FITC as a measure of apoptosis and the y-axis the measure of fluorescence intensity for intracellular HIV-1 core antigen.

Modification of apoptosis-related genes during GLA-induced cell death

As is typical of cells undergoing programmed cell death, the apoptosis defining characteristics - DNA fragmentation and phosphatidylserine externalization - seen in GLA-treated 8E5 cells are the result of specific signaling events occurring at molecular level. The signaling pathway involved is a function of cell type and death signal triggering the apoptosis. In order to identify the specific pathway mediating GLA-induced apoptosis, ribonuclease protection assay (RPA) was used to look for changes in expression of mRNA species of apoptosis-related genes in total RNA from untreated and GLA-treated A3.01 and 8E5 cells. RPA was performed using RiboQuant™ system (Pharmingen). This system utilizes anti-sense RNA probes from human apoptosis (hAPO) genes, including probes against two housekeeping genes –ribosomal protein L32 and glyceraldehydes 3-phosphate dehydrogenase (GAPDH), which control for sample loading variation. Results of RPA are shown in **Figure 11**. GLA did not cause modification of caspase gene expression in either A3.01 or 8E5 cell lines (panel A, **Fig. 11**). Of the two major initiator caspases, there was equal expression of caspase-8 message in both cell lines regardless of GLA treatment, and no signal was detected for caspase-9. At the other end, strong expression of caspase-3 transcripts was detected in all samples. The presence of initiator and effector caspase mRNA species in both apoptotic and normal cells is consistent with constitutive expression of these genes in most cells.

Since initiator caspase binding of receptor-associated death domain is a crucial step in initiation of the death cascade, we screened a set of templates (hAPO3) that assess expression of a group of death receptors and their ligands. These include death receptor 3 or DR3 (also known as Apo3, WSL-1, TRAMP or LARD), Fas (also called CD95 or Apo1) and tumor necrosis factor receptor 1 (TNFR1 or TNFRp55). The hAPO3 set is also composed of the Fas Ligand (FASL), TRAIL – which binds death receptor 5 (DR5 or Apo2) and the Fas associated death domain (FADD or Mort 1), which functions to couple Fas to another ingredient of the set – caspase-8 (also present in hAPO1c). Other components of the set include TNFR-associated death domain (TRADD), receptor interacting protein (RIP) with serine-threonine kinase activity, Fas-associated phosphatase (FAP) and Fas associated factor (FAF).

Using hAPO3, modulation of FADD mRNA expression in 8E5 cells following GLA treatment was demonstrated (**Lane 3 & 4, panel B, Fig. 11**). Whereas the signal intensity for FADD was similar in both untreated and GLA-treated A3.01 cells, there was significantly less

gene expression of this domain in control untreated 8E5 cells. Upon GLA treatment, the expression of FADD in 8E5 cells was upregulated. FADD is an adapter protein that binds through its death domain (DD) to trimerized death domains of Fas/CD95, TNFR1 or DR3 *[20, 11]*. After binding DD of these death receptors, FADD interacts with death effector domains (DED) of caspase-8 through its own DED to initiate apoptosis. With the exception of FAP, which was expressed in both control and GLA-treated A3.01 cells but not in 8E5 cells, the expression intensity of the remaining hAPO3 mRNAs species was not influenced by GLA treatment.

In addition to Fas-initiated death mechanisms, some cells, particularly cytotoxic T-lymphocytes, possess a distinct apoptosis pathway that relies on T-cell receptor (TCR)-induced release of granules containing perforin and serine-esterases called granzymes *[35]*. Using the hAPO4 set of probes, the presence and regulation of these mediators among the mRNA species of A3.01 and 8E5 was tested by RPA (panel **C, Fig. 11**). There was no discernible difference in expression of these transcripts in A3.01 and 8E5.

The third major component of the apoptosis program comprises members of the *Bcl-2* family of proteins. There are in excess of 18 members of this family possessing either anti-apoptotic or pro-apoptotic function in mammalian cells. In order to assay the expression of *Bcl-2* genes in response to GLA treatment, total RNA was isolated from A3.01 and 8E5 cells grown with or without 15 μg/ml GLA and subjected to RPA using the hAPO-2c multi-probe template set (Pharmingen). This set detects and quantifies mRNA species of nine *Bcl-2* family members, including the pro-apoptosis *bcl-x*, *bad*, *bak*, *bax* and *bik*, as well as the pro-survival *bcl-2*, *mcl-1*, *bcl-w*, *bfl-1* and *bcl-x* genes. This analysis revealed no obvious change in expression of any *Bcl-2* family genes resulting from GLA treatment (panel **D, Fig. 11**).

Expression of apoptosis-related genes in 8E5 cells exposed to GLA

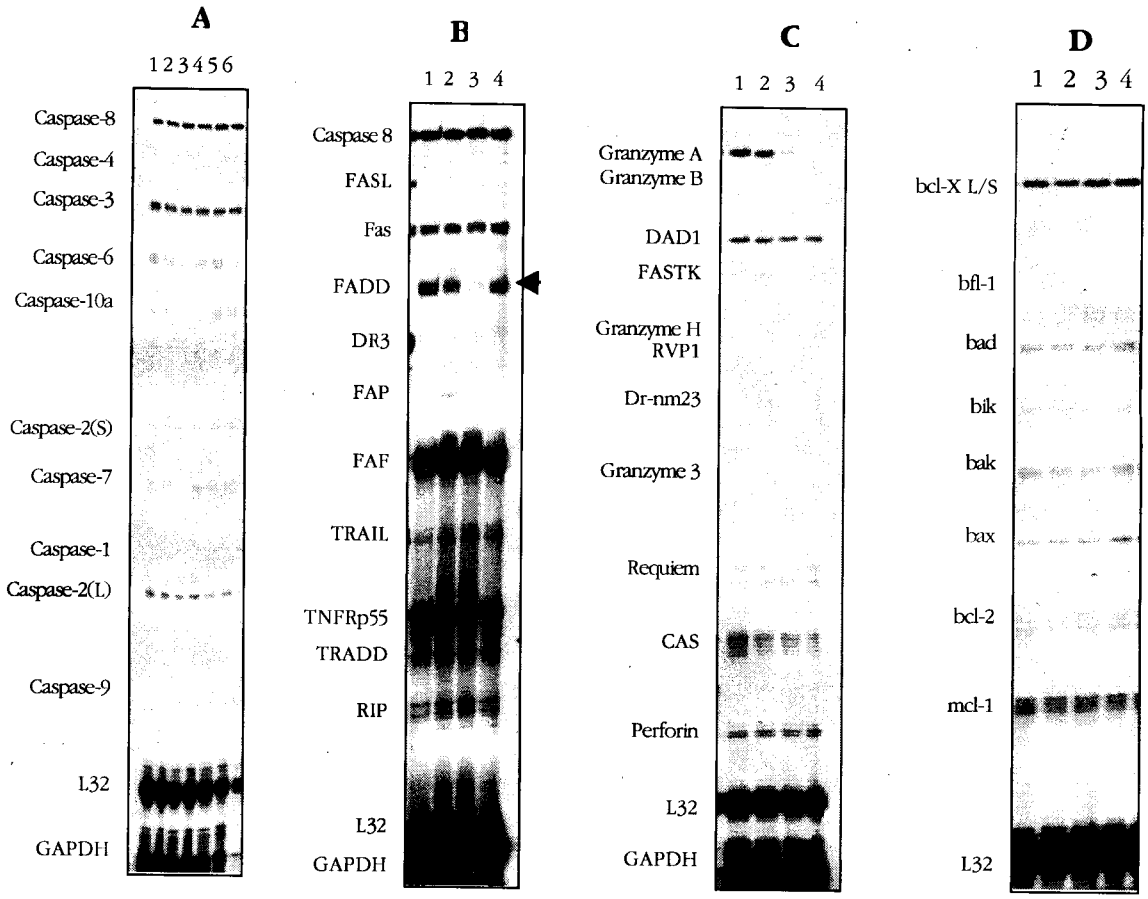

Figure 11: Ribonuclease protection assay (RPA) of A3.01 and 8E5 cells treated with 0 or 15 μg/ml GLA. Total RNA was extracted from 10^7 cells using TRIZOL (Life Technologies) and analyzed for distinct mRNA species using the RiboQuant multi-probe RPA system with hAPO-1c (**A**), hAPO-3 (**B**), hAPO-4 (**C**) or hAPO-2c (**D**) probe template sets (Pharmingen) as described in Materials and Methods. Hybridized samples were separated by gel electrophoresis using the NOVEX™ QuickPoint™ rapid nucleic acid separation system, transferred to a nylon membrane and detected by autoradiography. Panel A in the diagram above shows results obtained from A3.01 cells treated with 0 μg/ml GLA (Lane 1), 15 μg/ml GLA (Lane 2) or GLA + zVAD.fmk (Lane 3), and total RNA from 8E5 cells treated with 0 μg/ml GLA (Lane 4), 15 μg/ml GLA (Lane 5) or GLA + zVAD.fmk (Lane 6). Lanes 1 and 2 of panel B, C and D represent control and GLA-treated A3.01, respectively, while lanes 3 and 4 are their 8E5 equivalents. The identity and position of each mRNA species was determined based on appropriately sized, protected probe fragment band resolved on the same gel.

GLA induces apoptosis via a pathway that is blocked by a broad-spectrum inhibitor of caspases

The possible involvement of FADD in GLA-induced cell death gleamed from RPA results above suggests caspase activation by GLA despite lack of modification of caspase gene expression in treated cells. To investigate this, we examined the ability of two broad-spectrum caspase inhibitors, Z-Val-Ala-Asp(OMe)-CH_2F (or zVAD-FMK) and Boc-Asp(OMe)-CH_2F (or BD.fmk) (Calbiochem), to protect 8E5 cells against GLA-induced apoptosis. We also examined the similarity of GLA-induced apoptosis to that induced by engagement of CD95/Fas by its ligand. The ligand used in this case was an anti-Fas monoclonal antibody (clone CH-11) (Calbiochem). The apoptosis induced by CH-11 is inhibited by another clone of anti-Fas antibody - ZB4 (Calbiochem). Apoptosis induction was measured flow cytometrically by evaluating the extent of Annexin V binding as a reflection of PS exposure on the surface of cells undergoing apoptosis. Results of these experiments are summarized in **figure 12**. After 24 hours of incubation, 37% of cells were apoptotic by anti-Fas compared to 97% by GLA (panels **B** & **E**). The inhibitory anti-Fas antibody (ZB4) caused a three-fold (37% to 13%) reduction in the percentage of apoptotic cells resulting from CH-11 treatment (Panels **B** and **C**), but did not reduce percentage of apoptotic cells in GLA-treated cultures (97% versus 98%) (Panels **E** & **F**). Because ZB4 acts by recognizing the human cell surface Fas antigen, its inability to prevent GLA-induced cytotoxicity implies that GLA does not engage or stimulate Fas even though it may utilize a similar intracellular death-signaling pathway. GLA-induced apoptosis of 8E5 cells was overcome by the broad-spectrum caspase inhibitor BD.fmk, which reduced the percentage of apoptotic cells in GLA-treated cultures from 97% (Panel **E**) to 28% (Panel **G**). Another caspase inhibitor, zVAD.fmk, did not reduce percentage of cells undergoing apoptosis due to GLA treatment - 91% (Panel **H**) compared to GLA alone (97%). BD.fmk was partially effective at preventing death induced by CH-11, reducing the percentage of apoptotic cells from 37% (panel **B**) to 27% (panel **D**). Prevention of GLA-induced apoptosis by BD.fmk suggests that the caspase cascade is involved in GLA cytotoxicity despite the fact that similar results were not achieved with zVAD.fmk. This dichotomy is beyond the scope of this thesis but failure of peptidyl caspase inhibitors to suppress caspase-mediated apoptosis under some experimental conditions has been reported *[Reviewed in 59]*.

Effect of broad-spectrum caspase inhibitors on GLA and α-Fas-mediated programmed death of 8E5 cells

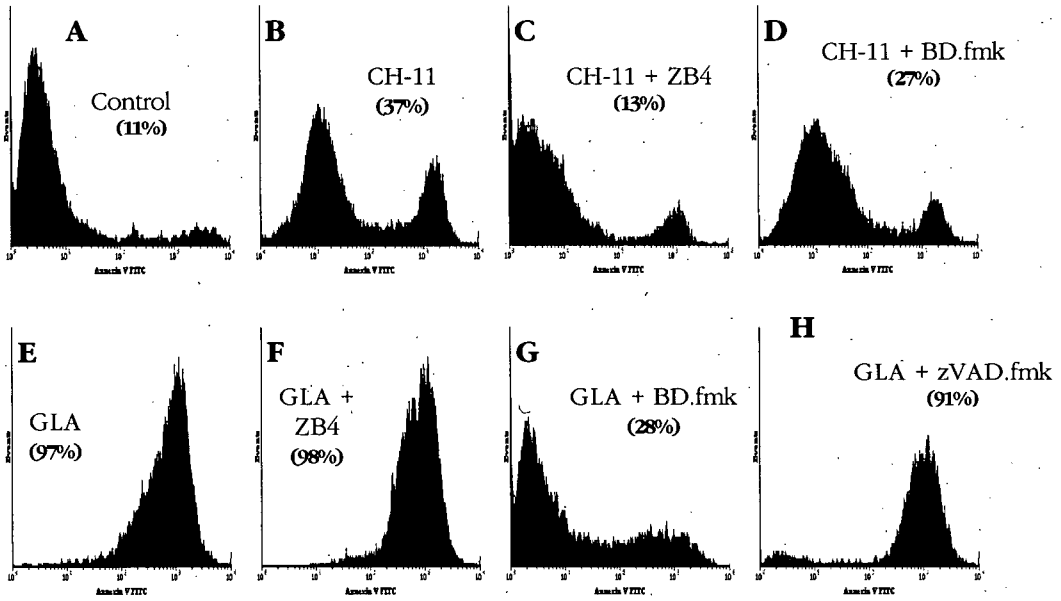

Figure 12: Flow cytometric analysis of 8E5 cells treated with GLA or anti-Fas antibody in the presence of select apoptosis inhibitors as indicated in the diagram. 8E5 cells cultured as described in Materials and Methods were preincubated for four hours with media containing inhibitor carrier (≤ 0.01% DMSO) (control), 500 ng/ml of α-Fas monoclonal antibody (clone ZB4) (Immunotech), 100 μM BD.fmk (Calbiochem), or 100 μM zVAD.fmk (Calbiochem). Then, either GLA (15 μg/ml final concentration) or α-Fas monoclonal antibody (clone CH-11) (Immunotech) (250 ng/ml final concentration) was added to appropriate wells and the cultures returned to the incubator for another 24 hours. Cells were then harvested, washed twice and incubated with Annexin V-FITC as described in the text. Within one hour, cells were analyzed on a Becton Dickinson FACScan flow cytometer for fluorescence intensity of Annexin V using the CellQuest acquisition environment. Results were analyzed using FCS Express software and presented as above with the x-axis showing fluorescence of Annexin V-FITC as a measure of apoptosis and the relative number of events on the y-axis. The percentage of apoptosis positive cells is shown in brackets.

Induction of apoptosis by GLA is associated with cleavage of caspase-3 and poly (ADP-ribose) polymerase (PARP)

Inhibition of GLA-induced apoptosis by BD.fmk implicates caspases in GLA-associated cell death despite lack of change in caspase gene expression as demonstrated by RPA. In most cells, caspases are constitutively expressed in inactive (zymogen) form and only become activated upon receiving proper stimuli. Therefore, in addition to caspase inhibition experiments, we looked for modulation of expression of FADD, caspase-8, cytochrome-C, caspase-9, caspase-3, caspase-7, Bcl-2 and Mcl-1 proteins using Western blot analysis. This was performed on cells from cultures supplemented with media alone, GLA or Fas for six or 12 hours, and cells preincubated with BD.fmk for four hours followed by incubation with GLA for eight hours. **Figure 13** shows the results of immunoblot analysis of upstream apoptosis proteins, namely FADD, caspase-8, caspase-9 and cytochrome C. Examination of lysates for FADD antigen was performed using an IgG anti-FADD polyclonal antibody (Santa Cruz Biotechnology) which reacts with a 23 kDa protein that associates with the death domains of both Fas and TNF-R1. As illustrated in **panel A**, only a slight increase in FADD protein expression in GLA-treated 8E5 cells was observed. This difference persisted following 6 or 12 hours of incubation. By contrast, the increase in FADD expression was higher in cells undergoing apoptosis due to incubation of cells for 12 hours with α-Fas antibody, as would be expected of cells dying via the CD95 pathway. Since FADD is not inhibited by caspase inhibitors, it is not clear why the slight upregulation of FADD expression seen in GLA-treated cells was abrogated by treatment with BD.fmk.

GLA- and α-Fas antibody- mediated regulation of upstream factors of the apoptosis cascade in apoptotic 8E5 cells

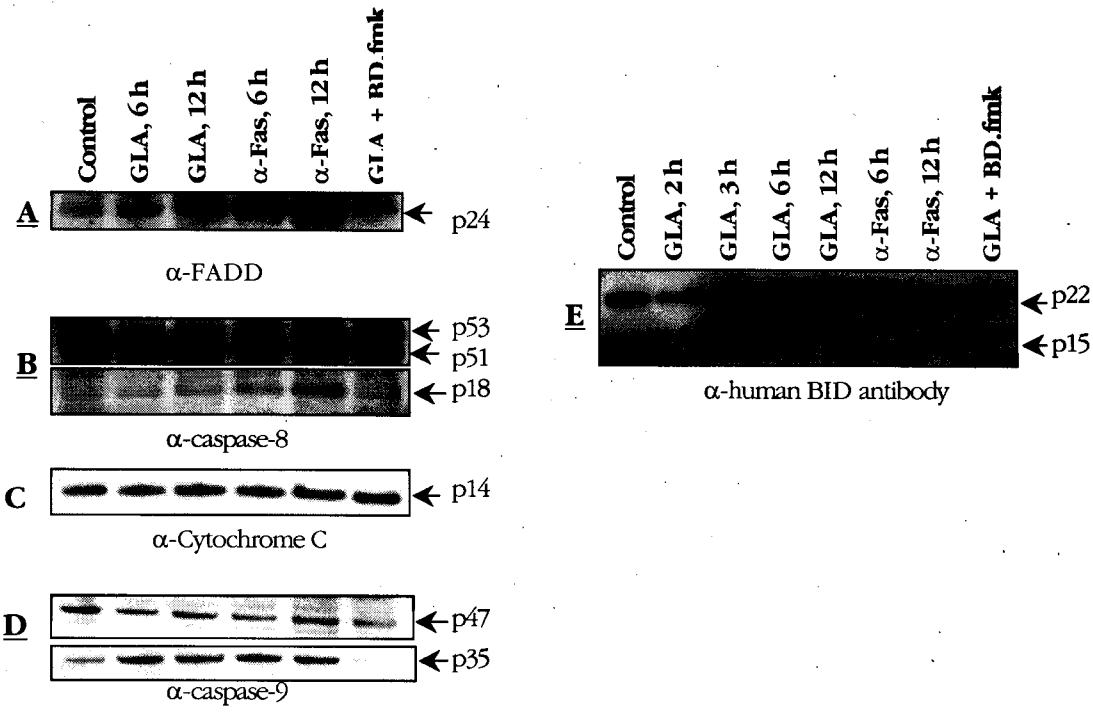

Figure 13: Western blot analysis of GLA or α-Fas antibody-treated 8E5 cells showing lack of FADD, caspase-8, cytochrome C, caspase-9 and BID protein activation. Cells were incubated with 15 μg/ml GLA or 0.25 μg/ml α-Fas for 6 or 12 hours, or 50 μM BD.fmk for 4 hours followed by incubation with GLA for another 8 hours. Cells were lysed as described previously and 20 μg of sample loaded into each well of a SDS-PAGE gel. An antibody against β-actin (Sigma) was used as control for protein input. The total protein was resolved and transferred to membrane, which was then subjected to immunoprecipitation with α-FADD (Santa Cruz Biotechnology), α-caspase-8 (Cell Signaling Technology), cytochrome C (Upstate Biotechnology), α-caspase-9 (Cell Signaling Technology) or α-human BID protein (Cell Signaling Technology) antibodies. Positions of specific immunoreactive bands are indicated with arrows. The figure represents results from one of two independent experiments that exhibited similar immunoreactive profiles. Band intensity was determined using TotalLab image analysis software (Phoretix).

We did not observe significant difference in caspase-8 expression in GLA-treated cells compared to untreated 8E5 cells using a polyclonal antibody that reacts with the p18/20 subunit and precursor of caspase-8 (Santa Cruz Biotechnology) (panels **B**). Similar results were seen using A3.01 cell lysates. Of the two native isoforms, the caspase-8/a (53 kDa) band predominated over that of caspase-8/b (51 kDa) in all lysates but was not upregulated in any of the lysates, perhaps reflecting its constitutive expression. In cells undergoing apoptosis via the Fas pathway, caspase-8 is activated by proteolytic cleavage into active 18 and 10 kDa subunits. Immunoblot analysis of GLA-treated cells did not detect any mature caspase-8 subunits. On the other hand, 8E5 cells exposed to α-Fas demonstrated a small but discernible increase in p18 caspase-8 cleavage subunit. It can be concluded from the totality of foregoing observations that GLA does not act through the caspase-8 pathway in its induction of apoptosis. This is with disregard to the modest reactivity of α-Fas-treated 8E5 cell lysates against α-cleaved caspase-8, which suggests that the antibody used may not be specific enough to identify the subunit of interest. However, using a monoclonal antibody (Cell Signaling, Beverly, MA) specifically directed against cleaved caspase-8 (10 kDa) small subunit confirmed the absence of caspase-8 cleavage in these samples (data not shown).

An alternative to Fas pathway is the mitochondrial or intrinsic route of apoptosis induction, which is mediated via release of cytochrome C from the mitochondria and subsequent caspase-9 activation. **Figure 13** (panel **C**) shows results of immunoblot analysis of 8E5 lysates using mouse IgG α-cytochrome C (Upstate Biotechnology), which reacts with the 14-kDa protein of cytochrome C. There was no difference among control untreated, GLA-treated and α-Fas-treated 8E5 cells with regards to cytochrome C protein levels. In a separate experiment, A3.01 cells were observed to express minimal amounts of cytochrome-C under all conditions (data not shown). However, lack of differential expression of cytochrome C between control and treated samples does not confirm lack of involvement of the intrinsic pathway in GLA-induced apoptosis. This is because cytochrome C needs only to be translocated from the mitochondria to the cytosol to initiate apoptosis.

The release of cytochrome C is preceded by collapse of the mitochondrial inner membrane potential ($\Delta\Psi_m$). Thus, measurement of changes in $\Delta\Psi_m$ is commonly used to detect

occurrence of apoptosis. An attempt was therefore made to measure changes in $\Delta\Psi_m$ by means of a fluorometric assay. Due to technical obstacles, these experiments did not yield conclusive results.

As described above (Introduction), the cytochrome C released from mitochondria during apoptosis binds to Apaf-1 together with dATP. The complex so formed then recruits Caspase-9 leading to its activation. Therefore, the expression of caspase-9 native protein and its cleaved mature subunit in 8E5 cells were assayed using two antibodies, one specific for the full length 47 kDa protein and another that recognizes either the large active 37 kDa (with prodomain) subunit or the 17 kDa subunit (without prodomain) (Cell Signaling Technology, Beverly, MA). The intensity of caspase-9 immunoreactive bands of GLA- and α-Fas- treated samples obtained from two experiments were analyzed using TotalLab software (Phoretix) and found to be three to four-fold higher than that of control (panel **D**, **Fig. 13**). Nonetheless, these differences in immunoreactivity of cleaved caspase-9 among control untreated, GLA-treated or α-Fas-treated cells were not statistically significant ($p = 0.51$).

Due to the small difference of caspase-9 processing observed, it is not possible to conclude from these results whether the difference was attributable to GLA. Further experimentation is necessary to confirm that GLA acts via the cytochrome C/caspase-9 pathway. Although α-Fas is known to act via the caspase-8 route, its slight increase of caspase-9 expression seen here could be explained by the 'cross-talk' between the two apoptosis pathways, which is mediated via caspase-8-initiated truncation of the Bcl-2 homologue BID protein. Although BID is anti-apoptotic in certain cells, its truncated subunit is known to signal the mitochondrion to trigger the intrinsic pathway of apoptosis through an unknown mechanism. However, immunoprecipitation of cell lysates using a human specific monoclonal antibody only revealed existence of the full-length protein (22 kDa) but not of the large fragment (15 kDa) or other cleavage products (panel **E**, **Fig. 13**), which are generated from caspase-8-induced proteolysis of BID. Though indirect, this provides further evidence implicating a lack of caspase-8 processing in GLA-treated cells.

Next, we looked at expression and activation of downstream or death effector caspases (caspase-3 and caspase-7) (Refer to Fig. 1). Caspase-3 is expressed in cells as an inactive 32-kDa (p32) precursor, which is proteolytically cleaved to yield two active effector subunits (p17 and p12) of apoptosis. Caspase-3 precursor is cleaved first to yield the p12 subunit and a p20

peptide, which in turn generates the p17 unit. Examination of caspase-3 expression was performed using a rabbit α-cleaved caspase-3 antibody (Cell Signaling Technology), which, among other subunits, recognizes the 17-kDa subunit of caspase-3. Results of Western blot analysis of cell lysates from GLA-treated and α-Fas-treated cultures using this antibody are shown in **figure 14** (panel **A**). The 20-kDa and 12-kDa subunits were dominant in GLA and α-Fas-treated 8E5 cells. A small band of the native precursor, but none of the active p20 or p12 cleavage products, was seen in control untreated cells. 8E5 cells pretreated with BD.fmk expressed neither the full-length caspase-3 nor the p20 and p12 active forms although a small band of around 17 kDa was seen instead (panel **A**, **Fig. 14**). A3.01 cells (control and GLA-treated) expressed neither inactive caspase-3 nor its cleaved subunits (Data not shown). The processing of caspase-3 was confirmed by control lysates of Jurkat cells treated with cytochrome C and the permeabilizing detergent CHAPS, which expressed mostly the 12 kDa cleavage product. Lysates from Jurkat cells treated with detergent alone did not show bands of caspase-3 fragments. Appearance of cleaved caspase-3 (p20) was evident in GLA-treated cells at six hours post-incubation (Panel **A**, **Fig. 14**). Activation of caspase-3 by GLA, similar to that by α-Fas antibody, and its inhibition by BD.fmk provide further evidence that GLA acts via the caspase pathway to induce apoptosis.

Western blot analysis of lysates for caspase-7 processing using an α-cleaved caspase-7 antibody (Cell Signaling Technology) revealed minor bands corresponding to the 21 kDa fragment only in cells treated with α-Fas antibody but not those treated with GLA. A large band was visible in positive control lysates of Jurkat cells treated with cytochrome C and CHAPS but not those treated with detergent alone (panel **B**, **Fig. 14**).

The main target of caspase-3 is poly (ADP-ribose) polymerase (PARP), a 116-kDa nuclear protein involved in DNA repair predominantly in response to environmental stress. Cleavage of PARP separates its amino-terminal DNA binding domain (24 kDa) from its carboxyl-terminal catalytic domain (89 kDa). We employed a rabbit polyclonal α-cleaved PARP antibody (Cell Signaling Technology) to detect the large fragment of human PARP produced by caspase-3 cleavage. In agreement with our data showing caspase-3 processing in response to treatment of 8E5 cells with GLA or α-Fas (CH-11) antibody, immunoblot analysis revealed cleavage of PARP (panel **C**, Fig. **14**). Cleavage of PARP in GLA-treated cells was prevented by

BD.fmk. Appearance of mature PARP after six hours of GLA incubation corresponded with that of caspase-3. Control lysates were prepared from Jurkat cells treated with the proteasome inhibitor etoposide and the detergent triton X-100, which showed a similar 89 kDa band as GLA-treated and α-Fas antibody-treated cells. These observations confirm the involvement of both caspase-3 and the caspase pathway in general in GLA-mediated cell death.

GLA- and α-Fas antibody- mediated cleavage of effector molecules of the apoptosis cascade in apoptotic 8E5 cells

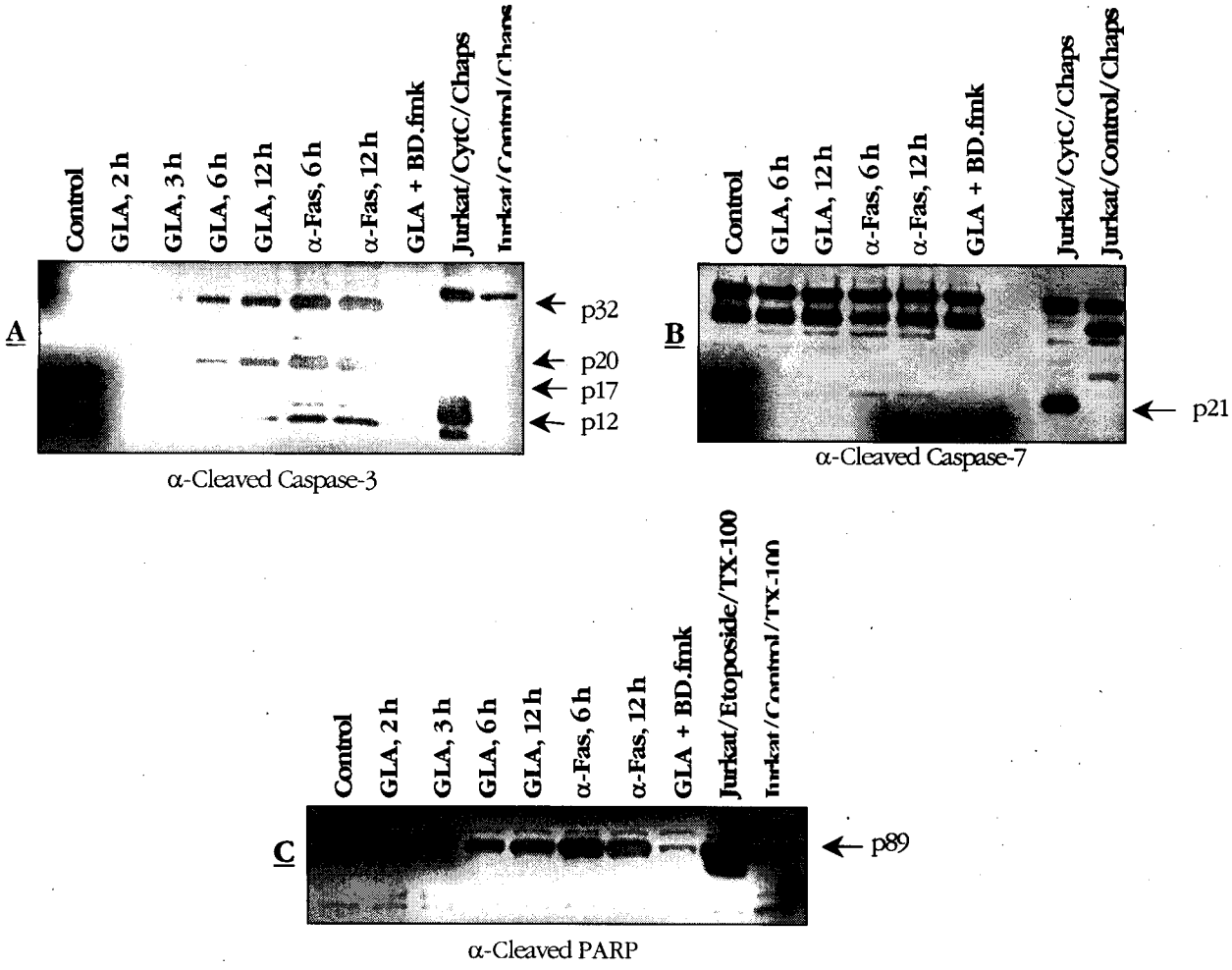

Figure 14: Western blot analysis of GLA- or α-Fas antibody- treated 8E5 cells showing processing of caspase-3 and PARP, and lack of caspase-7 cleavage. Cells were incubated with 15 μg/ml GLA for 2, 3, 6 or 12 hours, or 50 μM BD.fmk for 4 hours followed by incubation with GLA for another 8 hours. Simultaneously, some of the cultures were exposed to 0.25-μg/ml α-Fas antibody for 6 or 12 hours. At the end of the incubation, cells were harvested and lysed as described previously. 20 μg of total protein from each sample was electrophoresed and subjected to immunoprecipitation with α-cleaved caspase-3, α-cleaved caspase-7 or α-cleaved PARP (all from Cell Signaling Technology) along with controls made up of Jurkat cell lysates from cultures treated with either 0.25 mg/ml cytochrome C antibody or 25 μM etoposide as illustrated. The main immunoreactive bands are indicated with arrows.

Effect of GLA on primary $CD4^+$ T cells acutely infected with clinical and laboratory-adapted isolates of HIV-1

We have demonstrated differential induction of apoptosis by GLA in the chronically and productively HIV-infected 8E5 cell line in comparison to its parental uninfected A3.01 cell line. We have also identified the potential pathway of apoptosis by which GLA cytotoxicity is mediated and pointed to possible involvement of oxidative stress as the main predisposing factor. Finally, in the next set of experiments we examined whether the observed GLA cytotoxicity profile in the A3.01/8E5 *in vitro* model of HIV infection could be extended to primary $CD4^+$ T cells acutely infected with two clinical and three laboratory-adapted isolates of HIV-1. The toxicity of GLA in acutely infected donor cells was compared to that in uninfected HIV-seronegative donor cells.

Figure 15 shows results of a typical acute infection experiment. $CD8^+$-depleted mononuclear cells from a single donor were either mock infected or infected with clinical isolates HIV-1_{657} or HIV-1_{714}, or laboratory-adapted isolates HIV-1_{NL43} or HIV-1_{RF} (panel **A**). With results (not shown here) from previous experiments as a guide, we picked a MOI of 0.001 in order to achieve productive infection while minimizing virally induced cytotoxicity. Infected cells were grown for 11 days, at which point culture supernatants were drawn for HIV-1 p24 antigen ELISA, confirming that cells were productively infected. Cells were then exposed to GLA at concentrations shown and incubated for a further three days before assay of proliferation was carried out using WST-1 reagent. There was no difference in IC_{50} of GLA in mock-infected cultures compared to that in HIV-infected cultures infected with any of the four viral isolates. This lack of differential susceptibility to GLA-induced cytotoxicity was not altered by infecting $CD4^+$ cells (from the same donor) with HIV-1_{RF} at a lower MOI (0.0005) and culturing cells for 18 days prior to GLA exposure (panel **B**), even though cells were confirmed to be productively infected by HIV-1 p24 antigen ELISA.

Cytotoxicity of GLA in primary donor $CD4^+$ T cells acutely infected with HIV-1_{657}, HIV-1_{714}, HIV-1_{NL43} or HIV-1_{RF} isolates

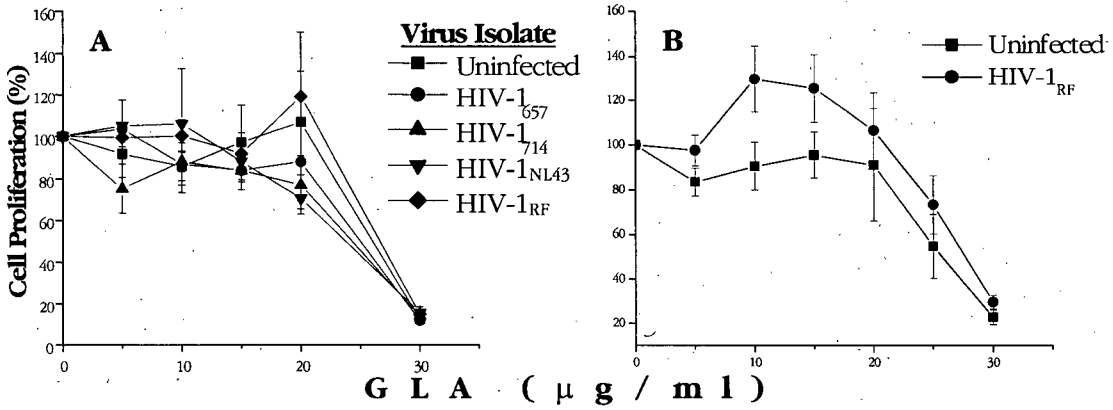

Figure 15: Mononuclear cells were isolated from HIV-1 seronegative donor blood by Ficoll gradient separation and enriched for $CD4^+$ T cells by CD8 T-cell depletion using immunomagnetic beads as described under Materials and Methods. Cells were stimulated with PHA for at least 72 hours and then were either mock-infected or infected with clinical HIV-1 isolates 657 or 714 from NIH, a HIV full-length infectious clone (HIV-1_{NL43}) or laboratory-adapted isolate HIV-1_{RF}, at a multiplicity of 0.001 (panel A), or HIV-1_{RF} isolate at a multiplicity of 0.0004 (B). Infected and mock-infected cells were grown for 11 days (A) or 18 days (B) and then transferred to GLA-supplemented media and incubated for a further three days on 96-well culture plates. Viability was subsequently determined using the WST-1 method as described earlier. Each point on the graph represents four independent measurements from the same experiment.

However, in a separate experiment in which cells were infected with the laboratory isolate HTLV-IIIB, GLA was shown to be five times more cytotoxic in infected cells than mock-infected cells (panel **A, Fig. 16**). Cells were infected with 0.001 infectious units ($TCID_{50}$) per cell following 72 hours of PHA stimulation, grown for seven days as usual, with a culture split on day 3, and then exposed to GLA for three days. The GLA IC_{50} values in mock infected and HTLV-IIIB-infected cells were 51.68 ± 5.45 and 10.18 ± 0.04, respectively. It appeared from these results that susceptibility to GLA-induced cytotoxicity in acute HIV infection *in vitro* models might depend, not only on the viral isolate used, but also on individual donor of $CD4^+$ cells. We addressed the latter question by carrying out a cytotoxicity assay in PBMC obtained from four different HIV-seronegative donors. We observed marked variations in GLA-

induced cytotoxicity against cells from different donors as is shown in panel **B** of figure **16**. $CD4^+$ cells from donor #2 & #3 were resistant to GLA-induced killing, showing proliferation of over 100% at 30 µg/ml GLA. Cells obtained from peripheral blood of donor #1 showed intermediate response to GLA, with approximately 65% cell proliferation at 30 µg/ml GLA compared to the untreated control. Cells from donor #4 exhibited the most susceptibility to GLA-induced cytotoxicity, with 0% cell proliferation at the highest concentration of GLA.

Cytotoxicity of GLA in donor $CD4^+$ T cells acutely infected with the HIV-1_{IIIB} isolate

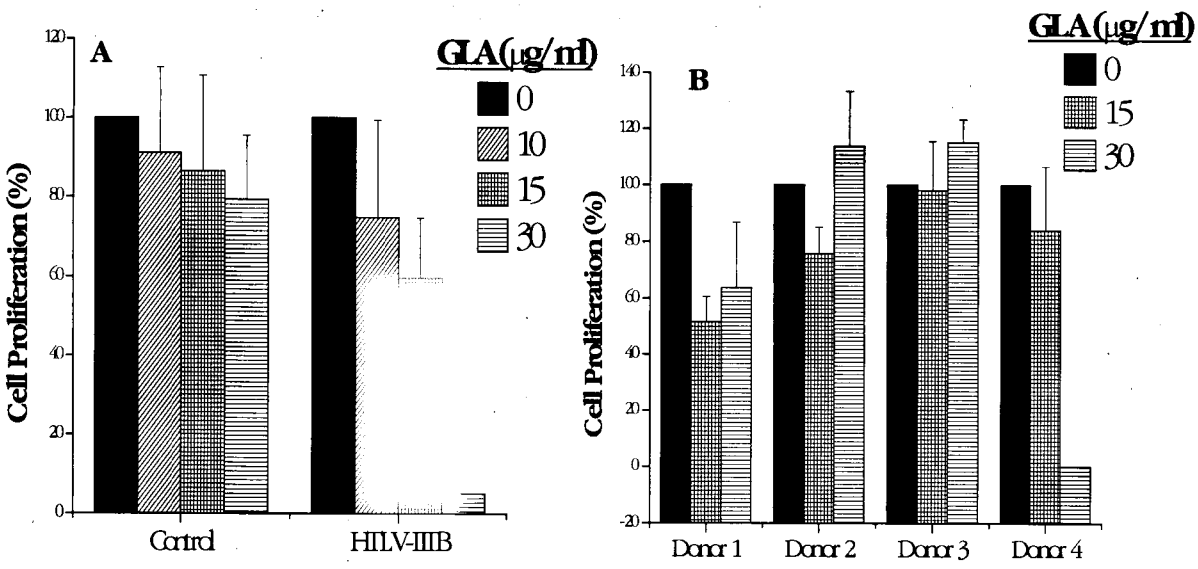

Figure 16: Mononuclear cells were isolated from HIV-1 seronegative donor blood by Ficoll gradient separation and enriched for $CD4^+$ T cells by CD8 T-cell depletion using immunomagnetic beads as described under Materials and Methods. Cells were stimulated with PHA for at least 72 hours and then were either mock infected or infected with HIV-$1_{HTLVIIIB}$ at a multiplicity of infection of 0.001 (panel **A**), grown for 11 days, transferred to GLA-supplemented media and incubated for a further three days on 96-well culture plates. Similarly, cells obtained from HIV-seronegative donors were stimulated with PHA, cultured for seven days and then exposed to GLA for a further 3 days (panel **B**). Viability in both cases was subsequently determined using the WST-1 method as described earlier. Each point on the graph represents four independent measurements from the same experiment.

GLA cytotoxicity against $CD4^+$ T cells isolated from HAART-treated AIDS patients is negatively correlated with patients' viral load

Compared to acute infection of donor T cells, $CD4^+$ T cells isolated from HIV-infected patients might provide a better model for studying GLA activity in primary mononuclear cells. T cells isolated from whole blood of AIDS patients are presumably more representative of *in vivo* populations with regards to oxidative stress as well as proportion of cells that are chronically infected. This is likely best represented in HAART-treated patients who may have fewer newly infected cells than quiescently and chronically infected ones. We therefore sought to establish whether the viral load measurements of HAART-treated patients correlated to GLA-induced cytotoxicity of $CD4^+$cells isolated from these individuals. We obtained $CD4^+$ cells from blood of 12 AIDS patients ranging in viral load from <50 to >30,000 HIV-1 mRNA copies/ml and subjected them to cytotoxicity assay as described in detail under Materials and Methods. Samples were subjectively divided into two categories comprising of 'low' (<2000 HIV-1 mRNA copies/ml) or 'high' (>2000 HIV-1 mRNA copies/ml) viral load. $CD4^+$ cells were isolated and grown in medium supplemented with 50 U/ml IL-2. Of the nine samples in the 'low' viral load category, three were exposed to GLA without undergoing PHA stimulation and the rest were stimulated using very low PHA (0.1 μg/ml) concentration to prevent mitogen-induced cytotoxicity. Notwithstanding PHA stimulation, no attempt was made to induce any of the cultures to produce HIV-1 antigen, which would have required longer incubation. Cells were grown for three days and then transferred to GLA-supplemented growth media. Cell proliferation was measured using WST-1 assay and the results used to determine GLA IC_{50} by means of Boltzman sigmoidal fit of the data. Results of the cytotoxicity assay are summarized in **figure 17**, and IC_{50} values are shown in **table 2** as are corresponding patient viral load measurements and $CD4^+$ cell count. The relationship between GLA cytotoxicity to viral load and CD4 cell count was deduced using correlation analysis. This analysis revealed that GLA cytotoxicity was negatively correlated to patient viral load (correlation coefficient = -0.55), meaning cells from high viral load patients had a tendency towards increased sensitivity to GLA-induced toxicity. Conversely, a positive but weaker correlation (correlation coefficient = 0.32) was observed with regards to CD4 cell count, indicating that cells obtained from individuals with high CD4 cell counts were slightly less sensitive to GLA-induced cytotoxicity.

Cytotoxicity of GLA in primary $CD4^+$ T cells isolated from HAART-treated HIV^+ patients

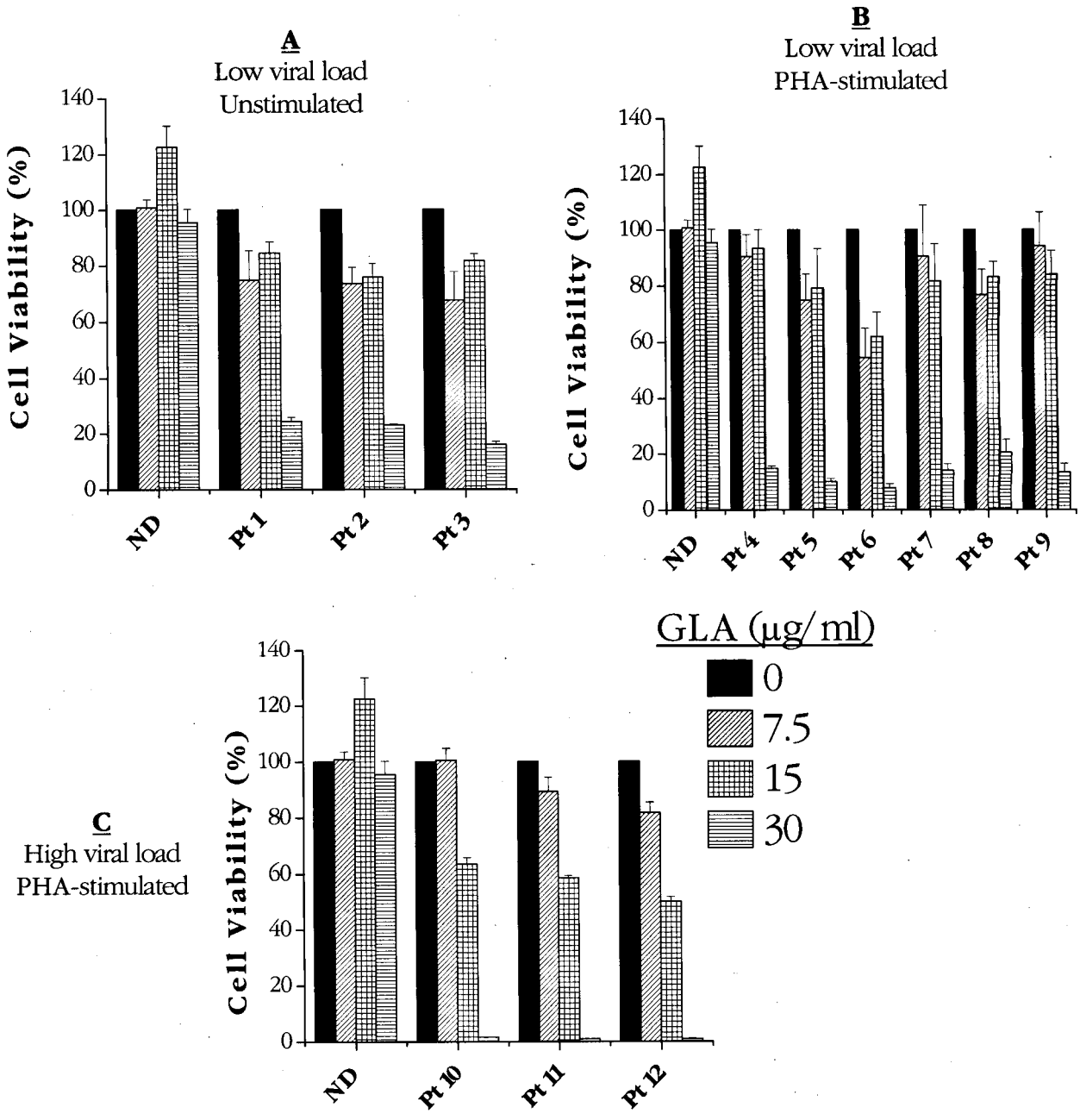

Figure 17: Mononuclear cells were isolated from peripheral blood of normal HIV seronegative donor or HIV^+ patients by Ficoll density gradient centrifugation and enriched for $CD4^+$ cells by $CD8^+$ cell depletion using immunomagnetic beads. Isolated cells were left unstimulated (A) or stimulated in growth media supplemented with 1 ng/ml PHA overnight. Cells were then transferred to IL-2 (50 U/ml) media and cultured for at least three days. After this period, cells were aliquoted to wells of a 96-well microculture plate and grown in media supplemented with GLA for 72 hours. Proliferation of cells was determined by incubating cells with the WST-1 as described in Materials and Methods. The results represent four measurements from one experiment. [ND = Normal (HIV-negative) Donor]

HIV-disease clinical characteristics of patient $CD4^+$ T cell donors and their correlation to GLA cytotoxicity.

Patient #	Viral Load (HIV-1 mRNA copies/ml)	CD4 Cell Count (per μl)	GLA IC_{50} (μg/ml)
1	64	1400	20.9 ± 0.3
2	154	1174	17.3 ± 0.4
3	<50	761	21.3 ± 0.2
4	1207	745	23.8 ± 0.2
5	<50	882	26.1 ± 0.5
6	346	586	12.5 ± 0.2
7	108	759	23.9 ± 0.3
8	1106	575	21.7 ± 0.4
9	<50	1118	21.8 ± 0.2
10	36554	235	15.1 ± 0.2
11	17225	558	16.8 ± 0.1
12	2314	855	14.9 ± 0.1
Correlation Coefficient *v* GLA IC_{50}:	**-0.54898**	**0.320752**	

Table 2: The proliferation data (optical density) from figure 17 were plotted against GLA concentration to generate dose response curves, which were then used to estimate the 50% inhibitory concentration (IC_{50}) for each sample by means of Boltzman sigmoidal fit in Origin™ software. Subsequently, correlation coefficients were calculated between GLA IC_{50} and logarithmic viral load values using MS Excel.

Chapter 4

DISCUSSION

The introduction of HAART regimens for treatment of AIDS has made it possible to suppress plasma viremia to undetectable levels (<50 copies of HIV mRNA/ml) *[56, 58]*. This advance in anti-HIV therapy has reduced morbidity and mortality rates among AIDS patients significantly. However, complete eradication of HIV has proven unworkable partly because of the existence of stable viral reservoirs that persist despite HAART *[21, 43, 58, 95, 128]*. The anatomic location and mechanism of establishment of the HIV reservoir have yet to be fully resolved but a number of anatomical and cellular sanctuaries have been proposed, and in some cases demonstrated. Anatomical sites include the central nervous system, lymphoid tissue of the gastrointestinal tract and genital tract. The main cellular compartments include tissue macrophages and latently infected resting $CD4^+$ T cells, as well as chronically virus-producing activated $CD4^+$ T cells (with undetectable viral replication) and follicular dendritic cells *[Reviewed in 113]*. A pool of latently infected, long-lived tissue macrophages may be maintained by in situ low level viral replication, incoming monocytes infected in peripheral blood and/or latently infected $CD34^+$ hematopoietic stem cells in bone marrow *[73]*. However, most attention has been paid to resting $CD4^+$ T cells latently infected with replication-competent virus. This compartment was the first to be described as a reservoir of HIV in HAART-treated patients *[21, 43, 128]*, and initiation of HAART even as early as 10 days after the onset of primary HIV infection did not prevent its establishment *[22]* thus casting doubt on early institution of HAART as a means to wade off HIV persistence. Subsequently, genomic analysis of rebounding virus after cessation of HAART has suggested that other as-yet-undefined compartments are probably more important sources of re-emerging virus *[24, 58]*. What is indisputable, however, is the need to target HIV reservoirs if eradication of HIV-1 in infected individuals is to be attempted. To achieve this goal, the use of IL-2, TNF-α, IL-6, α-CD3 antibody and therapeutic HIV-specific vaccines to induce the activation of HIV from latently infected, resting $CD4^+$ T cells has been researched with mixed success *[23, 47]*. Increasing attention is being focused on therapeutic strategies of selectively killing cells in

which the virus replicates and/or hides. Prominent among compounds that have been evaluated with some in vivo success in this regard are hydroxyurea (HU) [49, 79] and mycophenolic acid (MPA) [19]. HU works by depleting pools of deoxyribonucleoside triphosphates (dNTP) while MPA depletes pools of guanosine, in addition to direct antiviral activity by both compounds. As such, these two compounds do not selectively target HIV-infected cells so much as they inhibit proliferation of all activated T lymphocytes. We have carried out in vitro evaluation of the PUFA, GLA, that targets HIV-infected cells more specifically than can be achieved with non-specific immunosuppressants. In the past, GLA has been investigated extensively for its selective cytotoxicity in different malignant cells. A number of studies have examined whether GLA induces such selective cytotoxicity in cells infected with viruses, including HIV.

Several mechanisms of action have been proposed to account for GLA-associated cytotoxicity in both malignant and virally infected cells. Chief among these is increased oxidative stress in susceptible cells treated with GLA. We have presented data demonstrating that compared to the parental uninfected A3.01 cell line, GLA selectively kills the chronically and productively HIV-infected 8E5 cell line at a median concentration that is at least three-fold lower in 8E5 cells. Treatment of 8E5 cells with GLA was also associated with an increase in the concentration of MDA and 4-HNE, free radical products of oxidative metabolism which are indicative of increased oxidative stress. Such a GLA-induced increase in oxidative stress was neither observed in control untreated 8E5 cells nor the parental uninfected cell line A3.01. This implicates an inability by 8E5 cells to detoxify products of lipid peroxidation. Furthermore, GLA-induced inhibition of 8E5 cell proliferation was ameliorated by preincubating cells with 2-ME and to a lesser degree ebselen, providing more evidence that a redox imbalance in 8E5 cells predisposes them to GLA killing. The biological actions of 2-ME that might explain its antioxidant effects include enhancement of uptake of the amino acid cysteine, which in turn increases intracellular levels of GSH, and the induction of cells to release thiols into the extracellular milieu [90]. Unlike B-lymphocytes, human T lymphocytes do not require supplementation with 2-ME to prevent oxidation of intracellular SH-groups in culture. However, specific oxidation of SH-groups in human T cells results in apoptotic cell death via a thioredoxin, not GSH, dependent mechanism [111]. HIV infection is associated with systemic and intracellular deficiency of selenium, GSH, GPx and oxidized GSH disulfide

(GSSG)-reductase [92, 117, 118]. GSH is one of the ubiquitous nucleophiles and reducing agents in eukaryotic cells. Therefore, increased uptake of cysteine, resulting from 2-ME supplementation, would protect 8E5 cells against GLA-induced cytotoxicity. However, there is one report suggesting that 8E5 cells are deficient in GPx but express normal levels of glutathione [109]. Since the majority of reports demonstrate GSH deficiency in HIV-infected cells, it is possible the authors underestimated GSH deficiency in 8E5 cells. Alternatively, because the authors measured GPx enzymatic activity rather than its concentration, it is possible that a defect in the enzyme causes requirement of higher than usual intracellular GSH concentration for optimal peroxidase activity. Moreover, the existence of highly conserved open reading frame sequences in the HIV-1*env* gp41 region coding for a homologue of cellular GPx [122] might have bearing on 2-ME protective effect if it turns out that the putative viral peroxidase competitively antagonizes the cellular homologue. Finally, because 2-ME was more effective than Ebselen at inhibiting GLA-induced cytotoxicity, conceivably GSH impairment in 8E5 cells is more important than that of GPx as a determinant of susceptibility. Though indirect, this also provides further evidence in support of possible GSH deficiency in 8E5 cells. The thiol-containing antioxidant NAC is a commonly used inhibitor of T lymphocyte apoptosis, which is believed to undergo intracellular deacetylation and provide cysteine for GSH biosynthesis. NAC has been investigated extensively for potential application in the treatment of HIV infection largely based on its antioxidant properties, but also because it might possess direct anti-HIV-1 activity [17, 68, 101, 102]. Considering its antioxidant mechanism of action, NAC would be expected to provide a protective effect against GLA-induced cytotoxicity similar to that of 2-ME. However, NAC was less effective at protecting 8E5 cells from GLA-induced killing. This is possibly because, unlike 2-ME, NAC does not increase uptake of cysteine but rather undergoes intracellular deacetylation to yield cysteine, which can then be used for GSH biosynthesis. Such a mechanism of action might not be sufficient to overcome thiol antioxidant deficiencies that exist in 8E5 cells. In addition, the actual mechanism of NAC antioxidant activity is still controversial. Contrary to expectations, in one study the anti-apoptosis effects of NAC in the murine T-cell hybridoma DO-11.10 did not correlate with levels of GSH or GSSG [67].

Another major intracellular free radical scavenger that we evaluated in an attempt to block GLA-induced cytotoxicity was α-tocopherol or vitamin E. In our hands, supplementation with

vitamin E did not protect 8E5 cells against GLA-induced cytotoxicity. This is in contrast to reports showing successful inhibition of GLA cytotoxicity by vitamin E in other cell types. We suspect this difference relates to the mechanism of action of vitamin E as a free radical scavenger. Although vitamin E is a major intracellular peroxyl radical scavenger, it depends on other antioxidants; GSH, ascorbic acid and reduced ubiquinone (coenzyme Q), to reduce oxidized vitamin $E^{\bullet}$ (tocopheroxyl radical) back to the antioxidant form (vitamin E) *[16]*. The chemical and enzymatic pathways for regeneration of vitamin E by the three antioxidants as observed in human platelet homogenate are illustrated in **figure 18**. In this model, vitamin E regeneration from vitamin $E^{\bullet}$ depends on the presence of GSH and ascorbic acid. The oxidized form of glutathione, GSSG, is recycled to GSH by glutathione reductase enzyme and NADPH, as well as by reduction of dehydroascorbic acid to ascorbic acid in the presence of glutaredoxin *[16]*. GSH deficiency, as is known to occur in HIV-infected cells, would impair both the reduction of lipid free radicals by GPx as well as regeneration of reduced vitamin E. Since there is also evidence for vitamin C deficiency in HIV-infected cells, this and GSH deficiency could sufficiently explain the failure of vitamin E to prevent GLA-induced cytotoxicity in 8E5 cells.

SOD, a family of enzymes that convert the superoxide anion, $O_2^{\bullet-}$, to H_2O_2 was also not effective against GLA-induced cytotoxicity. Again, this is explainable by lack of catalase enzyme in 8E5 cells. Catalase is responsible for converting H_2O_2 to water. Although H_2O_2 is not as potent an oxidant as $O_2^{\bullet-}$, nevertheless it is toxic enough to induce severe cytotoxicity in susceptible cells.

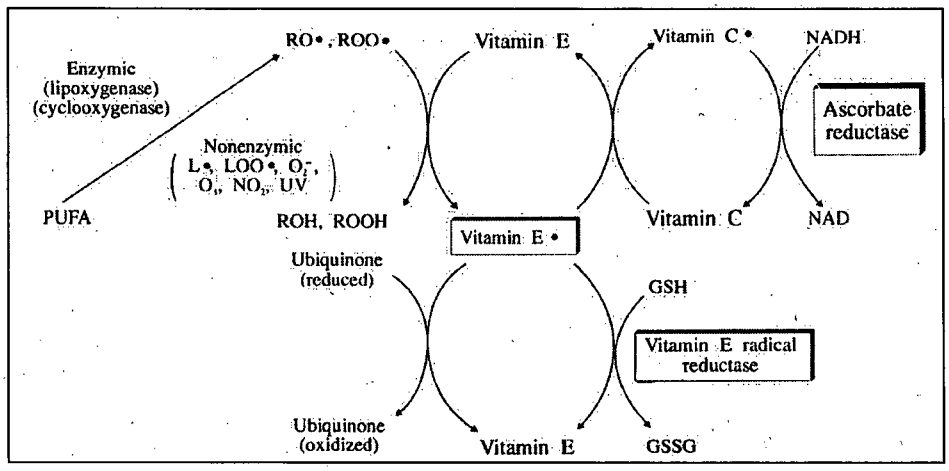

Figure 18: Interaction of antioxidants: Pathways for the oxidation and regeneration of vitamin E according to Chan et al *[16]*.

If GLA induces cytotoxicity via generation of lipid hydroperoxides, then examination of its metabolic transformation might shed light on the biochemical mechanism of this cytotoxicity. Immediately after dietary intake, GLA is converted to dihommo-gamma linolenic acid (DGLA), which then undergoes desaturation and elongation to arachidonic acid. Arachidonic acid is in turn oxidized via the lipoxygenase (LOX) and/or cyclooxygenase (COX) pathways to yield any number of prostaglandins, thromboxanes, leukotrienes, HETEs and lipoxins. In the course of this transformation, dioxygenation of arachidonic acid by one of the four members of the LOX family of enzymes (5-, 8-, 12- or 15-LOX) can result in the formation of active hydroxyperoxyeicosatetraenoic acids (5-, 8-, 12- or 15-HPETE). Because HPETEs have been shown previously to induce apoptosis in 8E5 cells *[109]*, we reasoned that inhibition of LOX in GLA-treated cells could potentially prevent GLA cytotoxicity. To this end, we used NDGA, a naturally occurring broad-spectrum LOX inhibiting lignan present in the evergreen shrub *Larrea divarita*. Low micro-molar concentrations of NDGA resulted in modest inhibition of GLA. However, at higher concentrations NDGA potentiated rather than attenuated GLA-induced cytotoxicity. In the absence of GLA, low to moderate concentrations of NDGA were generally stimulatory of 8E5 cell proliferation. Previous tests of NDGA in human leukocytes and platelets showed that it inhibited 5-, 12- and 15-LOX with IC_{50} values of 0.2, 30 and 30 μM *[61, 107]*. On the basis of this background, our data seem to suggest that it is the 5-LOX

isoform that mediates in GLA-induced cytotoxicity. Although 15-LOX and not 5-LOX was originally believed to be the main LOX isoform in T lymphocytes *[89]*, based on demonstration of 5-LOX activating protein (FLAP) expression, leukotriene A_4 hydrolase activity and response to 5-LOX-specific inhibitory response in monocyte-free environment, strong evidence is emerging that T lymphocytes express this isoform. Therefore, NDGA inhibition data from this study probably reflect the complexity of both NDGA actions and the role of LOX enzymes in cellular biochemistry *[30]*. LOX metabolites are capable of either stimulatory or suppressive effects depending on cell type and other factors *[94]*. The actions of NDGA and LOX inhibitors in general are equally complex. Although NDGA is a widely used LOX inhibitor, it also inhibits several T lymphocyte functions, including mitogen induced breakdown of inositol lipids, rise in cytosolic free Ca^{2+} and IL-2 production *[94]*. Moreover, structurally unrelated inhibitors of LOX, including NDGA, esculetin, AA861 and 5,8,11,14-eicosatetraynoic acid (ETYA), were shown to suppress mitogen-induced proliferation of PMBC by counteracting protein kinase C mediated events *[94]*. The optimal inhibitory concentration in this case was in the range of 16-33 μM for all compounds, and NDGA inhibited PKC-mediated proliferative response by 25-30% at 4 μM. It is noteworthy that GLA and its metabolite, DGLA, also suppress total PKC activity in human lymphocytes in response to PMA stimulation *[104]*. Although it is not clear whether similar inhibition would occur in established cell lines, mutual potentiation between GLA and NDGA is possible with regards to inhibition of PKC and T cell proliferation. Other actions of NDGA that are unrelated to its effect on LOX enzyme include inhibition of COX, phospholipase A_2 and cytochrome P-450, but these have not been demonstrated in lymphocytic cells *[25]*. NDGA was also demonstrated to trigger rapid lipid peroxidation in rat W256 monocytoid carcinosarcoma cells leading to depletion of cytosolic and mitochondrial GSH pools and induction of apoptosis *[3, 120]*. The authors stated that the LOX-unrelated effects of NDGA are generally elicited at ≥20 μM *[120]*. Therefore, lack of clear-cut inhibition of GLA-related cytotoxicity by NDGA is not conclusive evidence that LOX does not mediate GLA effects in 8E5 cells. Further experimentation is necessary to dissect the role of LOX enzymes in GLA-induced cytotoxicity. Although there was no prior evidence implicating COX pathway participation in GLA-induced cytotoxicity, it is pertinent that products of COX metabolism, notably E-series prostaglandins, have been shown to suppress proliferation of IL-2-dependent human T lymphocyte *[110]*.

Therefore, we examined the possible involvement of COX metabolic products in GLA-induced cytotoxicity using the COX inhibitor ibuprofen. Inhibition of COX with ibuprofen protected 8E5 cells against GLA-induced cytotoxicity at low to intermediate concentrations of the inhibitor, but caused greater cytotoxicity at higher doses than was seen in cultures treated with either GLA or ibuprofen alone. Metabolism of GLA via the COX pathway may therefore play a role in GLA cytotoxicity. In a study of DGLA, AA and eicosapentaenoic acid (EPA), three metabolites of GLA, authors concluded that inhibition of IL-2-dependent T cell growth was independent of COX metabolism *[82, 110]*. However, this determination was based on absence of prostaglandin production as a result of fatty acid treatment, and also lack of inhibition of cytotoxicity by COX antagonist indomethacin. Moreover, these observations involved high concentrations It is not clear which pathway, LOX or COX, is more important in this regard. It is also noteworthy that conversion of arachidonic acid by COX generates reactive oxygen intermediates that are reduced to upstream prostaglandins in a reaction involving a GSH-dependent peroxidase (PG hydroperoxidase) *[89]*. It is conceivable that deficiency of GSH in 8E5 cells might render them preferentially susceptible to toxicity induced by reactive lipid hydroperoxides generated during COX as well as LOX metabolism of PUFA. Oxidized lipid products as might be generated via the LOX or COX metabolic pathways play a crucial role in cell homeostasis, stimulating cell proliferation or triggering cellular cascades that may lead to apoptosis *[31, 78, 93]*.

Having demonstrated that GLA induced selective cytotoxicity in 8E5 cells with possible involvement of oxidative metabolic pathways, we next examined treated cells to determine the mechanism of cell death. Potential involvement of specific metabolic pathways would suggest that apoptosis rather than necrosis was the predominant mode of death in GLA treated cells. This is because, unlike necrosis, apoptosis is a genetically controlled and physiologically regulated process of cell death with characteristic morphologic and biochemical features. We examined apoptosis by two different methods and found that the cytotoxicity of GLA in 8E5 cells was associated with externalization of phosphatidylserine and increased DNA fragmentation, suggesting induction of apoptosis. The occurrence of apoptosis in HIV-infected cells, both in vivo and in vitro, is a subject of extensive investigation, with still many outstanding issues. Apoptosis is often cited as one of the phenomena leading to $CD4^+$ T cell depletion in HIV infected cells. There are likely multiple pathways of apoptosis stimulated by

HIV infection. Apoptosis has been demonstrated to be triggered by gp120 and gp41 expressed on the surface of infected cells, which interact with CD4 receptors on the surface of neighboring infected cells *[54, 74, 123]*. In addition, chronic stimulation of the immune system in HIV infection has been shown to deregulate Bcl-2, Fas and cytokine expression thus making T cells highly prone to spontaneous apoptosis in vitro *[53, 54]*. From these data, it would appear that prevention of apoptosis in HIV-infected cells has potential to curtail progression of HIV disease. However, although activation-dependent apoptosis of patient $CD4^+$ cells contributes to T helper cell depletion, the majority of dying cells in lymph nodes are bystander cells not producing HIV RNA *[42]*. Depletion of $CD4^+$ cells in peripheral blood is likely the result of these cells homing to lymph nodes from the periphery due to HIV-induced upregulation of the adhesion molecule L-selectin *[26]*. Furthermore, it has been proposed that a small population of latently HIV-1-infected long-lived cells may be responsible for most of the 'bystander' apoptosis by producing protease-defective , gp-120-containing (L2) particles that stimulate the $CD4^+/CD38^-$ subset of T cells to increase their surface expression of CD25 and become highly effective killers *[62]*. Regardless of the mechanism of 'bystander' apoptosis, the majority of the evidence implicates the infeted cell as the mediator of the apoptosis and immune depletion. Therefore, agents which selectively induce apoptosis in HIV infected cells should prove beneficial, particularly in combination with HAART therapy. *[5]*, This is critical especially since there is increasing evidence that HIV establishes long-lived reservoirs of infected cells partly by manipulating the apoptotic machinery in its favor *[8, 28, 50, 87, 103]* and the recent evidence that these reservoirs are resistant to HAART therapy . A logical approach would constitute promoting apoptosis in infected cells while protecting 'bystander' cells. Compounds like GLA which promote apoptosis of chronically HIV-infected cells have the potential to limit HIV cytopathicity if used in combination with HAART.

In order to determine the potential pathways of apoptosis induction by GLA, we performed RPA and Western blot screening of untreated and drug treated cells for expression of apoptosis-related genes and proteins, including death receptors, caspases, granzymes and Bcl-2 family of proteins. We did not observe substantial differences in mRNA expression of any caspase, granzyme or Bcl-2-type mRNAs between untreated and GLA treated cells of either A3.01 or 8E5 cell line. In contrast to A3.01 cells, however, control 8E5 cells did not express

FADD mRNA. Subsequent to GLA treatment of 8E5 cells, mRNA expression of this death domain was increased substantially. Although this might have suggested involvement of the CD95/Fas or extrinsic pathway of apoptosis in GLA-induced death of 8E5 cells, we could not detect differential expression of FADD protein in untreated and GLA-treated 8E5 cells by immunoprecipitation. The difference between A3.01 and 8E5 cells with respect to FADD mRNA expression is an interesting observation although we did not pursue it further for the purpose of this thesis. For one, it could represent a means for HIV to protect 8E5 cells against viral cytotoxicity. As further evidence for possible lack of involvement of the extrinsic pathway of apoptosis in GLA-mediated killing of 8E5 cells, immunoprecipitation did not demonstrate differential expression or processing of caspase-8 or caspase-10. On the other hand, although we observed neither GLA-related modification of TRAIL mRNA nor that of expression of cytochrome C in 8E5 cells, we observed a small but discernible increase in expression of the large active subunit of caspase-9. This suggests that GLA-induced apoptosis might be mediated via the intrinsic pathway although further experimentation is necessary to confirm this possibility. Especially since a similar increase in caspase-9 cleavage product was seen in 8E5 cells treated with the α-Fas antibody, which is known to cause apoptosis via the extrinsic pathway. Also, α-Fas antibody caused a demonstrable increase in expression of FADD protein and caspase-8 18 kDa subunit. Therefore, caspase-9 maturation seen in α-Fas treated cells could be explained by 'cross-talk' between intrinsic and extrinsic pathways of apoptosis, possibly mediated by the Bcl-2 family member Bid. However, Western blot analysis did not reveal processing of Bid to its active form in either GLA or α-Fas treated 8E5 cells, thus casting doubt on 'cross-talk' as an explanation for the slight increase in caspase-9 immunoreactivity. Since much is still unknown about the communication of the two apoptosis pathways, it could be possible that another as-yet-undetermined Bcl-2 homologues plays a similar role to that of Bid. It is also possible that the antibodies used to screen for either cleaved caspase-8 or caspase-9, or both, were not sensitive enough to detect these proteins. Alternative approaches to confirm involvement of the intrinsic apoptosis pathway in GLA-induced cytotoxicity would include assaying mitochondrial membrane versus cytosolic cytochrome C rather than total cellular protein, measuring changes in mitochondrial membrane potential ($\Delta\Psi_m$) and assaying for change in ATP production. Nonetheless, participation of caspases in GLA-mediated toxicity was proved by successful inhibition of

GLA-induced apoptosis in 8E5 cells by means of the broad-spectrum caspase inhibitor BD.fmk, and demonstration of cleavage of effector caspase-3. GLA-induced cleavage of caspase-3 led to processing of the nuclear protein PARP, which is involved in DNA repair resulting from stress-related stimuli.

In order to selectively target HIV-infected cells, which may be producing little or no viral proteins, for killing, it is necessary to identify biochemical markers that distinguish infected from uninfected cells.The 8E5 cell line provides a model in which to evaluate compounds such as GLA because of its resistance to HIV-induced programmed death. However, since each 8E5 cell contains an integrated copy of HIV genome, it is not possible, using this model, to compare the effect of GLA against infected and uninfected cells within one population. We addressed this methodological shortcoming using two approaches. The first was to compare the effects of GLA in 8E5 cells relative to the uninfected parental cell line, A3.01, as discussed above. We had also determined on the basis of mean fluorescence intensity data, that approximately 80% of 8E5 cells consistently stained bright for intracellular HIV core antigen. We interpreted this to mean that a proportion of cells expressed fewer molecules of the viral antigen at any given time. The second approach, therefore, was to carry out bivariate flow cytometric analysis of 8E5 cells and examine the apoptotic status of cells staining bright for intracellular HIV core antigen as opposed to those staining dim. GLA-treated cultures had a higher proportion of cells with low mean fluorescence for HIV-1 core antigen compared to control untreated cells. It appeared, therefore, that cells with low copy number of HIV core antigen molecules (dim) were less susceptible to GLA-induced apoptosis than those staining brightly. However, it was not possible to determine the lower limit for HIV core antigen positivity in this assay . Regardless , eventually all cells became apoptotic suggesting that there was no absolute association between apoptosis induction and viral antigen expression and that other viral induced cellular factors are likely involved. Theoretically, quiescently, chronically HIV-infected cell lines, e.g. U1 or OM-10.1, that produce viral antigen only upon stimulation with mitogens or cytokines would be better in vitro models for studying GLA-induced selective cytotoxicity. But in many cases induction of HIV in these cells results in some level of apoptosis inductions, thereby confounding any potential observations on cytotoxicity.

GLA induction of programmed death in 8E5 cells was also accompanied by arrest of cells in G_0/G_1 phase of the cell cycle. This is consistent with other studies which demonstrate GLA inhibition of cell division and cell cycle arrest [33, 34, 114]

Next, we extended the model to HIV infected cells in vivo by showing GLA-associated differential cytotoxicity in primary $CD4^+$ cells isolated from HAART-treated AIDS patients when compared to uninfected HIV-seronegative donor cells. The GLA-induced cytotoxicity correlated positively with increasing viral load in these HAART treated patients, in agreement with the 8E5 model in that infected cells were more sensitive to GLA treatment than uninfected controls. These observations strengthen the relevance of the 8E5 model to the situation *in vivo*. On the other hand,examination of GLA-induced cytotoxicity in primary mononuclear cells, either uninfected or infected *de novo* with laboratory or clinical HIV isolates, revealed selectivity in cells infected with one of the isolates, HIV-1 IIIB, but not in five others. Possible reasons for lack of clearly selective induction of cytotoxicity in the acute HIV-infection model include the probability that acutely infected T cells are at a relatively lower state of oxidative stress than chronically infected ones. Although this is testable by keeping HIV-infected cells in culture long enough to precipitate oxidative stress, such cultures lose viability within two to three weeks, thus making it difficult to establish a reproducible model. Secondly, viral isolates may engender differing degrees of oxidative stress depending on susceptibility of the cells to infection, cytopathicity of the isolate or other factors. Therefore, experimentation beyond the scope of this thesis appears necessary to reveal factors behind this variability and to develop a reproducible model to determine the effects, if any, of GLA in acute HIV infection *in vitro* and *in vivo*. Moreover, it appears likely that the extent of cytotoxicity in acutely HIV-infected primary $CD4^+$ T cells will vary according to donor. This is likely due to presence of cellular factors that may determine increased susceptibility to GLA among some individuals. It may also be a reflection of different levels of oxidative stress among donors.

In summary, previous work by ourselves and others have shown that GLA is cytotoxic to HIV-infected cells compared to the uninfected counterparts in T cell line models of productive infection. This study extends that work by demonstrating that several mechanisms contribute to GLA-induced cytopathicity. Not only does oxidative stress contribute to cytopathicity but apoptosis also plays a significant role and may be a consequence of GLA-

induced increase in oxidative stress. We demonstrated differential FADD gene expression between untreated and GLA-treated cells and specific cleavage of caspase-3 and PARP in 8E5 cells undergoing GLA-induced apoptosis. In addition, we showed a trend towards increased sensitivity to GLA-induced cytopathicity in PBMCs isolated from HAART treated AIDS patients as compared to PBMCs from HIV-negative donors. These data are of interest in light of recent studies showing rebound of HIV upon withdrawal of HAART therapy and provide a basis for further evaluation of combination therapies that include cytotoxic compounds such as GLA. The selectivity of GLA for HIV-infected cells and its relatively low toxicity to normal cells could provide a means to target long-lived, productively infected cells that comprise part of the HIV reservoir for eradication.

REFERENCE:

1. Adachi A, Gendelman H, Koenig S, Folks T, Willey R, Rabson A and Martin M. Production of acquired immunodeficiency syndrome-associated retrovirus in human and nonhuman cells transfected with an infectious molecular clone. *Journal of Virology* **59**, 284-291 (1986)
2. Adams J and Cory S. The *bcl-2* protein family: arbiters of cell survival. *Science* **281**, 1322-26 (1998)
3. Agarwal R, Wang Z, Bik D and Mukhtar H. Nordihydroguaiaretic acid, an inhibitor of lipoxygenase, also inhibits cytochrome P-450-mediated monooygenase activity in rat epidermal and hepatic microsomes. *Drug Metabolism and Disposition* **19**, 620-624 (1991)
4. Anel A, Naval J, Desportes P, Gonzalez B, Uriel J and Pineiro A. Increased cytotoxicity of polyunsaturated fatty acids on human tumoral B and T-cell lines compared with normal lymphocytes. *Leukemia* **6**, 680-688 (1984)
5. Antoni B, Sabbatini P, Rabson A and White E. Inhibition of apoptosis in human immunodeficiency virus-infected cells enhances virus production and facilitates persistent infection. *Journal of Virology* **69**, 2384-92 (1995)
6. Aoki K, Nakashima H, Hattori T, Shiokawa D, Ni-imi E, Tanimoto Y, Maruta H, Uchumi F, Kochi M, Yamamoto N et al. Sodium benzylideneascorbate induces apoptosis in HIV-replicating U1 cells. *FEBS Letters* **351**, 105-108 (1994)
7. Aukrust P, Svardal A, Muller F, Lunden B, Berge R, Ueland P and Froland S. Increased levels of oxidized glutathione in $CD4^+$ lymphocytes associated with distrubed intracellular redox balance in human immunodeficiency virus type 1 infection. *Blood* **86**, 258-267 (1995)
8. Azad A. Could Nef and Vpr proteins contribute to disease progression by promoting depletion of bystander cells and prolonged survival of HIV-infected cells? *Biochemical and Biophysical Research Communications* **267**, 677-685 (2000)
9. Bégin M, Ells G and Horrobin D. Polyunsaturated fatty acid-induced cytotoxicity against tumor cells and its relationship to lipid peroxidation. *Journal of the National Cancer Institute* **80**, 188-194 (1988)
10. Begin M, Ells G, Das U and Horrobin D. Differential killing of human carcinoma cells supplemented with n-3 and n-6 polyunsaturated fatty acids. *Journal of the National Cancer Institute* **77**, 1053-1062 (1986)
11. Boldin M, Mett I, Varfolomeev E, Chumakov I, Shemer-Avni Y, Camonis J, Wallach D. Self-association of the 'death domains' of the p55 tumor necrosis factor (TNF) receptor and Fas/APO1 prompts signaling for TNF and Fas/APO1 effects. *Journal of Biological Chemistry* **270**, 387-91 (1995)
12. Brick D, Burke R, Minkley A and Upton C. Ectromelia virus virulence factor p28 acts upstream of caspase-3 in response to UV light-induced apoptosis. *Journal of General Virology* **81**, 1087-1097 (2000)
13. Buhl R, Jaffe H, Holroyd K, Wells F, Mastrangeli A, Saltini C, Cantin A and Crystal R. Systemic glutathione deficiency in symptom-free HIV-seropositive individuals. *The Lancet* **2**, 1294-1298 (1989)
14. Buttke TM & Folks T. Complete replacement of membrane cholesterol with 4,4',14-trimethyl sterols in a human T cell line defective in lanosterol demethylation. *Journal of Biological Chemistry* **267**, 8819-8826 (1992)
15. Cayota A, VuillierF, Gonzalez G, and Dighiero G. In vitro antioxidant

treatment recovers proliferative responses of anergic CD4+ lymphocytes from human immunodeficiency virus-infected individuals. *Blood* **87**, 4746-4753 (1996)
16. Chan A, Chow C and Chiu D. Interaction of antioxidants and their implication in genetic anemia. *Experimental Biology and Medicine* **222**, 274-282.
17. Chandra A, Demirhan I, Arya S and Chandra P. D-penicillamine inhibits transactivation of human immunodeficiency virus type-1 (HIV-1) LTR by transactivator protein. *FEBS Letters* **236**, 282-286 (1988)
18. Chang S, Bowman B, Weiss J, Garcia R and White T. The origin of HIV-1 isolate HTLV-IIIB. Nature **363**, 466-469 (1993)
19. Chapuis A, Rizzardi G, D'Agostino C, Attinger A, Knabenhans C, Fleury S, Acha-Orbea H and Pantaleo G. Effects of mycophenolic acid on human immunodeficiency virus infection in vitro and in vivo. *Nature Medicine* **6**, 762-768 (2000)
20. Chinnaiyan A, O'Rourke K, Tewari M, Dixit V. FADD, a novel death domain-containing protein, interacts with the death domain of Fas and initiates apoptosis. *Cell* **81**, 505-12 (1995)
21. Chun T, Stuyver L, Mizell S, Ehler L, Mican J, Baseler M, Lloyd A, Nowak M and Fauci A. Presence of an inducible HIV-1 latent reservoir during highly active antiretroviral therapy. *Proceedings of the National Academy of Sciences* **USA 94**; 13193-13197 (1997).
22. Chun T-W, Engel D, Berrey M, Shea T, Corey L and Fauci A. Early establishment of a pool of latently infected, resting CD4+ T cells during primary HIV-1 infection. *Proceedings of the National Academy of Sciences USA* **95**, 8869-8873 (1998)
23. Chun T-W and Fauci A. Latent reservoirs of HIV: Obstacles to the eradication of virus. *Proceedings of the National Academy of Sciences USA* **96**, 10958-10961 (1999)
24. Chun T, Davey R Jr, Ostrowski M, Shawn J, Engel D, Mullins J and Fauci A. Relationship between pre-existing viral reservoir and the re-emergence of plasma viremia after discontinuation of highly active anti-retroviral therapy. *Nature Medicine* **6**, 757-761 (2000)
25. Chung-Ren J and Ching-Jiunn T. Mechanisms of nordihydroguaiaretic acid-induced $[Ca^{2+}]_i$ increases in MDCK cells. *Life Sciences* **66**, 1753-1762 (2000)
26. Cloyd M, Chen J and Wang L. How does HIV cause AIDS? The homing theory. *Molecular Medicine Today* **6**, 108-111 (2000)
27. Cohen O and Fauci A. HIV/AIDS in 1998—gaining the upper hand? *Journal of the American Medical Association* **280**, 87-88 (1998)
28. Conti L, Matarrese P, Varano B, Gauzzi M, Sato A, Malorni W, Belardelli F and Gessani S. Dual role of the HIV-1 Vpr protein in the modulation of the apoptotic response of T cells. *The Journal of Immunology* **165**, 3293-3300 (2000)
29. Coppola S and Ghibelli L. GSH extrusion and the mitochondrial pathway of apoptotic signalling. *Biochemical Society Transactions* **28**, 56-61 (2000)
30. Dailey L and Imming P. 12-lipoxygenase: classification, possible therapeutic benefits from inhibition, and inhibitors. *Current Medicinal Chemistry* **6**, 389-98 (1999)
31. Datta K, Biswal S, Xu J, Towndrow K, Feng X and Kehrer J. A relationship between 5-lipoxygenase-activating protein and bcl-X_L expression in murine pro-B lymphocytic FL5.12 cells. *Journal of Biological Chemistry* **273**, 28163-169 (1998)
32. de Kock M, Lottering M.-L, Grobler J, Viljoen C, le Roux M and Seegers J. The induction of apoptosis in human cervical carcinoma (HeLa) cells by gamma-linolenic acid. *Prostaglandins, Leukotrienes and Essential Fatty Acids* **55**, 403-411 (1996)

33. De Kock M, Lottering M and Seegers J. Differential cytotoxic effects of gamma-linolenic acid on MG-63 and HeLa cells. *Prostaglandins, leukotrienes and essential Fatty acids* **51**, 109-120 (1994)
34. De Kock M, Seegers J and Els H. Effects of gamma-linolenic acid on mitosis and nuclear morphology in osteogenic sarcoma cells. *South Africa Medical Journal* **81**, 467-72 (1992)
35. Depraetere V and Golstein P. Fas and other cell death signaling pathways. *Seminars in immunology* **9**, 93-107 (1997)
36. Dornadula G, Zhang H, VanUitert B, Stern J, Livornese L Jr, Ingerman M, Witek J, Kedanis R, Natkin J, DeSimone J and Pomerantz R. Residual HIV-1 RNA in blood plasma of patients taking suppressive highly active antiretroviral therapy. *Journal of the American Medical Association* **282**, 1663-1668 (1999)
37. Duvall E and Wyllie A. Death and the cell. *Immunology Today* **7**, 115-9 (1986)
38. Eck H-P, Gmunder H, Hartmann M, Petzoldt D, Daniel V and Droge W. Low concentrations of acid-soluble thiol (cysteine) in the blood plasma of HIV-1-infected patients. *Biological Chemistry Hoppe Seyler* **370**, 101-108 (1989)
39. Ells G, Chisholm K, Simmons V and Horrobin D. Vitamin E blocks the cytotoxic effect of γ-linolenic acid when administered as late as the time of onset of cell death – insight into the mechanism of fatty acid induced cytotoxicity. *Cancer Letters* **98**, 207-11 (1996)
40. Favier A, Sappey C, Leclerc P, Faure P and Micoud M. Antioxidant status and lipid peroxidation in patients infected with HIV. *Chemico-Biological Interactions* **91**, 165-180 (1994)
41. Finkel T and Banda N. Indirect mechanisms of HIV pathogenesis: how does HIV kill T cells?. *Current Opinion in Immunology* **6**, 605-615 (1994)
42. Finkel T, Tudor Williams G, Banda N, Cotton M, Curiel T, Monks C, Baba T, Ruprecht R and Kupfer A. Apoptosis occurs predominantly in bystander cells and not in productively infected cells of HIV- and SIV-infected lymph nodes. *Nature Medicine* **2**, 129-134 (1994)
43. Finzi D, Hermankova M, Pierson T, Carruth L, Buck C, Chaisson R, Quinn T, Chadwick K, Margolick J, Brookmeyer R, Gallant J, Markowitz M, Ho D, Richman D and Siliciano R. *Science* **278**, 1295-1300 (1997)
44. Foley G, Lazarus H, Farber S, Uzman B, Boone B and McCarthy R. Continuous culture of human lymphoblasts from peripheral blood of a child with acute keukemia. *Cancer* **18**, 522-529 (1965)
45. Folks T, Powel D, Lightfoote M, Koenig S, Fauci A, Benn S, Rabson A, Daugherty D, Gendelman, H, Hoggan M, et al. Biological and biochemical characterization of a cloned Leu-3-cell surviving infection with the acquired immune deficiency syndrome retrovirus. *Journal of Experimental Medicine* **164**, 280-290 (1986)
46. Folks T, Benn S, Rabson A, Theodore T, Hoggan M, Martin M, Lightfoote M and Sell K. Characterization of a continuous T-cell line susceptible to the cytopathic effects of the acquired immunodeficiency syndrome (AIDS)-associated retrovirus. *Proceedings of the National Academy of Sciences USA* **82**, 4539-4543 (1985)
47. Fraser C, Ferguson N, Ghani A, Prins J, Lange J, Goudsmit J, Anderson R and de Wolf F. Reduction of the HIV-1-infected T-cell reservoir by immune activation treatment is dose-dependent and restricted by the potency of antiretroviral drugs. *AIDS* **14**, 659-669 (2000)
48. Furtado M, Callaway D, Phair J, Kunstman K, Stanton J, Macken C, Perelson A and Wolinsky S. Persistence of HIV-1 transcription in peripheral-blood mononuclear cells in patients receiving potent antiretroviral therapy. *New England Journal of Medicine* **340**, 1614-1622 (1999)

49. Gao W, Johns D and Mitsuya H. Anti-human immunodeficiency virus type 1 activity of hydroxyurea in combination with 2',3'-dideoxynucleosides. *Molecular Pharmacology* **46**, 767-772 (1994)
50. Geleziunas R, Xu W, Takeda K, Ichijo H and Greene W. HIV-1 Nef inhibits ASK-1-dependent death signalling providing a potential mechanism for protecting the infected host cell. *Nature* **410**, 834-838 (2001)
51. Gendelman H, Theodore T, Willey R, McCoy J, Adachi A, Mervis R, Venkatesan S and Martin M. Molecular characterization of a polymerase mutant human immunodeficiency virus. *Virology* **160**, 323-329 (1987)
52. Gibellini D, Caputo A, Celeghini C, Bassini A, La Placa M, Capitani S and Zauli G. Tat-expressing Jurkat cells show an increased resistance to different apoptotic stimuli, including acute human immunodeficiency virus-type 1 (HIV-1) infection. *British Journal of Haematology* **89**, 24-33 (1995)
53. Gougeon M. Programmed cell death in HIV infection: Dysregulation of Bcl-2 and Fas pathways and contribution to AIDS pathogenesis. *Psychoneuroendocrinology* **22**, S33-S39 (1997)
54. Gougeon M.-L and Montagnier L. Programmed cell death as a mechanism of CD4 and CD8 T cell deletion in AIDS. Molecular control and effect of highly active anti-retroviral therapy. *Annals of the New York Academy of Sciences* **887**, 199-212 (1999)
55. Greenway A, Azad A and McPhee D. Human immunodeficiency virus tpe 1 Nef protein inhibits activation pathways in peripheral blood mononuclear cells and T-cell lines. *Journal of Virology* **69**, 1842-1850 (1995)
56. Gulick R, Mellors J, Havlir D, Eron J, Gonzalez C, McMahon D, Richman D, Valentine F, Jonas L, Meibohm A, Aemini E and Chodakewitz J. Treatment with indinavir, zidovudine, and lamivudine in adults with human immunodficiency virus infection and prior antiretroviral therapy. *New England Journal of Medicine* **337**, 734-739 (1997)
57. Hakem R, Hakem A, Duncan G, Henderson J, Woo M, Soengas M, Elia A, de la Pompa J, Kagi D, Khoo W, Potter J, Yoshida R, Kaufman S, Lowe S, Penninger J and Mak T. Differential requirement for caspase 9 in apoptotic pathways in vivo. *Cell* **94**, 339-352 (1998)
58. Hammer S, Squires K, Hughes M, Grimes J, Demeter L, Currier J, Eron J Jr, Feinberg J, Balfour H Jr, Deyton L, Chodakewitz J and Fischl M. A controlled trial of two nucleoside analogues plus indinavir in persons with human immunodeficiency virus infection and CD4 cell counts of 200 per cubic milimeter or less. AIDS Clinical Trials Group 320 Study Team. *New England Journal of Medicine* **337**; 725-733 (1997)
59. Henkart P. ICE family proteases: Mediators of all apoptotic cell death? *Immunity* **4**, 195-201 (1996)
60. Hildeman D, Mitchell T, Teague T, Henson P, Day B, Kappler J and Marrack P. Reactive oxygen species regulate activation-induced T cell apoptosis. *Immunity* **10**, 735-744 (1999)
61. Hope W, Welton A, Nagy-Fiedler C, Bernardo-Batula C and Coffey J. In vitro inhibition of the biosynthesis of slow reacting substance of anaphylaxis (SRS-A) and lipoxygenase activity by quercetin. *Biochemical Pharmacology* **32**, 367-371 (1983)
62. Ikuta K, Kameoka M and Luftig R. AIDS pathogenesis: the role of accessory gene mutations, leading to formation of long-lived persistently infected cells and/or apoptosis-inducing HIV-1 particles. *Virus Research* **52**, 145-156 (1997)
63. Inglot A, Piasecki E, Zaczynska E and Zielinska-Jenczylik J. Seleno-organic compounds induce interferon and tumor necrosis factor in human but not in rat or mouse lymphoid cells. *Archium Immunologiae et Therapiae Experimentalis* **40**, 169-173 (1992)

64. Ishiyama M, Tominaga H, Shiga M, Sasamoto K, Ohkura Y and Ueno K. A combined assay of cell viability and in vitro cytotoxicity with a highly water-soluble tetrazolium salt, neutral red and crystal violet. *Biological & Pharmaceutical Bulletin* **19**, 1518-1520 (1996)
65. Jayadev S, Linardic C and Hannun Y. Identification of arachidonic acid as a mediator of sphingomyelin hydrolysis in response to tumor necrosis factor α. *Journal of Biological Chemistry* **269**, 5757-5763 (1994)
66. Jiang W, Hiscox S, Horrobin D, Hallett M, Mansel R and Puntis M. Expression of catenins in human cancer cells and its regulation by n-6 polyunsaturated fatty acids. *Anticancer Research* **15**, 2569-2574 (1995)
67. Jones D, Maellaro E, Jiang S, Slater A and Orrenius S. Effects of N-acetyl-L-cysteine on T-cell apoptosis are not mediated by increased cellular glutathione. *Immunology Letters* **45**, 205-209 (1995)
68. Kalebic T, Kinter A, Poli G, Anderson M, Meister A and Fauci A. Suppression of human immunodeficiency virus expression in chronically infected monocytic cells by glutathione, glutathione ester, and N-acetylcysteine. *Proceedings of the National Academy of Sciences* USA **88**, 986-990 (1991)
69. Kerr J, Wyllie A and Currie A. Apoptosis: A basic biological phenomenon with wide-ranging implications in tissue kinetics. *British Journal of Cancer* **26**, 239-57 (1972)
70. Kinchington D, Randall S, Winther M and Horrobin D. Lithium γ-linolenate-induced cytotoxicity against cells chronically infected with HIV-1. *FEBS Letters* **330**, 219-21 (1993)
71. Kubota S, Zhang H, Kitahara S and Pomerantz R. Role of lentiviral lytic polypeptide I (LLP-I) in the selective cytotoxicity of gamma-glutamylcysteine ethyl ester against human immunodeficiciency virus type 1-producing cells. *Antiviral Chemistry and Chemotherapy* **10**, 121-127 (1999)
72. Kuida K, Haydar T, Kuan C, Gu Y, Taya C, Karasuyama H, Su M, Rakic P and Flavell R. Reduced apoptosis and cytochrome c-mediated caspase activation in mice lacking caspase 9. *Cell* **94**, 325-337 (1998)
73. Lambotte O, Taoufik Y, de Goër M, Wallon C, Goujard C and Delfraissy J. Detection of infectious HIV in circulating monocytes from patients on prolonged highly active antiretroviral therapy. *Journal of acquired immune deficiency syndromes* **23**, 114-119 (2000)
74. Laurent-Crawford A, Krus B, Muller S, Rivière Y, Rey-Cuillé, Béchet J.-M, Montagnier L and Hovanessian A. The cytopathic effect of HIV is associated with apoptosis. *Virology* **185**, 829-839 (1991)
75. Lennon S, Martin S and Cotter T. Dose-dependent induction of apoptosis in human tumour cell lines by widely diverging stimuli. *Cell Proliferation* **24**, 203-214 (1991)
76. Levy J. HIV research: a need to focus on the right target. *The Lancet* **345**, 1619-1621 (1995)
77. Li P, Nijhawan D, Budihardjo I, Srinivasula S, Ahmad M, AlnemriE and Wang X. Cytochrome c and dATP-dependent fomration of Apaf-1/caspase-9 complex initiates an apoptotic protease cascade. *Cell* **91**, 479-489 (1997)
78. Liu W, Masashi K, Akhand A, Hayakawa A, Haruhiko S, Miyata T, Kurokawa K, Hotta Y, Ishikawa N and Nakashima I. 4-hydroxynonenal induces a cellular redox status-related activation of the caspase cascade for apoptotic cell death. *Journal of Cell Science* **113**, 635-641 (2000)
79. Lori F, Malykh A, Cara A, Sun D, Weinstein J, Lisziewicz J and Gallo R. Hydroxyurea as an inhibitor of human immunodeficiency virus-type 1 replication. *Science* **266**, 801-805 (1994)
80. Lukashov V and Goudsmit J. HIV heteroneneity and disease progression in AIDS: a model of continuous virus

adaptation. *AIDS* **12 Suppl. A**, S43-52 (1998J)
81. Ma Y, Ogino T, Kawabata T, Li J, Eguchi K and Okada S. Cupric nitrilotriacetate-induced apoptosis in HL-60 cells association with lipid peroxidation, release of cytochrome C from mitochondria, and activation of caspase-3. *Free Radical Biology & Medicine* **27**, 227-233 (1999)
82. Madhavi N, Das U, Prabha P, Kumar G, Koratkar R and Sagar P. Suppression of human T-cell growth in vitro by cis-unsaturated fatty acids: Relationship to free radicals and lipid peroxidation. *Prostaglandins leukotrienes and essential fatty acids* **51**, 33-40 (1994).
83. Masutani H. Oxidative stress response and signaling in hematological malignancies and HIV infection. *International Journal f Hematology* **71**, 25-32 (2000)
84. Mayes PA (1997) in Textbook of Biochemistry with Clinical Correlations: Metabolism of Unsaturated Fatty Acids & Eicosanoids (Devlin TM ed.) pp. 236-244. A John Wiley & Sons, N.Y.
85. McConkey D and Orrenius S. Cellular signaling in thymocyte apoptosis. In: Apoptosis: The molecular basis of cell death. 1st edn. (Tomei L and Cope F, eds) p227. Cold Spring Harbor Laboratory Press, N.Y. (1991)
86. McFadden G. Even viruses can learn to cope with stress. *Science* **279**, 40-41 (1998)
87. McCloskey T, Ott M, Tribble E, Khan S, Teichberg S, Paul M, Pahwa S, Verdin E and Chirmule N. Dual role of HIV Tat in regulation of apoptosis in T cells. *The Journal of Immunology* **158**, 1014-1019 (1997)
88. Mpanju O, Winther M, Manning J, Craib K, Montaner J, O'Shaugnessy M and Conway B. Selective cytotoxicity of lithium γ-linolenic acid in human T cells chronically and productively infected with HIV. *Antiviral Therapy* **2**, 13-19 (1997)
89. Murray R, Granner D, Mayes P and Rodwell V in Harper's Biochemistry: Lipoxygenase and Oxy-Eicosatetraenoic Acids. Pp 436-441. Appleton & Lange, Stamford, CT (1996)
90. Neumann D, Zierke M and Martin M. Withdrawal of 2-mercaptoethanol induces apoptosis in a B-cell line via Fas upregulation. *Journal of Cellular Physiology* **177**, 68-75 (1998)
91. Obeid L and Hannun Y. Ceramide: a stress signal and mediator of growth suppression and apoptosis. *Journal of Cell Biochemistry* **58**, 191-198 (1995)
92. Paolicchi A, Tonarelli P, Silva S, Bandecchi P and Malvaldi G. Changes in glutathione metabolism during feline immunodeficiency virus infection. *Journal of Acquired Immune Deficiency Syndrome* **13**, 94-96 (1996)
93. Papa S and Skulachev V. Reactive oxygen species, mitochondria, apoptosis and aging. *Molecular and Cellular Biochemistry* **174**, 305-319 (1997)
94. Papadogiannakis N and Barbieri B. Lipoxygenase inhibitors counteract protein kinase C mediated events in human T lymphocyte proliferation. *International Journal of Immunopharmacology* **19**, 263-75 (1997)
95. Perelson A, Essunger P, Cao Y, Vesanen M, Hurley A, Saksela K, Markowitz M and Ho D.Decay characteristics of HIV-1-infected compartments during combination therapy. *Nature* **387**, 188-191 (1997)
96. Popovic M, Read-Connole E and Gallo R. T4 positive human neoplastic cell lines susceptible to and permissive for HTLV-III. *Lancet* **ii**, 1472-1473 (1984)
97. Popovic M, Samgadharan M, Read E and Gallo R. Detection, isolation, and continuous production of cytopathic retroviruses (HTLV-III) from patients with AIDS and pre-AIDS. *Science* **224**, 497-500 (1984)
98. Quillent C, Dumey N, Dauguet C and Clavel F. Reversion of a polymerase-defective integrated HIV-1 genome. *AIDS Research & Human Retroviruses* **9**, 1031-1037 (1993)
99. Ratner L, Haseltine W, Patarca R, Livak K, Starcich B, Josephs S, Doran E,

Rafalski J, Whitehorn E, Baumeister K, Ivanoff L, Petteway S Jr, Pearson M, Lautenberger J, Papas T, Ghrayab J, Chang N, Gallo R and Wong-Staal F. *Nature* **313**, 277-283 (1985)

100. Robbins M, Ali K, McCaw R, Olsen J, Vartak S and Lubaroff D. γ-Linolenic acid (GLA)-mediated cytotoxicity in human prostate cancer cells. *Advances in Experimental Medicine & Biology* **469**, 499-504 (1999)

101. Roederer M, Staal F, Raju P, Ela S, Herzenberg L and Herzenberg L. Cytokine-stimulated human immunodeficiency virus replication is inhibited by N-acetyl-L-cytsteine. *Proceedings of the National Academy of Sciences USA* **87**, 4884-4888 (1990)

102. Roederer M, Ela S, Staal F, Herzenberg L and Herzenberg L N-acetylcysteine: a new approach to anti-HIV therapy. *AIDS Research & Human Retroviruses* **8**, 209-217 (1992)

103. Ross T. Using death to one's advantage: HIV modulation of apoptosis. *Leukemia* **15**, 332-341 (2001)

104. Rossetti R, Seiler C, Laposata M and Zurier R. Differential regulation of human T lymphocyte protein kinase C activity by unsaturated fatty acids. *Clinical Immunology and Immunopathology* **76**, 220-224 (1995).

105. Roy S and Nicholson D. Cross-Talk in cell death signaling. *Journal of Experimental Medicine* **192**, F21-F25 (2000)

106. Saag M and Kilby J. HIV-1 and HAART: a time to cure, a time to kill. *Nature Medicine* **5**, 609-611 (1999)

107. Salari H, Braquet P and Borgeat P. Comparative effects of indomethacin, acetylenic acids, 15-HETE, nordihydroguaiaretic acid and BW755C on the metabolism of acrachidonic acid in human leukocytes and platelets. *Prostaglandins Leukotrienes and Medicine* **13**, 53-60 (1984)

108. Sandstrom P, Roberts B, Folks T and Buttke T. HIV gene expression enhances T cell susceptibility to hydrogen peroxide-induced apoptosis. *AIDS Research and Human Retroviruses* **9**, 1107-13 (1993)

109. Sandstrom P, Tebbey P, Van Cleave and Buttke T. Lipid hydroperoxides induce apoptosis in T cells displaying a HIV-associated glutathione peroxidase deficiency. *Journal of Biological Chemistry* **269**, 798-801 (1994)

110. Santoli D, Phillips P, Colt T and Zurier R. Suppression of interleukin 2-dependent human T cell growth in vitro by prostaglandin E (PGE) and their precursor fatty acids. *Journal of Clinical Investigation* **85**, 424-32 (1990)

111. Sato N, Iwata S, Nakamura K, Hori T, Mori K and Yodoi J. Thiol-mediated redox regulation of apoptosis. Possible roles of cellular thiols other than glutathione in T cell apoptosis. *Journal of Immunology* **154**, 3194-3203 (1995)

112. Schewe T. Molecular actions of Ebselen-an anti-inflammatory antioxidant. *General Pharmacology* **26**, 1153-1169 (1995)

113. Schrager L and D'Souza P. Cellular and anatomical reservoirs of HIV-1 in patients receiving potent antiretroviral combination therapy. *Journal of the American Medical Association* **280**, 67-71 (1998)

114. Seegers J, de Kock M, Lottering M.-L, Grobler C, van Papendrop D, Shou Y, Habbersett R and Lehnert B. Effects of gamma-linolenic acid and arachidonic acid on cell cycle progression and apoptosis induction in normal and transformed cells. *Prostaglandins, Leukotrienes and Essential Fatty Acids* **56**, 271-80 (1997)

115. Shisler J, Senkevich T, Berry M and Moss B. Ultraviolet-induced cell death blocked by a selenoprotein from a human dermatotropic pox virus. *Science* **279**, 102-105 (1998)

116. Skinner et. al. (1990) in: Omega-6 Essential Fatty Acids: Pathophysiology and Roles in Clinical Medicine (Horrobin D.F. Ed.) pp. 261-273, Alan R. Liss. N.Y.

117. Skurnick J, Bogden J, Baker H, Kemp F, Sheffet A, Quattrone G and Louria

D. Micronutrient profiles in HIV-1-infected heterosexual adults. *Journal of Acquired Immune Deficiency Syndromes and Human Retrovirology* **12**, 75-83 (1996)
118. Staal F, Roederer M, Israelski D, Bubp J, Mole L, McShane D, Deresinski S, Ross W, Sussman H, Raju P, Anderson M, Moore W, Ela S, Herzenberg L and Herzenberg L. Intracellular glutathione levles in T cell subsets decrease in HIV-infected individuals. *AIDS Research and Human Retroviruses* **2**, 305-311 (1992)
119. Starcich B, Hahn B, Shaw G, McNeely P, Modrow S, Wolf H, Parks E, Parks W, Josephs S, Gallo R, et al. Identification and characterization of conserved and variable regions in the envelope gene of HTLV-III/LAV, the retrovirus of AIDS. *Cell* **45**, 637-678 (1986)
120. Tang D and Honn K. Apoptosis of W256 carcinosarcoma cells of the monocytoid origin induced by NDGA involves lipid peroxidation and depletion of GSH: Role of 12-lipoxygenase in regulating tumor cell survival. *Journal of Cellular Physiology* **172**, 155-170 (1997)
121. Taylor E, Nadimpalli R and Ramanathan C. Genomic structures of viral agents in relation to the biosynthesis of selenoproteins. *Biological Trace Elements Research* **56**, 63-91 (1997)
122. Taylor E, Bhat A, Nadimpalli R, Zhang W and Kececioglu J. HIV-1 encodes a sequence overlapping env gp41 with highly significant similarity to selenium-dependent glutathione peroxidases. *Journal of Acquired Immune Deficiency Syndromes and Human Retrovirology* **15**, 393-394 (1997)
123. Terai C, Kornbluth R, Pauza C, Richman D and Carson D. Apoptosis as a mechanism of cell death in clutured T lymphoblasts acutely infected with HIV-1. *Journal of Clinical Investigation* **87**, 1710-1715 (1991)
124. The Division of AIDS, National Institutes of Allergy & Infectious Diseases, National Institutes of Health and Collaborating Investigators. Virus stock infectivity titration. In: DAIDS Virology Manual for HIV Laboratories, Version January 1997 (Beatty C, Bradley M, Brambilla D et al, eds) pp 81-83.
125. Tortorella D, Gewurz B, Furman M, Schust D and Ploegh H. Viral subversion of the immune system. *Annual Review of Immunology* **18**, 861-926 (2000)
126. Vartak S, Robbins M and Spector A. The selective cytotoxicity of γ-linolenic acid (GLA) is associated with increased oxidative stress. *Advances in Experimental Medicine & Biology* **469**, 493-8 (1999)
127. Westendorp M, Frank R, Ochsenbauer C, Stricker K, Dhein J, Walczak H, Debatin K and Krammer P. Sensitization of T cells to CD95-mediated apoptosis by HIV-1 Tat and gp120. *Nature* **375**, 497-500 (1995)
128. Wong J, Hezareh M, Gunthard H, Havlir D, Ignacio C, Spina C and Richman D. Recovery of replication-competent HIV despite prolonged suppression of plasma viremia. *Science* **278**, 1291-1295 (1997)
129. Wyllie A, Kerr J and Currie A. Cell death: The significance of apoptosis. *International Review of Cytology* **68**, 251-306 (1980)
130. Yerly S, Kaiser L, Perneger T, Cone R, Opravil M, Chave J, Furrer H, Hirschel B and Perrin L. Time of initiation of antiretroviral therapy: impact on HIV-1 viraemia. The Swiss HIV Cohort Study. *AIDS* **14**, 243-249 (2000)
131. Zauli G, Gibellini D, Milani D, Mazzoni M, Borgatti P, La Placa M and Capitani S. Human immunodeficiency virus type 1 Tat protein protects lymphoid, epithelial, and neuronal cell lines from death by apoptosis. *Cancer Research* **53**, 4481-4485 (1993)
132. Zhang L, Ramratnam B, Tenner-Racz K, He Y, Vesanen M, Lewin S, Talal A, Racz P, Perelson A, Koerber B, Markowitz M and Ho D. Quantifying residual HIV-1 replication in patients erceiving combination antiretroviral therapy. *New England Journal of Medicine* **340**, 1605-1613 (1999)

133. Zhong L, Sarafian T, Kane D, Charles A, Mah S, Edwards R and Bredesen D. Bcl-2 inhibits death of central neural cells induced by multiple agents. *Proceedings of the National Academy of Sciences USA* **90**, 4533-4537 (1993)